Mining the SAIGUP data, phase 1

Norsk Regnesentral
ANVENDT DATAFORSKNING
Norwegian Computing Center/Applied Research and Development

NOTAT/NOTE

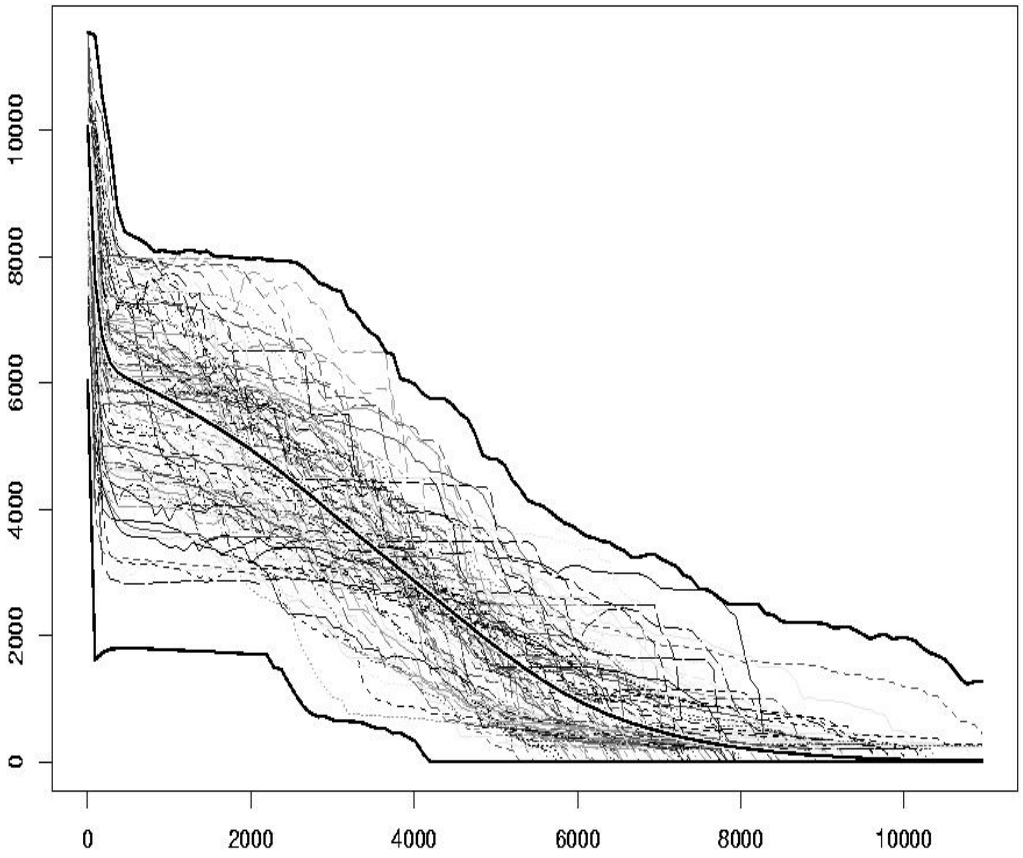

SAND/06/02

Odd Kolbjørnsen
Arne Skorstad
Lars Holden

OSLO
December 2002

Norsk Regnesentral
ANVENDT DATAFORSKNING

NR-notat/NR Note

Tittel/Title: Mining the SAIGUP data, phase 1.

Dato/Date: December
År/Year: 2002
Notat nr: SAND/06/02
Note no:

Forfatter/Author: Odd Kolbjørnsen, Arne Skorstad and Lars Holden

Sammendrag/Abstract: In the current report data from phase one of the SAIGUP project is analyzed. The data consist of 9072 production scenarios given from 81 geological models, 28 fault models and four production strategies. The models contain structural factors that are typical for shallow marine hydrocarbon reservoirs. The objective is to identify the structural factors that give the largest contribution to the variability in the output, and to identify the geological variables that contribute the most to the main effect of geology in the output.

For variables related to the produced oil volume, geological effects are dominant; this is in part because fault models are adjusted such that oil in place is determined by geological factors. For overall recovery fault effects are largest. The production strategy has larger influence on the time of production than on the cumulated amounts.

Emneord/Keywords: Oil production, structural factors, shallow marine hydrocarbon reservoirs, variance components, model

Tilgjengelighet/Availability: Open

Prosjektnr./Project no.: 912010

Satsningsfelt/Research field: Structural factors in oil production

Antall sider/No. of pages: 83

Norsk Regnesentral / Norwegian Computing Center
Gaustadalléen 23, Postboks 114 Blindern, 0314 Oslo, Norway
Telefon 22 85 25 00, telefax 22 69 76 60

Mining the SAIGUP data, phase 1

Odd Kolbjørnsen, Arne Skorstad and Lars Holden

December 2002

Abstract

In the currentreport data from phase one of the SAIGUP project is analysed. The data consist of 9072 production scenarios given from 81 geological models, 28 fault models and four production strategies. The models contain structural factors that are typical for shallow marine hydrocarbon reservoirs. The objective is to identify the structural factors that give the largest contribution to the variability in the output, and to identify the geological variables that contribute the most to the main effect of geology in the output.

For variables related to the produced oil volume, geological effects are dominant; this is in part because fault models are adjusted such that oil in place is determined by geological factors. For overall recovery fault effects are largest. The production strategy has larger influence on the time of production than on the cumulated amounts.

Keywords: Oil production, structural factors, shallow marine hydrocarbon reservoirs, variance components, model selection.

1 Introduction

The project "Sensitivity analysis of the impact of geological uncertainties on production forecasting in clastic hydrocarbon reservoirs", SAIGUP for short, is designed to quantify objectively the sensitivity of geological complexity on production forecast as a function of generic aspects of sedimentological architecture and fault structure of shallow marine hydrocarbon reservoirs.

In the current report data from phase one of the SAIGUP project are described and analysed. The data consist of 9072 production scenarios given from 81 geological models, 28 fault models and four production strategies. There are two objectives of the current analysis. Firstly to explain the variability in scalar response variables related to recovery and production by causes related to geology, faults, production strategy, and interactions of these effects. Next to obtain a simplified relation between the scalar response and explanatory variables related to geology. A similar study is the great reservoir uncertainty study (GRUS), (Lia, Omre, Tjelmeland, Holden, Egeland, Andersen, MacDonald, Hustad and Qi, 1995). The data analysis in GRUS is reported in Egeland, Omre, Lia, Tjelmeland, Holden and Andersen (1994).

For a full set of explanatory variables, the relation between the response and the explanatory variables is given by flow equations,

$$y = K_0 + K(\mathbf{G}, \mathbf{F}, \mathbf{P}), \tag{1}$$

with y being a scalar response; $\mathbf{G}$, $\mathbf{F}$ and $\mathbf{P}$ being explanatory variables related to geology faulting and production strategy respectively; K_0 being the average level of y; and K being a function describing the variability around K_0. The function $K_0 + K(\mathbf{G}, \mathbf{F}, \mathbf{P})$ is implicitly defined by flow equations. Notice there is no error term in Expression (1), since y is simulated and not observed. In the statistical analysis the function K is broken down into orthogonal effects,

$$\begin{array}{rcccccc} K(\mathbf{G},\mathbf{F},\mathbf{P}) & = & K_{\mathbf{G}}(\mathbf{G}) & + & K_{\mathbf{F}}(\mathbf{F}) & + & K_{\mathbf{P}}(\mathbf{P}) \\ & + & K_{\mathbf{GF}}(\mathbf{G},\mathbf{F}) & + & K_{\mathbf{GP}}(\mathbf{G},\mathbf{P}) & + & K_{\mathbf{FP}}(\mathbf{F},\mathbf{P}) \\ & + & K_{\mathbf{GFP}}(\mathbf{G},\mathbf{F},\mathbf{P}) & & & & \end{array}, \tag{2}$$

with $K_{\mathbf{G}}(\mathbf{G})$, $K_{\mathbf{F}}(\mathbf{F})$ and $K_{\mathbf{P}}(\mathbf{P})$, being main effects of geology, faulting and production strategy respectively; $K_{\mathbf{GF}}(\mathbf{G},\mathbf{F})$, $K_{\mathbf{GP}}(\mathbf{G},\mathbf{P})$, and $K_{\mathbf{FP}}(\mathbf{F},\mathbf{P})$ being second order interactions and $K_{\mathbf{GFP}}(\mathbf{G},\mathbf{F},\mathbf{P})$

being third order interactions. In the statistical analysis these functions are variance components. The total variability of a production variable y is $K(\mathbf{G}, \mathbf{F}, \mathbf{P})$, the total variance is $\|K\|^2$. The total variability is obtained when all factors are allowed to vary freely. The variance component due to the main effect of a factor, i.e. $\|K_{\mathbf{G}}\|^2$, $\|K_{\mathbf{F}}\|^2$, and $\|K_{\mathbf{P}}\|^2$, is the decrease in variance when this factor is fixed. If two factors are fixed, the decrease in variance is generally larger than the sum of the two main effects. The additional decrease of variance is the variance component due to second order interaction of the two effects, i.e. $\|K_{\mathbf{GF}}\|^2$, $\|K_{\mathbf{GP}}\|^2$, and $\|K_{\mathbf{FP}}\|^2$. Variance components due to higher order interactions are defined correspondingly, as the additional variance reduction when all lower order interactions are subtracted. Note that if one factor is allowed to vary and all other factors are kept fixed, the variance that is observed is the sum of the main effect of this factor and all interaction effects that include this factor; hence this will generally be larger than the main effect.

2 SAIGUP experimental design

The SAIGUP data is generated by input from 81 distinct geological models, 28 distinct fault patterns and four distinct production strategies. The flow simulator is run for all combinations producing a total of 9072 responses.

The geological models are constructed to capture the main features in shallow marine hydrocarbon reservoirs. Figure 1 display three of the 81 geological models, in the figure the facies are assigned colour codes. The geological models have six facies types being, channels (red), coastal plane (green), upper shore face (yellow), lower shore face (brown), offshore transition zone (dark brown), and offshore (grey). The models all have four layers. The layering is particularly easy to see in Figure 1 (b). The sedimentological architecture is in addition determined by four factors that are assigned to three different levels. The shoreline curvature, determines the curvature of the facies, as being no curvature, see Figure 1 (a); one lobe, see Figure 1 (b); or two lobes, see Figure 1 (c). The progradation direction determines the shoreline relative to the orientation of the reservoir. The angle of the progradation direction increases clockwise, with north being 0^o. The cases considered are 90^o, see Figure 1 (b); 180^o see Figure 1 (a); and 270^o, see Figure 1 (c). The aggradation angle determines the transition between facies within a zone, the angel varies in the four zones and is drawn uniformly in the intervals 6^o to 17^o, see Figure 1 (a); 28^o to 45^o, see Figure 1 (c); or 57^o to 80^o, see Figure 1 (b). The geological models contain flow barriers, these are located along surfaces going through the reservoir. The surfaces that contain the barriers are both vertical and horizontal. The shape of the vertical surfaces depend on the facies transitions trough a set of hyper parameters that give the shape of the shore line curvature. The horizontal surfaces separate the geological layers. The barriers are completely sealing but do not cover the entire surface. The barrier coverage is 10%, 50% or 90% in the geological models. Petrophysical properties are generated independently within each facies type, and for each geological model, according to a random rule. All combinations of the four factors are investigated, yielding 81 geological models, $\mathbf{G}_i \; ; \;\; i = 1, ..., 81$.

The fault patterns represent typical fault patterns that are observed in shallow marine hydrocarbon reservoirs. The fault models are determined by three factors. Figure 2 display the three main fault structures are investigated. Structure a is a predominantly strike-parallel fault case, Structure b is a compartmentalised fault system, and structure c is a strike perpendicular fault case. The fault density varies at four levels, from fully faulted (level 1), to an unfaulted model (level 4), see bottom Figure 2. The unfaulted model is common for all three fault structures. The fault rock properties are selected based on relationships derived from core analysis. Three different fault rock permeability predictors are assigned to each faulted model. The design yield a total of 27 fault models and one unfaulted model, $\mathbf{F}_j \; ; \;\; j = 1, ..., 28$.

Three production strategies are designed to be optimal for each of the three main structures in the fault pattern. In addition one production strategy is designed for the unfaulted model, giving the four production strategies, $\mathbf{P}_k \; ; \;\; k = 1, ..., 4$.

In order to generate the data in the database, all combinations of geological model, fault models and production strategies are run through the flow simulator, hence all production strategies are applied to all fault structures regardless whether it was designed for the particular fault structure or not. The total number of responses is hence 9072,

$$y_{ijk} = K_0 + K(\mathbf{G}_i, \mathbf{F}_j, \mathbf{P}_k) \; ; \;\; i = 1, ..., 81; \;\; j = 1, ..., 28; \;\; k = 1, ..., 4. \tag{3}$$

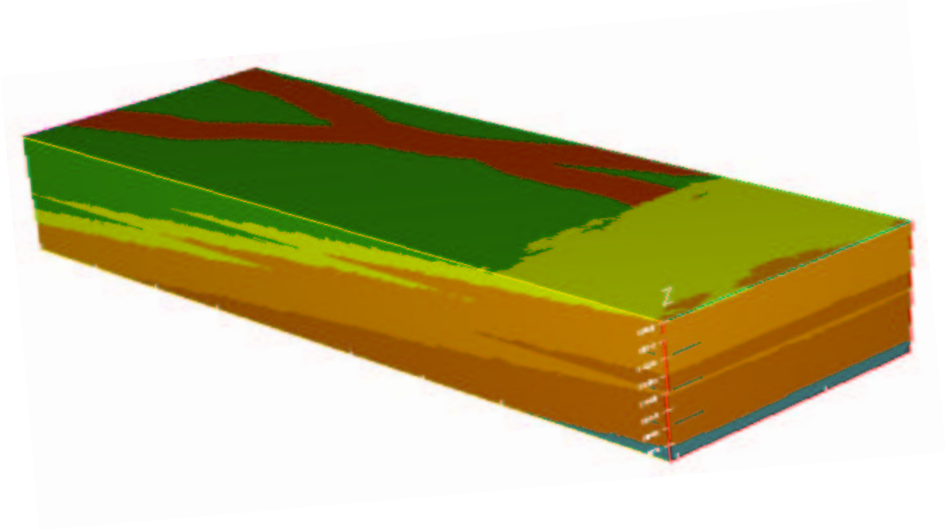

(a)

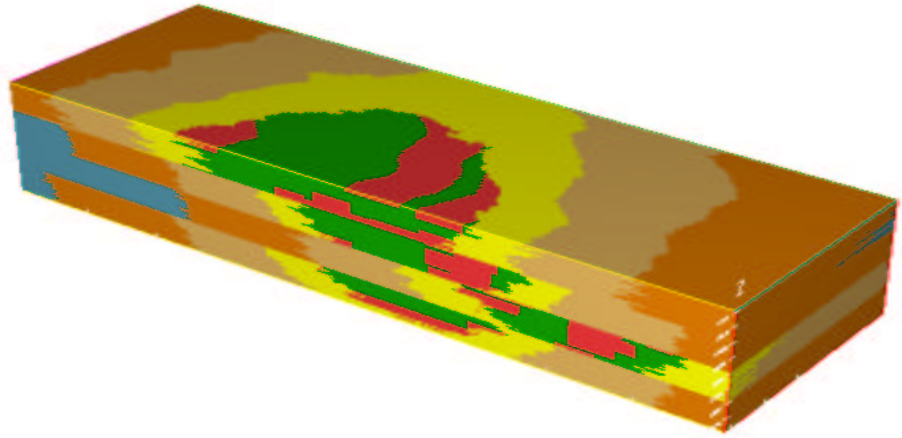

(b)

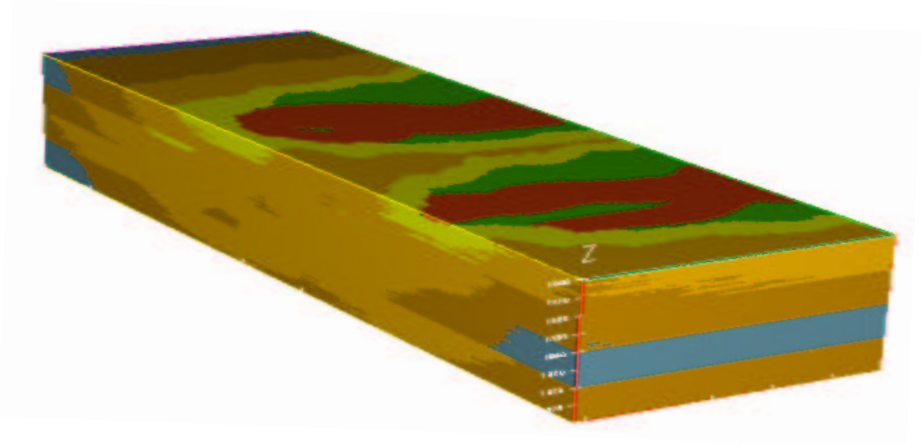

(c)

Figure 1: Geological models. Three of the geological design parameters are illustrated. The shoreline curvature, aggradation angle and progradation direction is; no curvature, low and 180^o (a); single lobe, high, and 90^o (b); double lobe, medium, and 270^o (c);

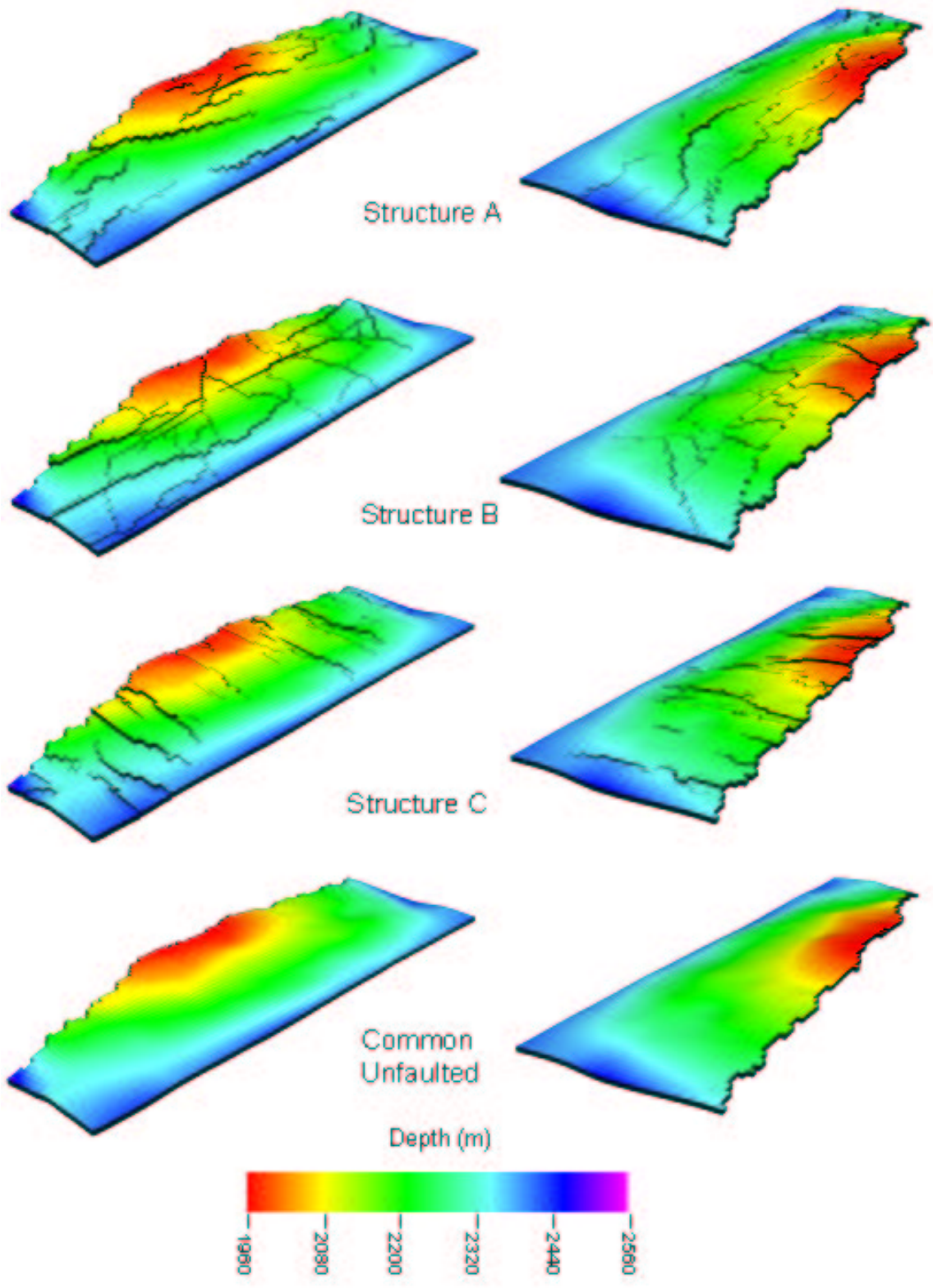

Figure 2: Structural deformations. The figure displays the main structure of the reservoir in the unfaulted case, bottom and the three main fault structures above. The three structures are, predominantly strike-parallel fault case (Structure A), a compartmentalised fault system (Structure B), and a strike perpendicular fault case (Structure C).

3 Descriptive statistics

The current section reports sample statistics of geological and production variables and plots illustrating the joint distribution of production variables, and conditional distribution of production variables given some of the categorical design variables. The sample statistics and the plots are generated by using the statistical program Splus.

Geological summary variables are listed in Table 1. The variables above the line are sampled as a part of the procedure for generating the Geological models. The variable denoting fraction of upper shore face is one minus the other facies fractions, and is hence not included. The variables below the line are quantities computed from the resulting Geological models. In Table 2 some summary statistics of the geological variables are reported.

In Table 3 the pairs of variables having a correlation larger than 0.5 in absolute value are listed. The correlations depend on the sampling design used for generating the 81 geological models, and should not be given weight as natural phenomena. In order to compute the aggregate summary variables quantities are averaged over different facies types this may cause correlation between variables that are uncorrelated within the facies. The correlations in Table 3 are relevant in Section 5 and 6 where the geological variables are used as explanatory variables in regression analysis.

Table 1: Description of geological variables;

Variable name	Description
COS.PROG	Cosine of progradation direction 0, -1 or 0 for $90^o, 180^o$ or 270^o
SIN.PROG	Sine of progradation direction 1, 0 or -1 for $90^o, 180^o$ or 270^o
BARR	Expected barrier coverage $10\%, 50\%$, or 90%
AGGR.aZ	Average aggradation angle all zones
KXY.ARITH	Average lateral permeability (log transformed)
KXmY.ARITH	Average difference in X and Y permeability (log transformed)
KZ.ARITH	Average Z-direction permeability (log transformed)
CLIN.aZ	Average angle of clinoform from all zones
OFFSET.aZ	Average offset all zones
PORO.ARITH.aZ	Average Porosity in all zones
VSHALE.ARITH.aZ	Average Shale fraction in all zones
THICK.LSF.aZ	Average Thickness of LSF all zones
THICK.USF.aZ	Average Thickness of USF all zones
THICK.OTZ.aZ	Average Thickness of OTZ all zones
CH.FM.aZ	Fraction of channels in all zones in flow model
CP.FM.aZ	Fraction of coastal plane in all zones in flow model
LSF.FM.aZ	Fraction of lower shore face in all zones in flow model
OFF.FM.aZ	Fraction of offshore in all zones in flow model
OTZ.FM.aZ	Fraction of offshore transition zone in all zones in flow model
KX.PRES.SOLVE	Upscaled permeability in X-direction (log transformed)
KY.PRES.SOLVE	Upscaled permeability in Y-direction (log transformed)
KZ.PRES.SOLVE	Upscaled permeability in Z-direction (log transformed)
HETRX	Heterogeneity measure in X-direction. The ratio of the upscaled to the arithmetic permeability, the permeabilities are not log transformed.
HETRY	Heterogeneity measure in Y-direction. The ratio of the upscaled to the arithmetic permeability, the permeabilities are not log transformed.
HETRZ	Heterogeneity measure in Z-direction. The ratio of the upscaled to the arithmetic permeability, the permeabilities are not log transformed.

Table 2: Summary statistics of aggregate geological variables, based on 81 Geological models

Variable name	Mean	Standard deviation	Median	Minimum	Maximum
COS.PROG	-0.333	0.474	0.000	-1.000	0.000
SIN.PROG	0.000	0.822	0.000	-1.000	1.000
BARR	0.500	0.329	0.500	0.100	0.900
AGGR.aZ	0.684	0.405	0.642	0.153	1.298
CLIN.aZ	0.505	0.001	0.505	0.501	0.508
KXY.ARITH	5.233	0.268	5.215	4.698	5.835
KXmY.ARITH	0.000	0.003	0.000	-0.010	0.005
KZ.ARITH	2.979	0.356	2.930	2.350	3.790
OFFSET.aZ	1727.000	1664.876	917.800	166.600	5671.000
PORO.ARITH.aZ	0.138	0.011	0.141	0.116	0.158
THICK.LSF.aZ	14.980	0.715	15.050	13.170	16.470
THICK.OTZ.aZ	19.940	0.718	19.900	18.620	21.990
THICK.USF.aZ	6.561	0.444	6.666	5.558	7.242
VSHALE.ARITH.aZ	0.304	0.031	0.306	0.248	0.367
CH.FM.aZ	0.042	0.025	0.032	0.008	0.112
CP.FM.aZ	0.133	0.093	0.120	0.016	0.335
LSF.FM.aZ	0.396	0.083	0.407	0.209	0.546
OFF.FM.aZ	0.031	0.056	0.001	0.000	0.258
OTZ.FM.aZ	0.206	0.115	0.206	0.000	0.534
KX.PRES.SOLVE	5.017	0.280	5.041	4.322	5.600
KY.PRES.SOLVE	5.008	0.349	4.989	3.997	5.790
KZ.PRES.SOLVE	-1.433	0.940	-1.482	-3.193	0.890
HETRX	0.814	0.111	0.847	0.413	0.968
HETRY	0.807	0.113	0.832	0.440	0.954
HETRZ	0.017	0.014	0.010	0.003	0.059

Table 3: The correlations of geological variables exceeding 0.5 in absolute value

Variable name 1	Variable name 2	Correlation
KZ.ARITH	KXY.ARITH	0.936
VSHALE.ARITH.aZ	PORO.ARITH.aZ	−0.908
KXY.ARITH	KY.PRES.SOLVE	0.905
KY.PRES.SOLVE	KX.PRES.SOLVE	0.897
OFFSET.aZ	AGGR.aZ	−0.883
KZ.PRES.SOLVE	HETRZ	0.857
KXY.ARITH	KX.PRES.SOLVE	0.847
OTZ.FM.aZ	KZ.ARITH	−0.828
KZ.ARITH	KY.PRES.SOLVE	0.818
OTZ.FM.aZ	KXY.ARITH	−0.800
LSF.FM.aZ	PORO.ARITH.aZ	0.789
VSHALE.ARITH.aZ	KXY.ARITH	−0.747
LSF.FM.aZ	VSHALE.ARITH.aZ	−0.747
KZ.ARITH	KX.PRES.SOLVE	0.736
PORO.ARITH.aZ	KXY.ARITH	0.721
OTZ.FM.aZ	KY.PRES.SOLVE	−0.715
VSHALE.ARITH.aZ	KZ.ARITH	−0.713
BARR	HETRZ	−0.705
VSHALE.ARITH.aZ	KY.PRES.SOLVE	−0.705
KY.PRES.SOLVE	HETRY	0.690
OTZ.FM.aZ	VSHALE.ARITH.aZ	0.669
PORO.ARITH.aZ	KY.PRES.SOLVE	0.667
KXmY.ARITH	HETRX	0.655
BARR	KZ.PRES.SOLVE	−0.647
PORO.ARITH.aZ	KX.PRES.SOLVE	0.64
VSHALE.ARITH.aZ	KX.PRES.SOLVE	−0.627
PORO.ARITH.aZ	KZ.ARITH	0.615
SIN.PDIR	CP.FM.aZ	0.601
OTZ.FM.aZ	KX.PRES.SOLVE	−0.597
OTZ.FM.aZ	OFFSET.aZ	0.595
KZ.PRES.SOLVE	KY.PRES.SOLVE	0.586
BARR	HETRX	−0.571
BARR	HETRY	−0.568
OTZ.FM.aZ	KZ.PRES.SOLVE	−0.564
KX.PRES.SOLVE	HETRY	0.564
KZ.PRES.SOLVE	KX.PRES.SOLVE	0.554
AGGR.aZ	HETRX	−0.523
KZ.ARITH	KZ.PRES.SOLVE	0.517
OFFSET.aZ	KZ.PRES.SOLVE	−0.516
OFF.FM.aZ	PORO.ARITH.aZ	−0.514
OFF.FM.aZ	VSHALE.ARITH.aZ	0.506
CH.FM.aZ	KXmY.ARITH	−0.504
OFFSET.aZ	HETRX	0.503

Figure 3 (a) display 100 of the 9072 production profiles and indicate the pointwise maximum and minimum production rate. The production variables that will be considered in this article are listed in Table 4. The variables above the line in the table are of natural interest. The variables PROD.PC1, PROD.PC2 and PROD.PC3 are the first three principal components of the oil production profile. These summary variables explains 50%, 31%, and 8%, of the variance in the production profile respectively. The production profiles constructed by using only the largest, two largest and three largest principal components are displayed in Figure 3 (b), (c) and (d) respectively. The variables are hence coefficients in a generalised Fourier series that describe the production profile. In Figure 4 the mean production and the functions corresponding to the three principal components are displayed. The first production component, can be said to discriminate on the amount of oil produced the first ten years, see Figure 4 (b). The second production component , can be said to discriminate on the amount of oil produced between 10 and 20 years, see Figure 4 (c) The last production component discriminate on the time the oil is produced, i.e. if this coefficient has a positive sign, it pushes production away from ten years to both sides, see Figure 4 (d). The functions in Figure 4 (b), (c), and (d), are scaled to reflect the variability range. The coefficients corresponding to the functions, i.e. PROD.PC1, PROD.PC2 and PROD.PC3, are hence centred with unit variance.

Table 4: Production Variables

Variable name	Description
FIOP.0	Volume of oil in place prior to production
GOPT.END	Total oil volume produced at the end
LNOPT.END	Total oil volume produced at the end (log transformed)
DISK.PROD.10	Total oil volume produced discounted by 10% per year after start
ROPT.END	Recovery factor for production after 30 years
ROPT.PV20	Recovery factor for production at an injected pore volume of 20%.
GWPT.END	Total water volume produced at the end
ROWPT.END	Ratio oil/water production at the end
PROD.PC1	Component yielding maximum variability in production profile
PROD.PC2	Component yielding second most variability in production profile
PROD.PC3	Component yielding third most variability in production profile

Figure 5 show how the variability in the production profile is reduced when the variability due to the production components are extracted. In Figure 5 (a) the total variability is displayed. The variability remaining after extracting the largest, two largest and three largest principal components are displayed in Figure 5 (b), (c) and (d) respectively.

Table 5 present summary statistics of the production variables. The values in the table are sample values for the production variables. Each variable has 9072 samples. The samples are however dependent because there are only $81 + 28 + 4 = 113$ independent factors in the input, in which are combined to $81 \cdot 28 \cdot 4 = 9072$ outputs.

In Table 6 the pairs of production variables having a correlation larger than 0.5 in absolute value are listed. The correlations must be taken into account when the results of the analysis is interpreted. If two production variables have high correlation common factors in the design influence both variables. The dependencies of the production variables are also illustrated in the Figures 6, 7, and 8; which display scatter plots for some pairs of production variables. Each entry in the matrix of scatter plots in the Figures 6, 7, and 8 is the scatter plot of the two variables on the corresponding diagonal elements, the scatter plot matrices are symmetric.

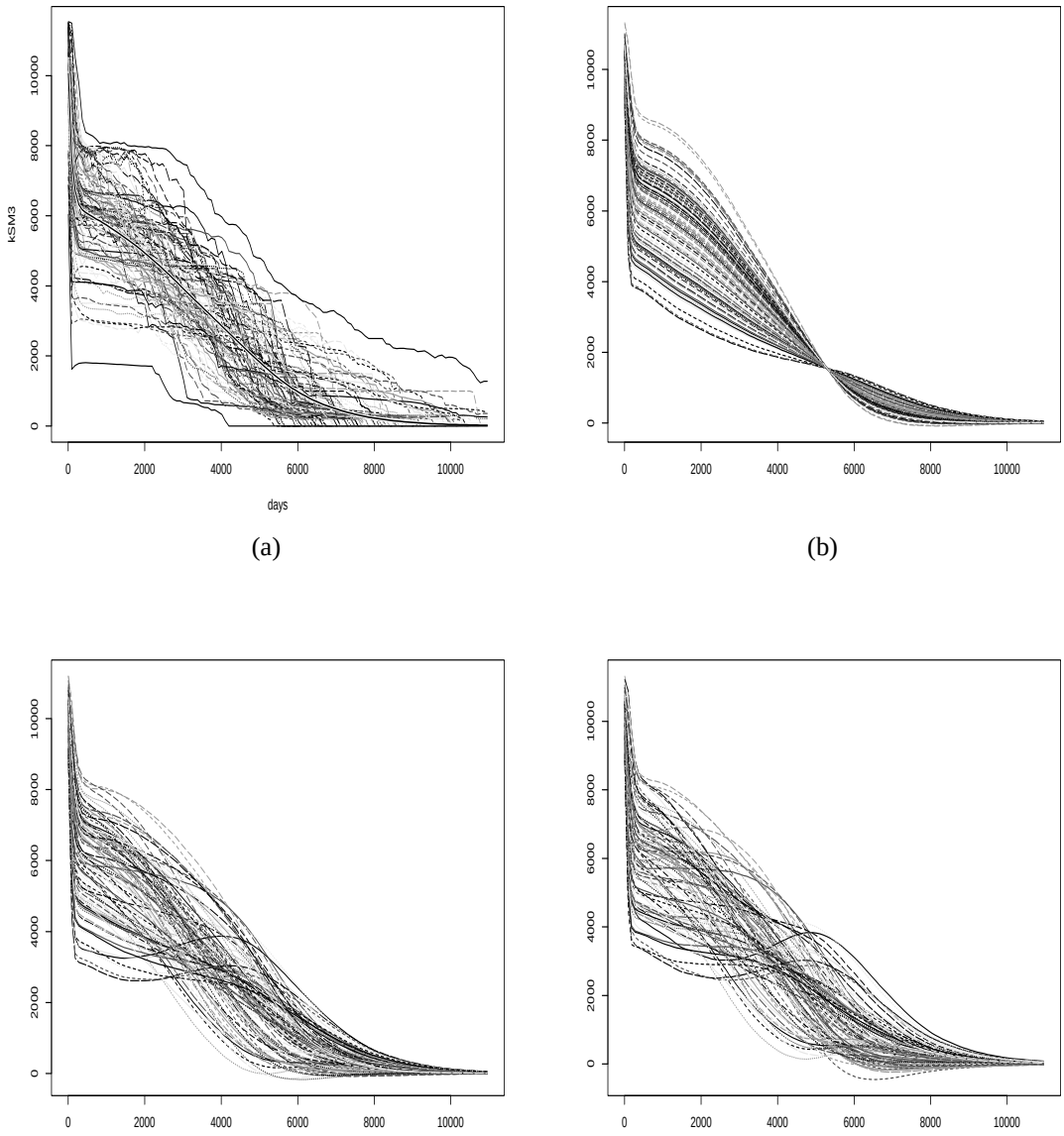

(a) (b)

(c) (d)

Figure 3: Total production rate in the field; In figure (a) Total production rate for 100 production scenarios are displayed together with the pointwise mean, maximum, and minimum production rate. Figures (b)-(d) display the approximate production profiles if only the first component (b); the two first (c); the three first (d) principal components of are used.

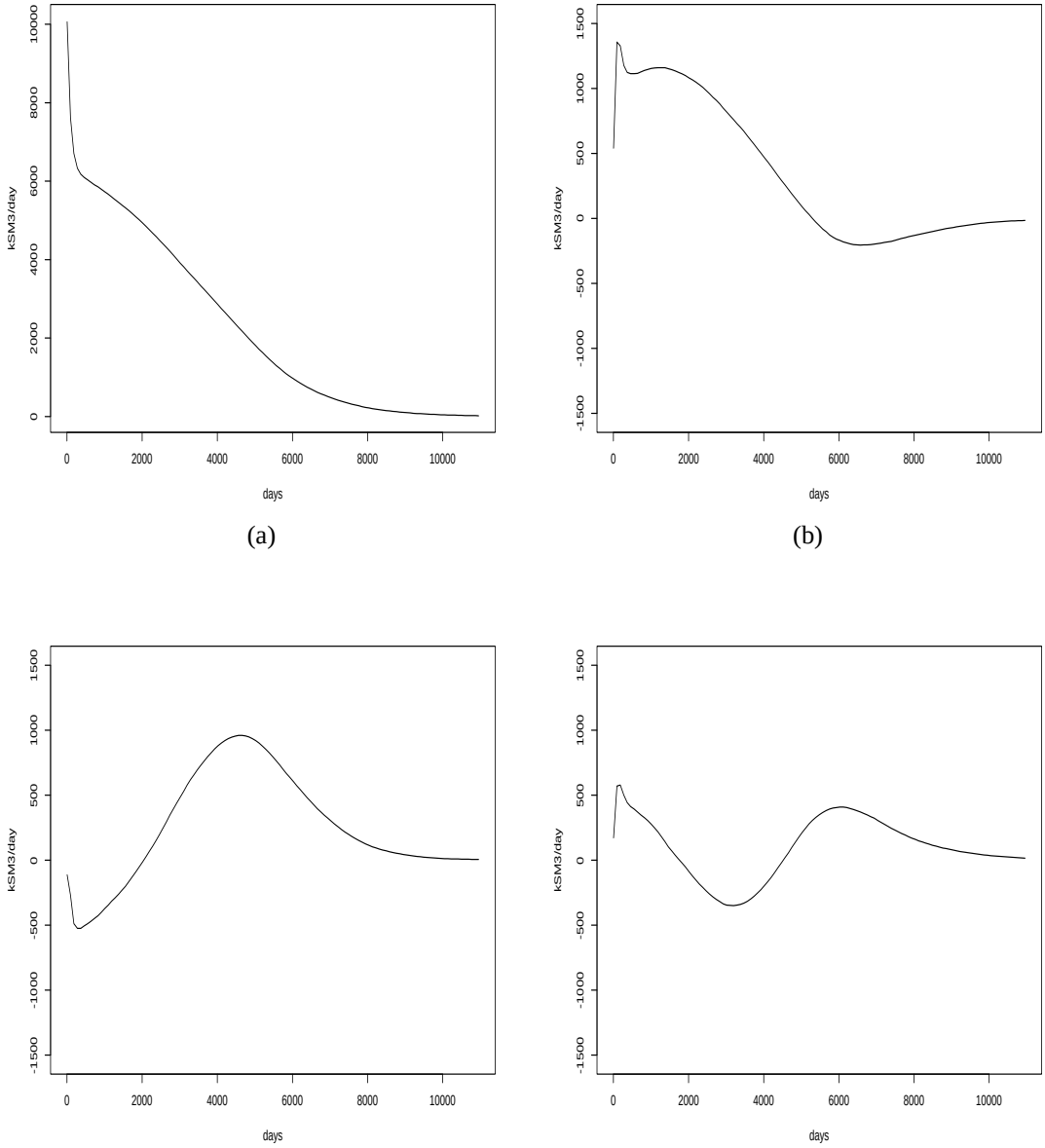

(a) (b)

(c) (d)

Figure 4: Mean and components of variability in production profile. The mean production (a); the first component (b); the second component (c); and the third component (d).

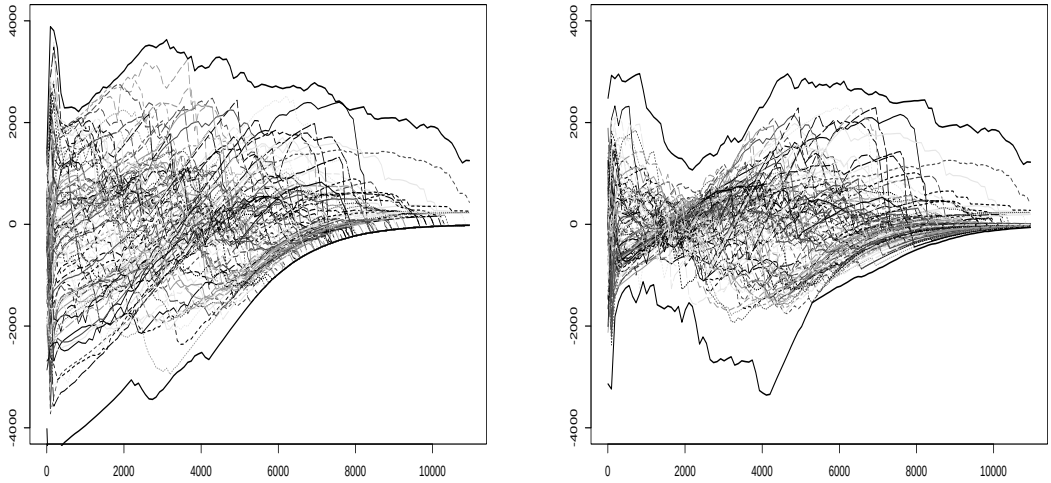

(a) (b)

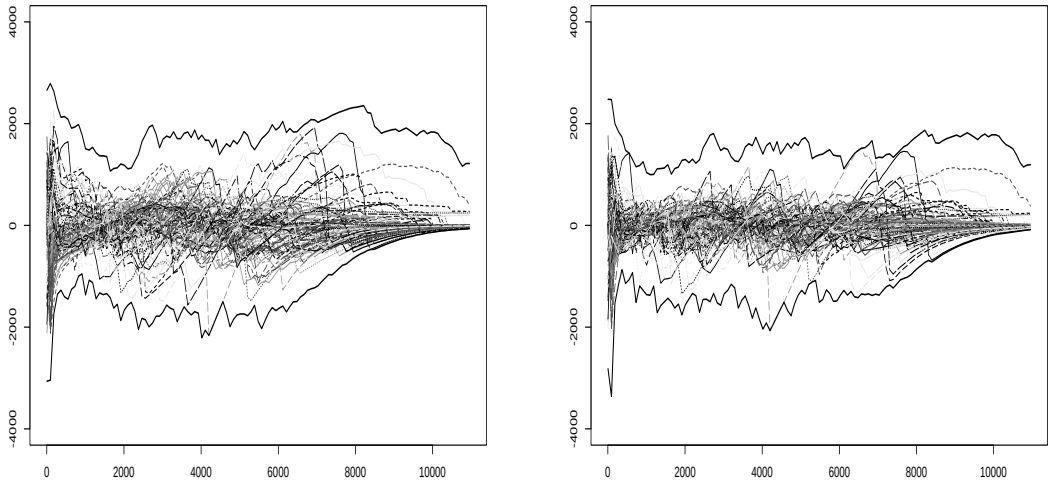

(c) (d)

Figure 5: Variability in production rate in the field. The variability in 100 production scenarios (a); the variability remaining after: the most important (b): the two most important(c); The three most important (d); components are extracted.

Table 5: Summary statistics of production variables, based on 9072 observations

Variable name	Mean	Standard deviation	Median	Minimum	Maximum
FIOP.0	54690.000	7022.392	53710.000	39860.000	70500.000
GOPT.END	24550.000	4733.821	23810.000	11620.000	38690.000
LNOPT.END	10.090	0.192	10.080	9.361	10.560
DISK.PROD.10	14770.000	2655.863	14530.000	6597.000	21790.000
ROPT.END	0.446	0.039	0.450	0.277	0.552
ROPT.PV20	0.099	0.009	0.100	0.062	0.125
GWPT.END	1510.000	378.397	1507.000	387.800	3131.000
ROWPT.END	17.040	4.416	16.260	8.917	41.020
PROD.PC1	0.000	1.000	-0.022	-3.286	2.557
PROD.PC2	0.000	1.000	0.059	-2.376	2.423
PROD.PC3	0.000	1.000	-0.079	-2.428	3.877

Table 6: The correlations of production variables exceeding 0.5 in absolute value

Variable name 1	Variable name 2	Correlation
LNOPT.END	GOPT.END	0.992
DISK.PROD.10	PROD.PC1	0.973
ROPT.END	ROPT.PV20	0.954
FIOP.0	GOPT.END	0.923
LNOPT.END	FIOP.0	0.915
GOPT.END	DISK.PROD.10	0.884
LNOPT.END	DISK.PROD.10	0.876
LNOPT.END	ROPT.PV20	0.844
LNOPT.END	ROPT.END	0.835
GOPT.END	ROPT.PV20	0.831
ROPT.END	GOPT.END	0.825
FIOP.0	DISK.PROD.10	0.824
GOPT.END	PROD.PC1	0.765
LNOPT.END	PROD.PC1	0.761
ROPT.PV20	DISK.PROD.10	0.726
FIOP.0	PROD.PC1	0.724
ROPT.END	DISK.PROD.10	0.717
ROWPT.END	GWPT.END	-0.708
ROPT.PV20	PROD.PC1	0.622
ROPT.END	PROD.PC1	0.609
FIOP.0	ROPT.PV20	0.592
LNOPT.END	PROD.PC2	0.589
GOPT.END	PROD.PC2	0.582
FIOP.0	PROD.PC2	0.551
FIOP.0	ROPT.END	0.550

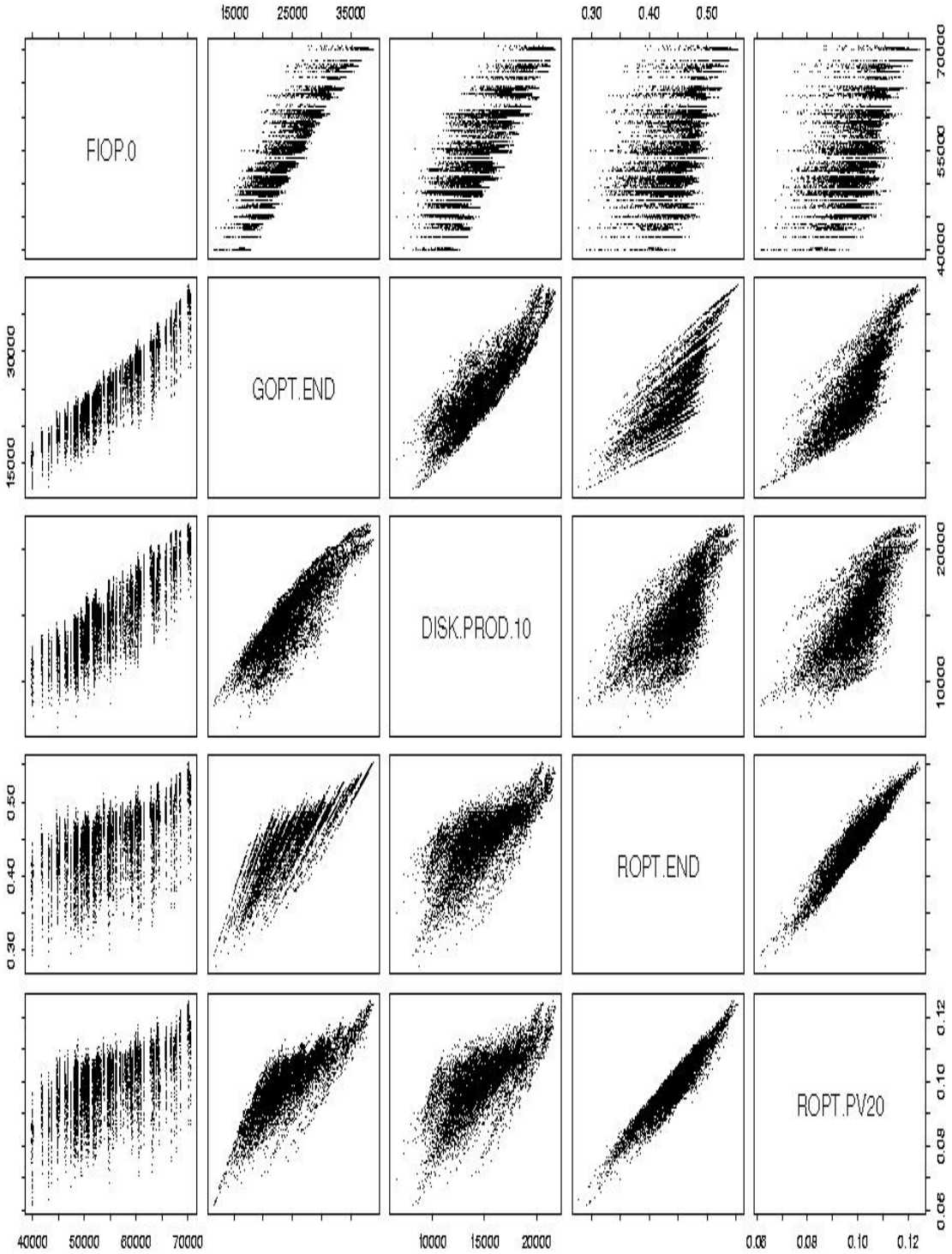

Figure 6: Scatter plot of variables related to oil production and recovery. Each entry in the matrix of scatter plots is the scatter plot of the two variables on the corresponding diagonal elements, the matrix is symmetric. The description of the variables is given in Table 4.

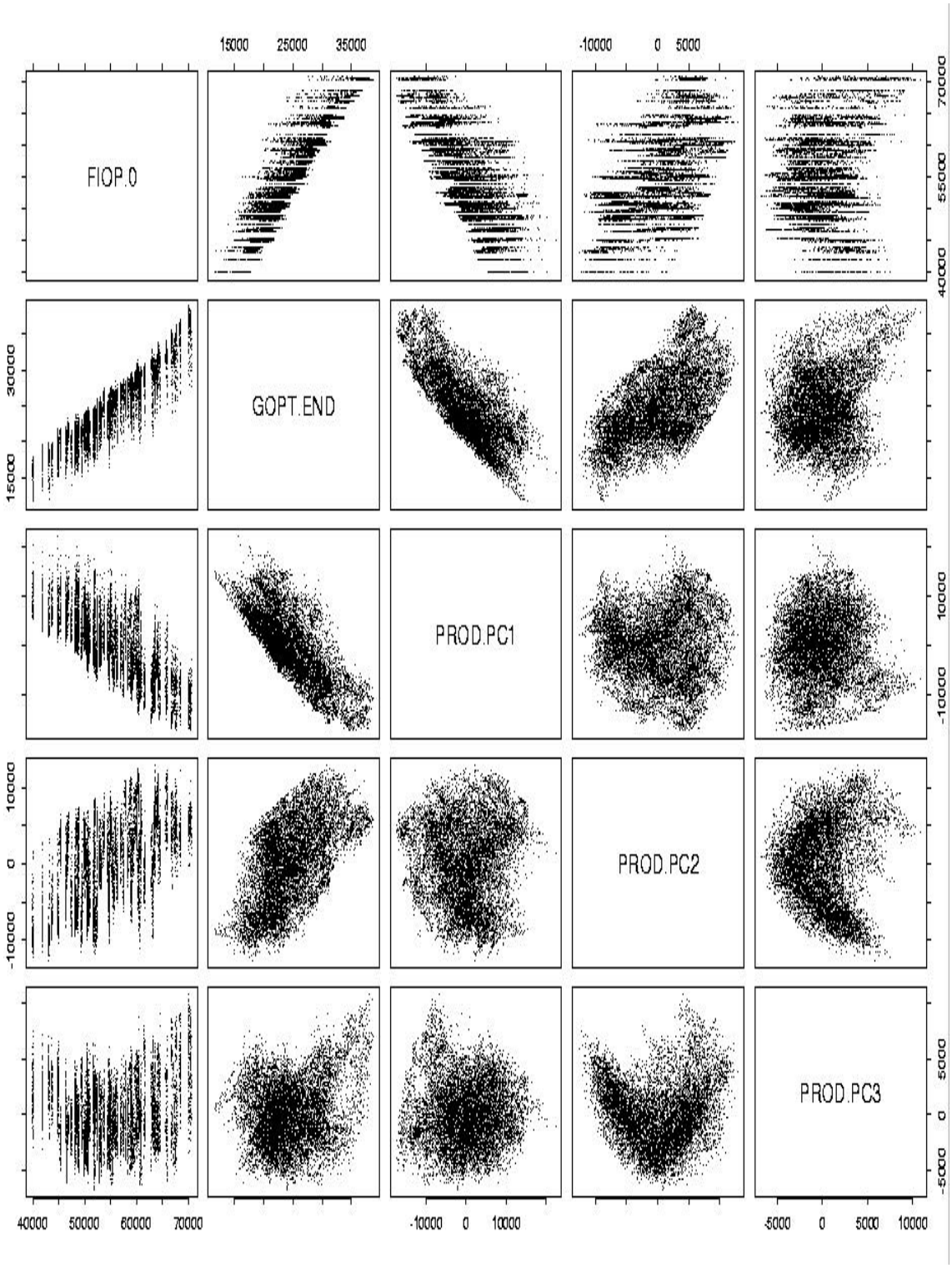

Figure 7: Scatter plot of variables related to oil production and production components. Each entry in the matrix of scatter plots is the scatter plot of the two variables on the corresponding diagonal elements, the matrix is symmetric. The description of the variables is given in Table 4.

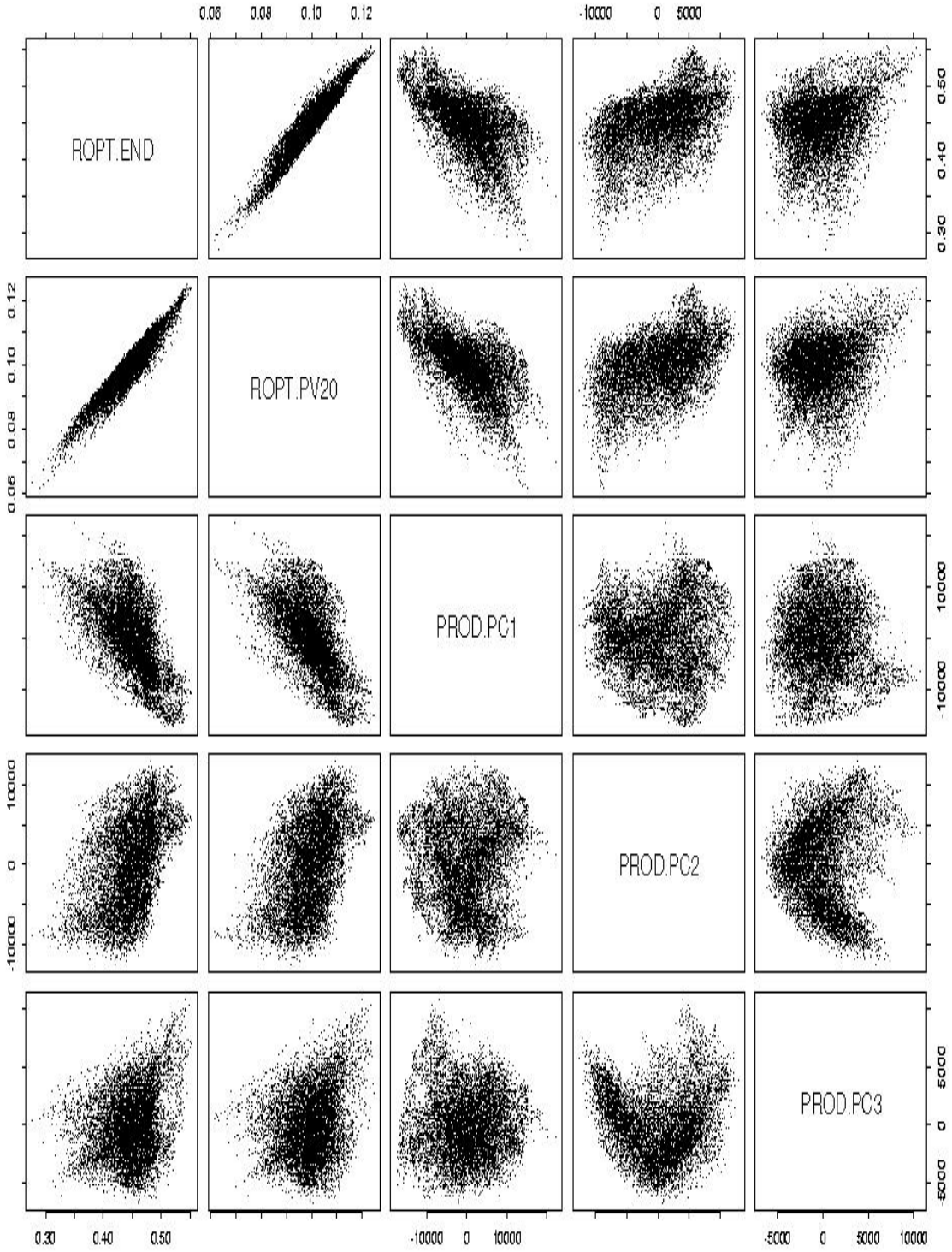

Figure 8: Scatter plot of variables related to recovery and production components. Each entry in the matrix of scatter plots is the scatter plot of the two variables on the corresponding diagonal elements, the matrix is symmetric. The description of the variables is given in Table 4.

The distribution of the production variables given design parameters are illustrated by boxplots. A standard boxplot indicate median, quartiles and extreme values. The event that a sample lie more than 1.5 interquartile range away from the median is considered as extreme, if this is the case for one or several samples, the box plot indicate the limit of 1.5 interquartile range, the samples further away are marked individually.

In Figure 9 through 19 the production variables are broken down by parameters in the fault design and in the production strategy. The subfigures (a), (b), and (c) correspond to the fault structures a, b and c. In each subfigure the first four boxplots are for PDO a, the next four for PDO b, next four PDO c, and last four for PDO u. In the four boxplots having the same fault structure and PDO, the fault density ranges from fully faulted to none faulting. The unfaulted model is identical for all three fault structures. Note that PDO's are designed for the fault structures, i.e. a to a, b to b, c to c, hence in Figures 9 through 19 the set of boxplots having a match between PDO and fault structure are special. The design variables that are not used in the split, i.e. fault permeability predictor,aggradation angle, progradation direction,barrier coverage, and curvature, each vary at three levels. Each boxplot contain values that correspond to all combinations of levels in these five variables hence, there are 243 values underlying each boxplot. The exception is the boxplots that correspond to an unfaulted model, for which the fault permeability predictor do not influence the results hence, each plot contain only 81 values.

In Figure 20 through 30 the production variables are broken down by parameters in the geological design. The design variables are curvature, aggradation angle and progradation direction. In the subfigures (a), (b), and (c), the curvature changes from no curvature in subfigure (a); single lobe in subfigure (b); and double lobe in subfigure (c). The aggradation angle is assigned to three levels, see Section 2, where the three first, three next and three last boxplots in a subfigure have different levels of aggradation angle. In the three box plots having identical curvature and aggradation angle, the progradation direction is 90^o, 180^o and 270^o. The design variables, barrier coverage, fault structure, fault density, fault permeability predictor, and PDO are not used in the split. Each boxplot contain values that correspond to all combinations of the levels in these five variables resulting in $3 \cdot (3^3 + 1) \cdot 4 = 336$ values underlying each boxplot.

Note that Figures 9 through 30 illustrate the results in the current experiment and that the outcome is dependent on the experimental design, it can only be interpreted in the context of the SAIGUP project. That is if parameters that are fixed throughout the SAIGUP project are altered the distributions in Figures 9 through 30 will no longer be valid, with respect to spread and centring. A basic assumption underlying the analysis is however that the general trends found in the figures are representative for real reservoirs. The figures are commented together with the result of the analysis in Section 7.

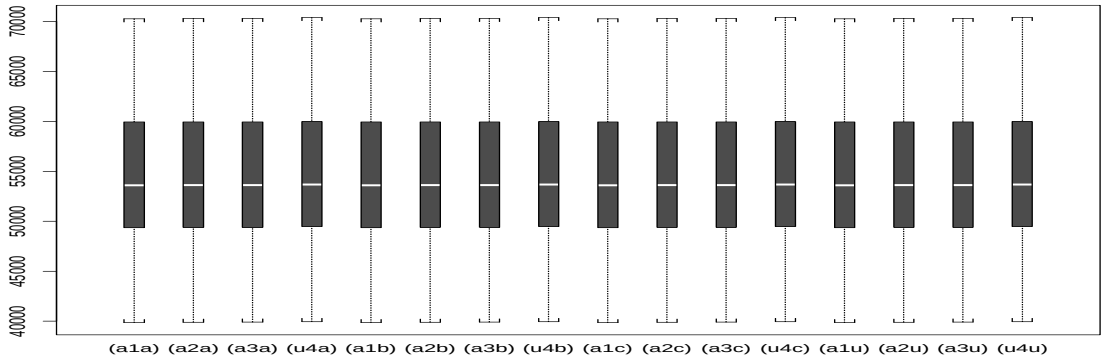

(a)

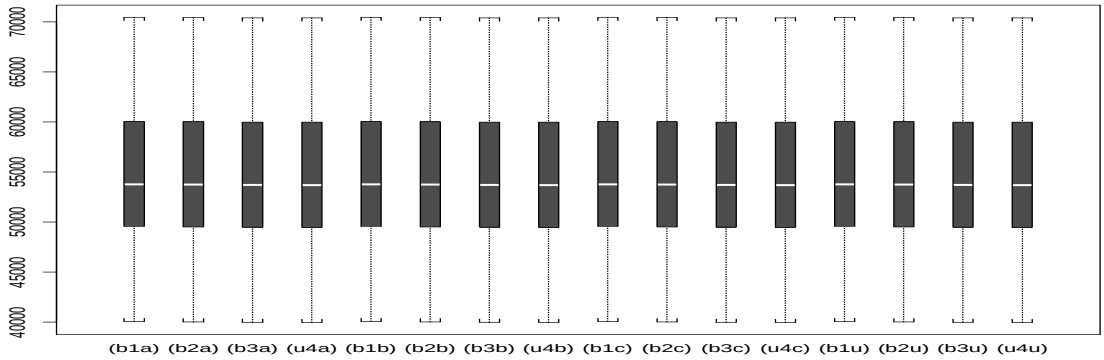

(b)

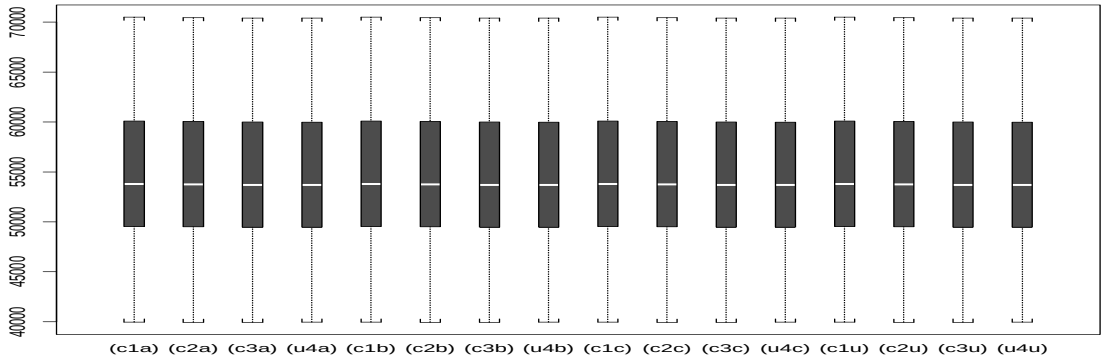

(c)

Figure 9: Oil in place by fault structure, fault density and PDO. Fault structure a, b and c are displayed in the corresponding figures. In each figure the first four boxplots are for PDO a, the next four for PDO b, next four PDO c, and last four for PDO u. In the four boxplots having the same fault structure and PDO, the fault density ranges from fully faulted to none faulting, i.e. 1 trough 4. The unfaulted model is identical for all three fault structures. The data in each boxplot correspond to assigning the three different fault permeability predictors to each of the 81 geological models. All boxplots are identical in this case.

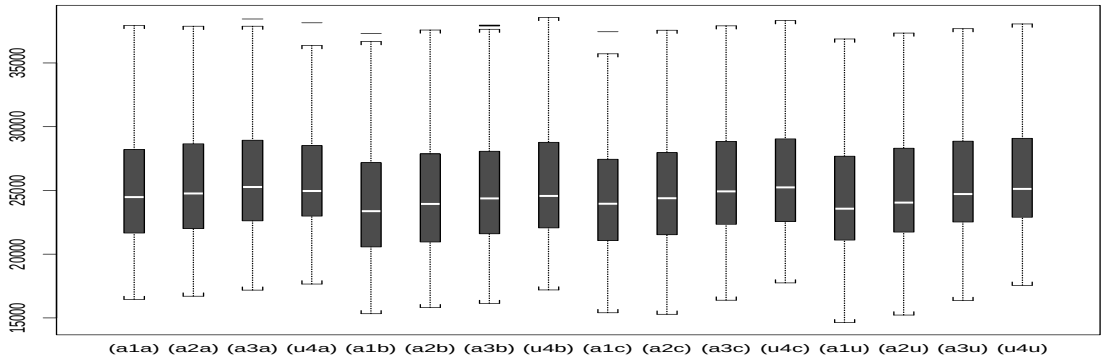

(a)

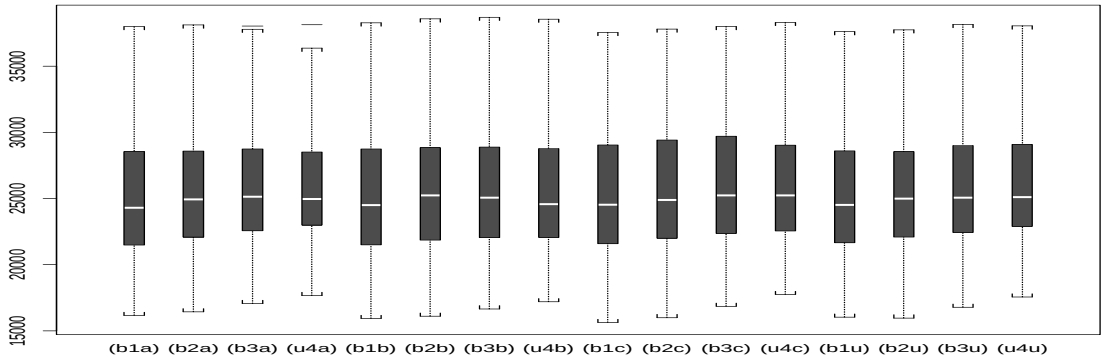

(b)

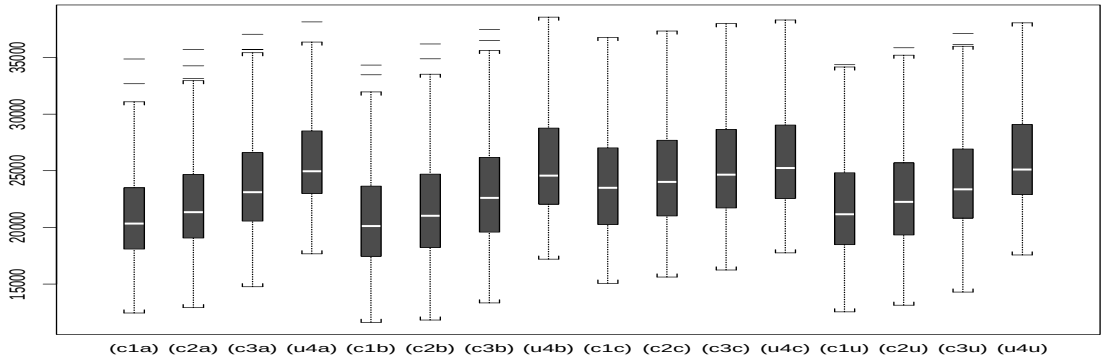

(c)

Figure 10: Total oil production by fault structure, fault density and PDO. Fault structure a, b and c are displayed in the corresponding figures. In each figure the first four boxplots are for PDO a, the next four for PDO b, next four PDO c, and last four for PDO u. In the four boxplots having the same fault structure and PDO, the fault density ranges from fully faulted to none faulting, i.e. 1 through 4. The unfaulted model is identical for all three fault structures. The data in each boxplot correspond to assigning the three different fault permeability predictors to each of the 81 geological models.

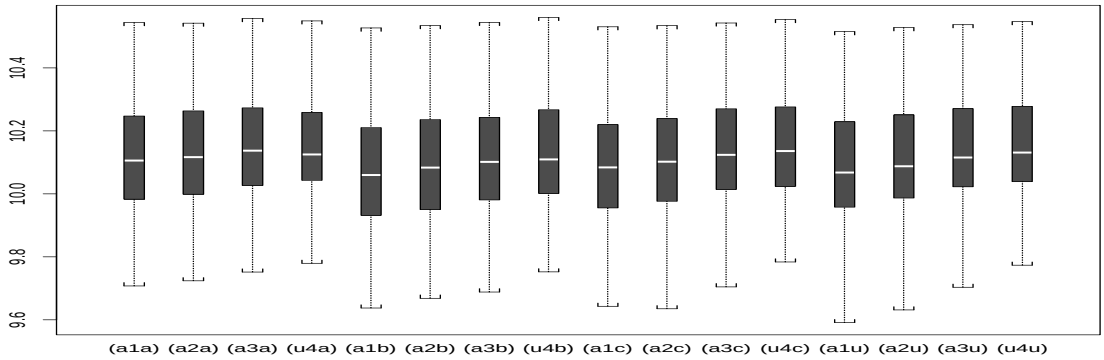

(a)

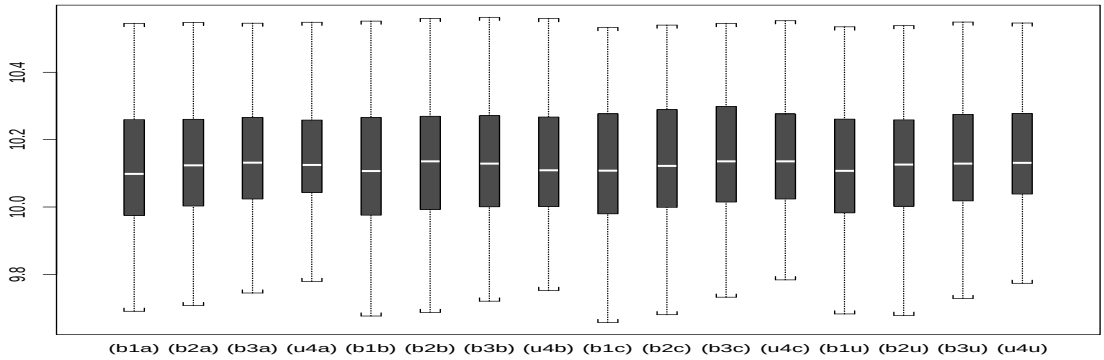

(b)

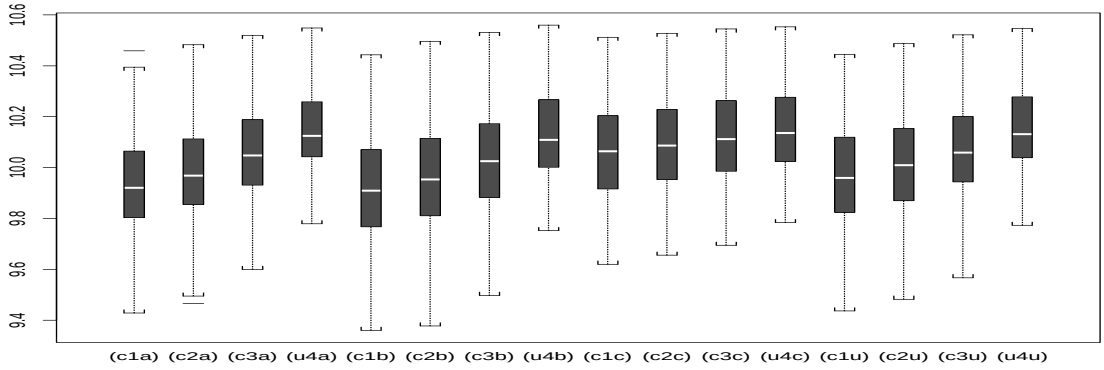

(c)

Figure 11: Logarithm of total oil production by fault structure, fault density and PDO. Fault structure a, b and c are displayed in the corresponding figures. In each figure the first four boxplots are for PDO a, the next four for PDO b, next four PDO c, and last four for PDO u. In the four boxplots having the same fault structure and PDO, the fault density ranges from fully faulted to none faulting, i.e. 1 through 4. The unfaulted model is identical for all three fault structures. The data in each boxplot correspond to assigning the three different fault permeability predictors to each of the 81 geological models.

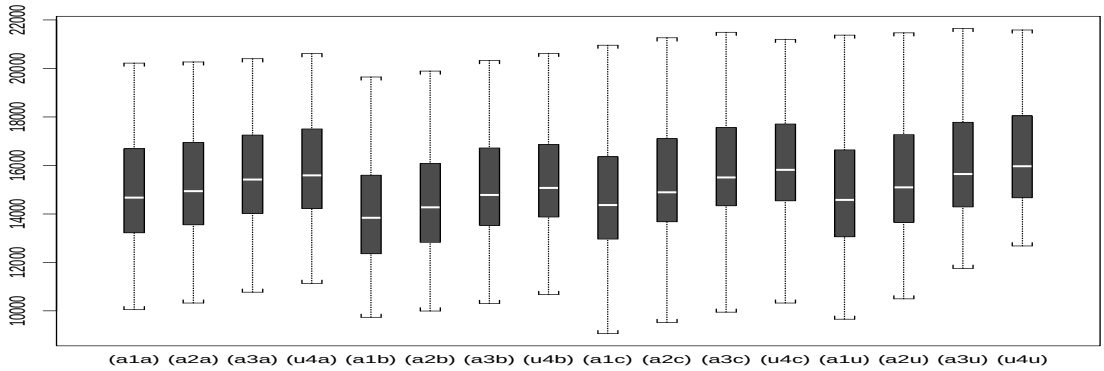

(a)

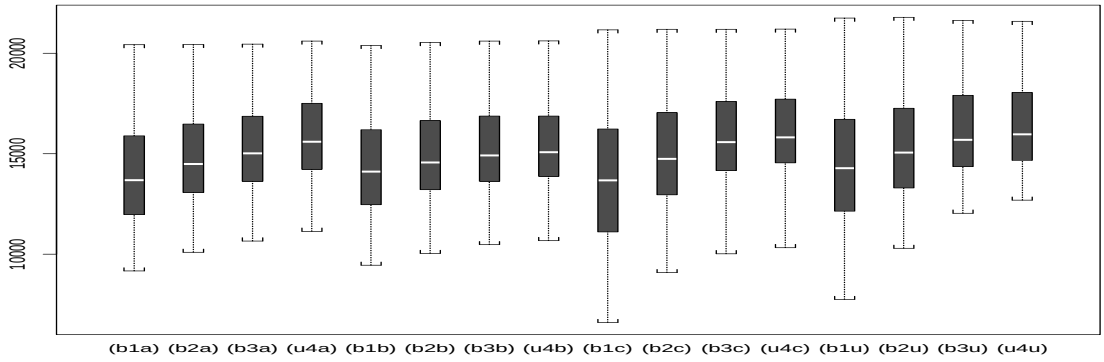

(b)

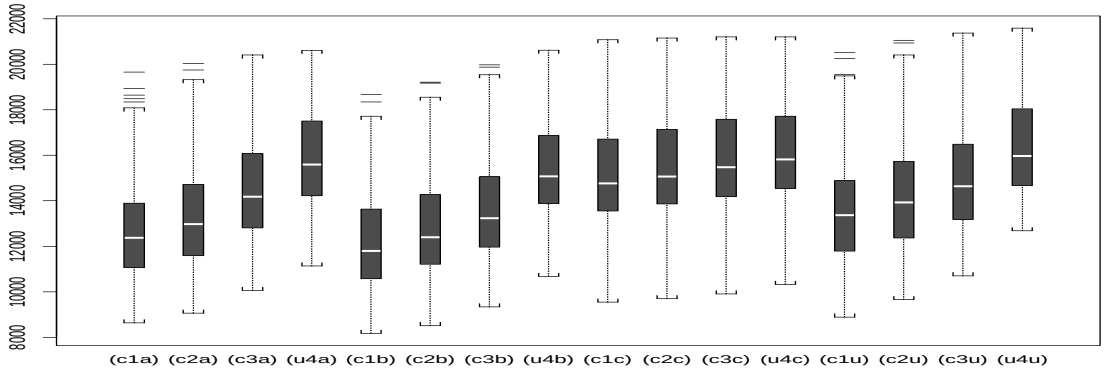

(c)

Figure 12: Discounted oil production by fault structure, fault density and PDO. Fault structure a, b and c are displayed in the corresponding figures. In each figure the first four boxplots are for PDO a, the next four for PDO b, next four PDO c, and last four for PDO u. In the four boxplots having the same fault structure and PDO, the fault density ranges from fully faulted to none faulting, i.e. 1 through 4. The unfaulted model is identical for all three fault structures. The data in each boxplot correspond to assigning the three different fault permeability predictors to each of the 81 geological models.

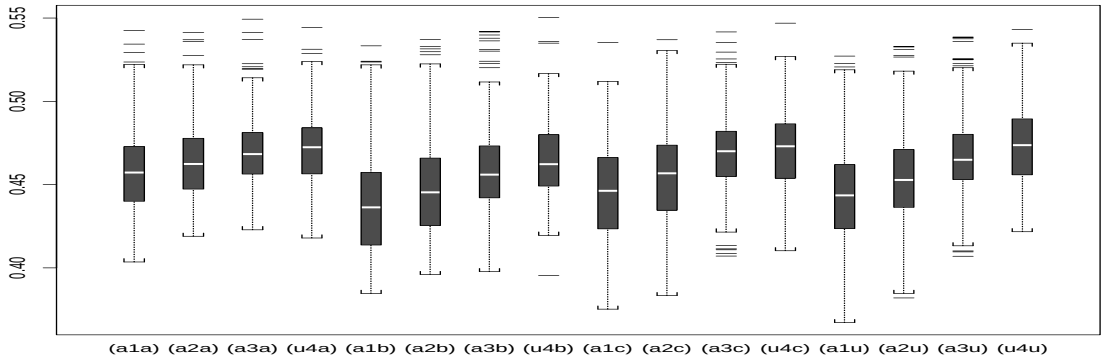

(a)

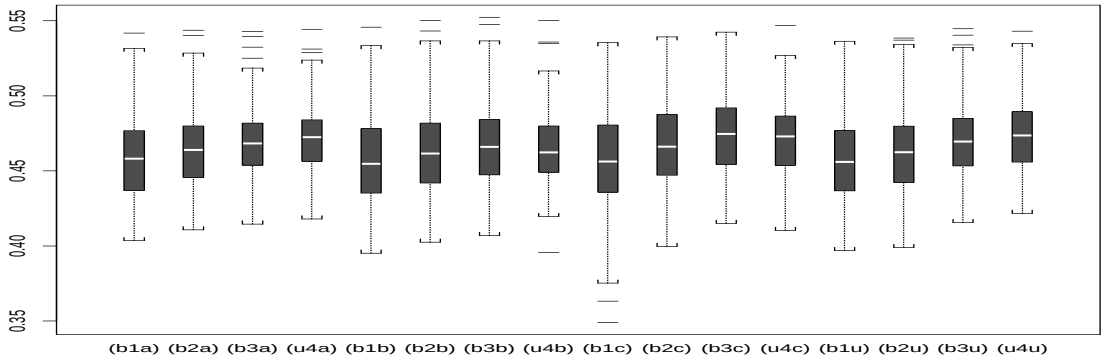

(b)

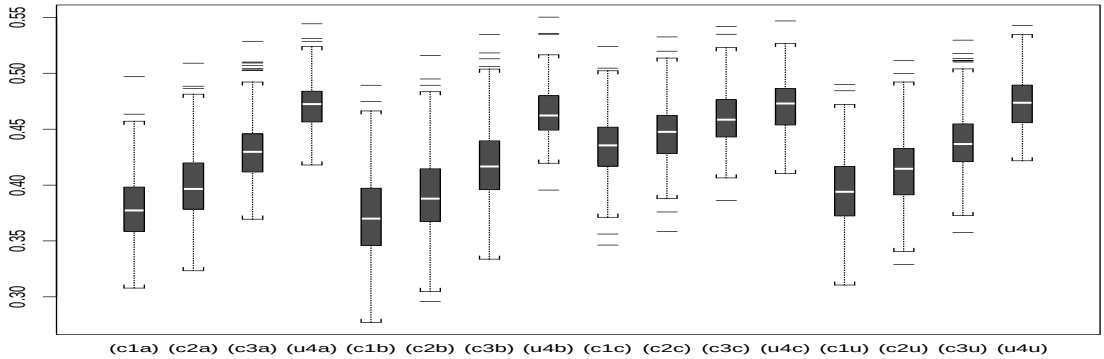

(c)

Figure 13: Recovery factor by fault structure, fault density and PDO. Fault structure a, b and c are displayed in the corresponding figures. In each figure the first four boxplots are for PDO a, the next four for PDO b, next four PDO c, and last four for PDO u. In the four boxplots having the same fault structure and PDO, the fault density ranges from fully faulted to none faulting, i.e. 1 through 4. The unfaulted model is identical for all three fault structures. The data in each boxplot correspond to assigning the three different fault permeability predictors to each of the 81 geological models.

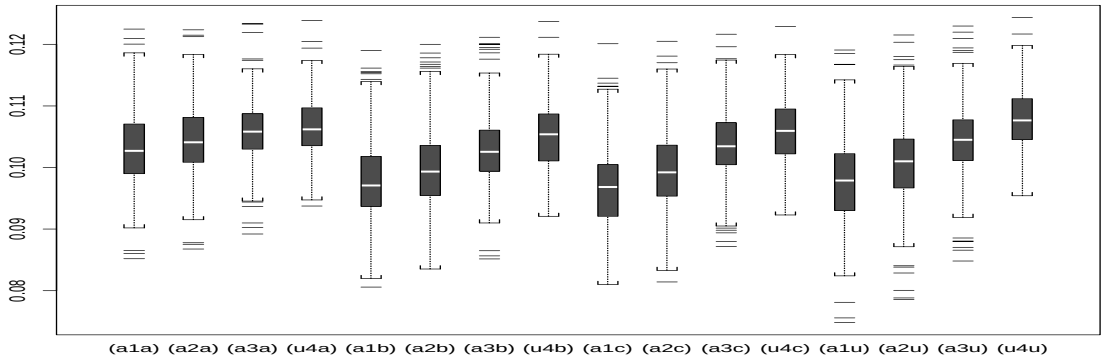

(a)

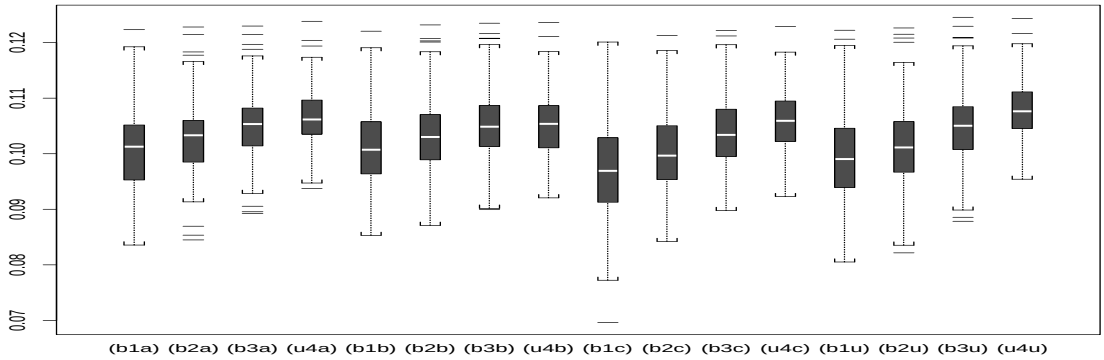

(b)

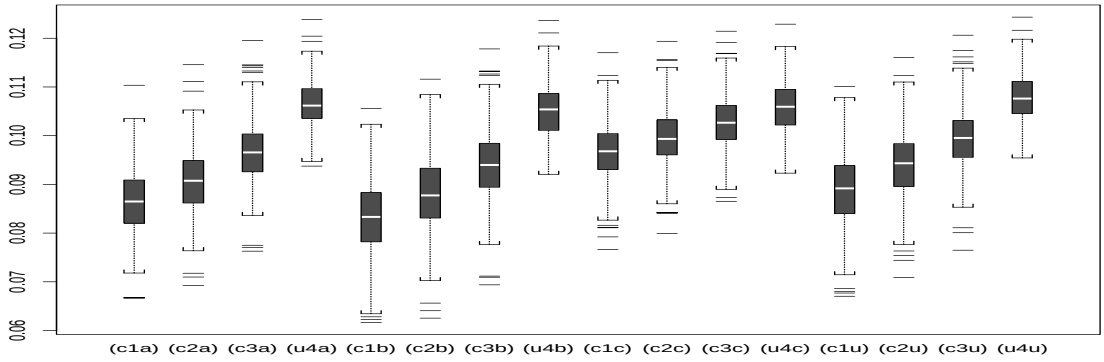

(c)

Figure 14: Recovery factor at 20% water injection by fault structure, fault density and PDO. Fault structure a, b and c are displayed in the corresponding figures. In each figure the first four boxplots are for PDO a, the next four for PDO b, next four PDO c, and last four for PDO u. In the four boxplots having the same fault structure and PDO, the fault density ranges from fully faulted to none faulting, i.e. 1 through 4. The unfaulted model is identical for all three fault structures. The data in each boxplot correspond to assigning the three different fault permeability predictors to each of the 81 geological models.

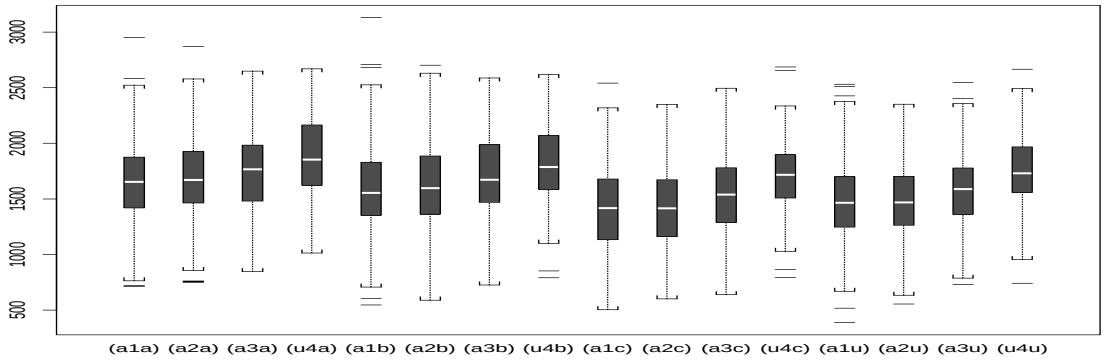

(a)

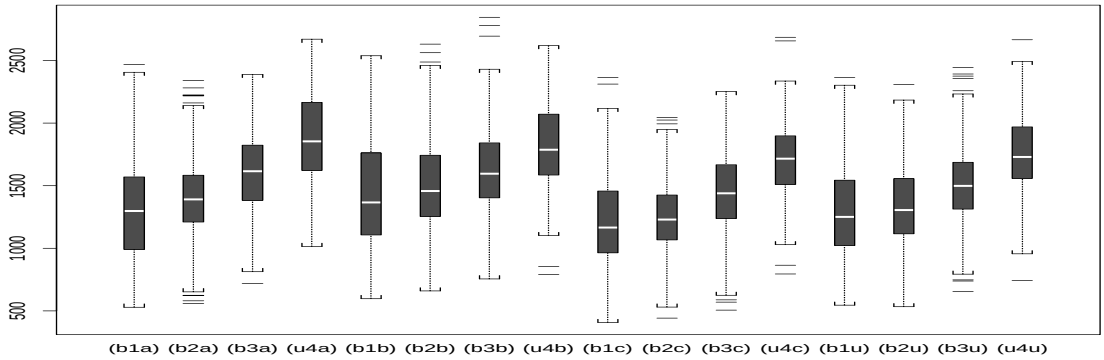

(b)

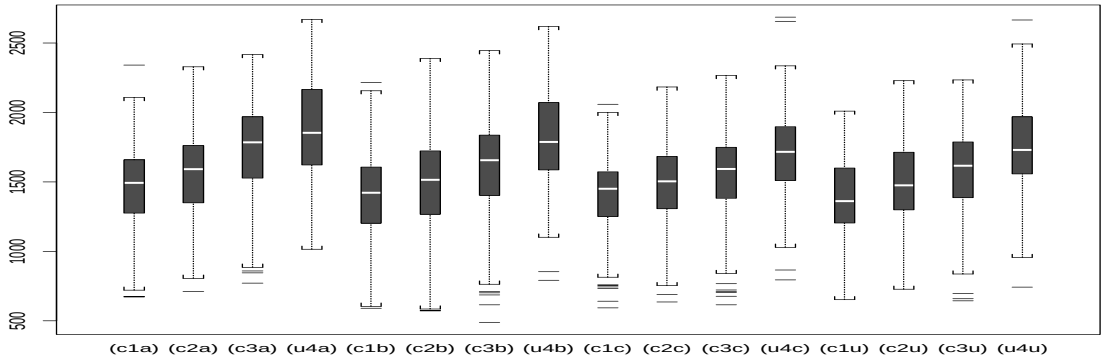

(c)

Figure 15: Total water production by fault structure, fault density and PDO. Fault structure a, b and c are displayed in the corresponding figures. In each figure the first four boxplots are for PDO a, the next four for PDO b, next four PDO c, and last four for PDO u. In the four boxplots having the same fault structure and PDO, the fault density ranges from fully faulted to none faulting, i.e. 1 through 4. The unfaulted model is identical for all three fault structures. The data in each boxplot correspond to assigning the three different fault permeability predictors to each of the 81 geological models.

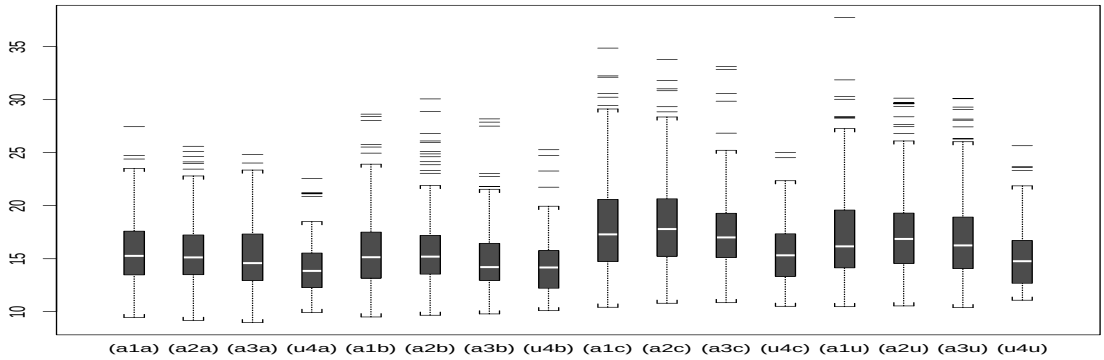

(a)

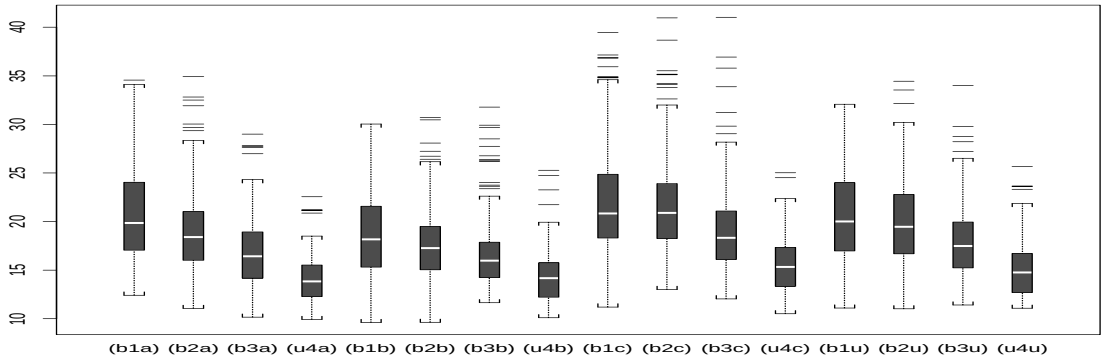

(b)

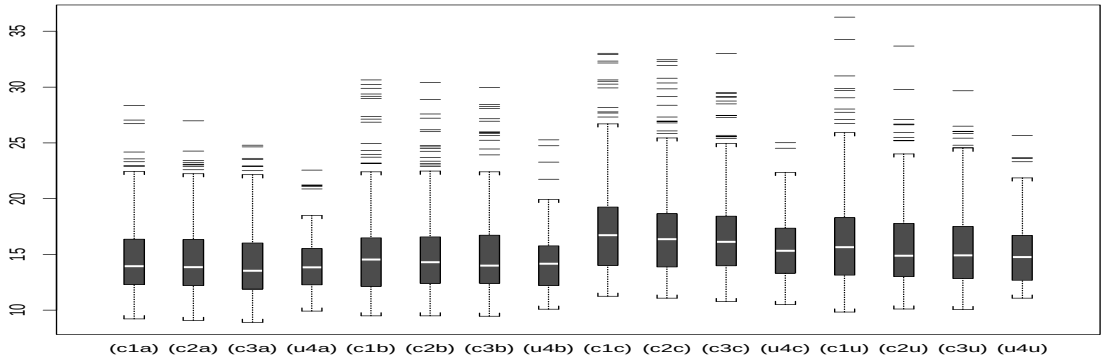

(c)

Figure 16: Ratio of oil/water production by fault structure, fault density and PDO. Fault structure a, b and c are displayed in the corresponding figures. In each figure the first four boxplots are for PDO a, the next four for PDO b, next four PDO c, and last four for PDO u. In the four boxplots having the same fault structure and PDO, the fault density ranges from fully faulted to none faulting, i.e. 1 through 4. The unfaulted model is identical for all three fault structures. The data in each boxplot correspond to assigning the three different fault permeability predictors to each of the 81 geological models.

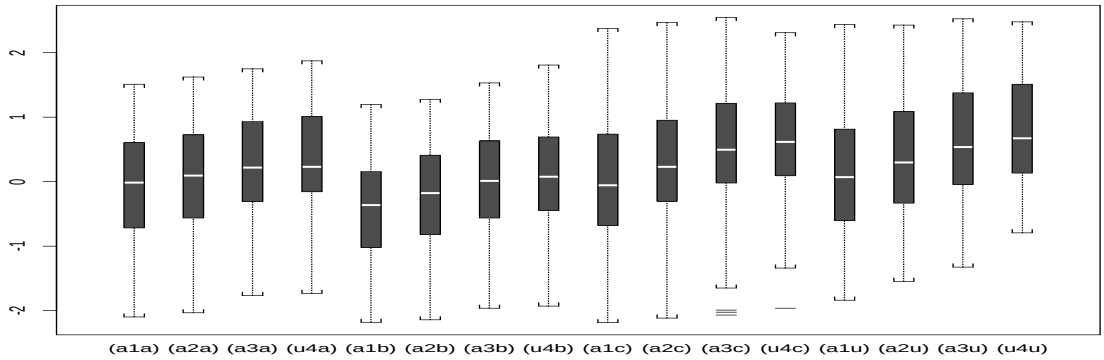

(a)

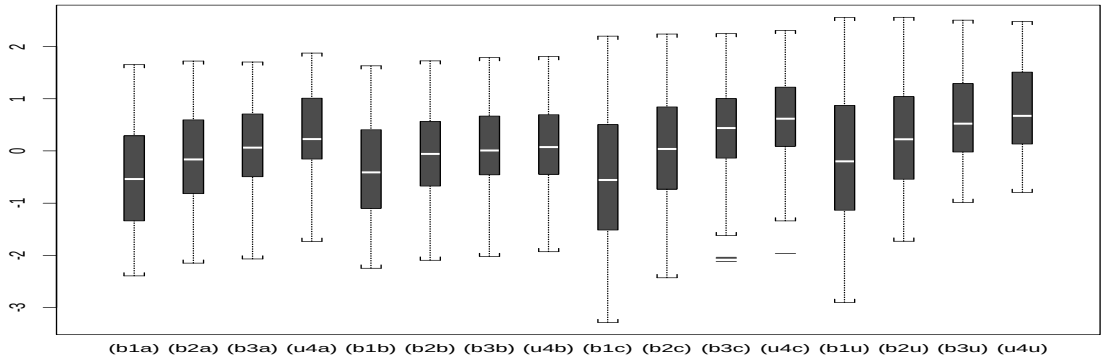

(b)

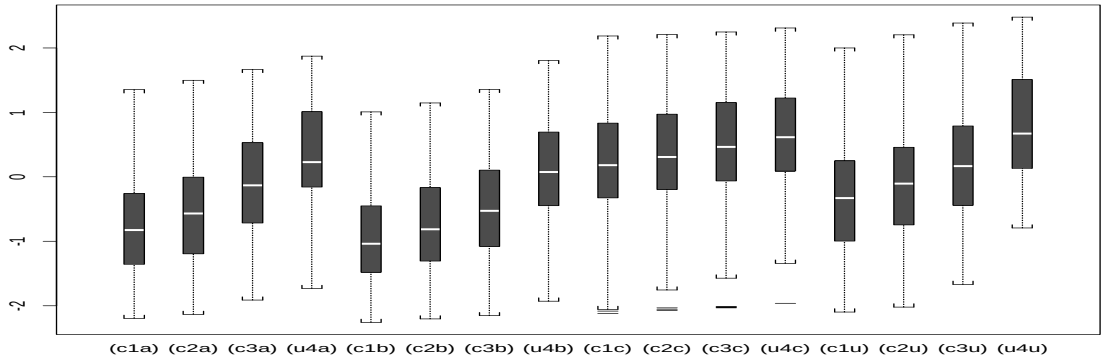

(c)

Figure 17: First component of variability by fault structure, fault density and PDO. Fault structure a, b and c are displayed in the corresponding figures. In each figure the first four boxplots are for PDO a, the next four for PDO b, next four PDO c, and last four for PDO u. In the four boxplots having the same fault structure and PDO, the fault density ranges from fully faulted to none faulting, i.e. 1 through 4. The unfaulted model is identical for all three fault structures. The data in each boxplot correspond to assigning the three different fault permeability predictors to each of the 81 geological models.

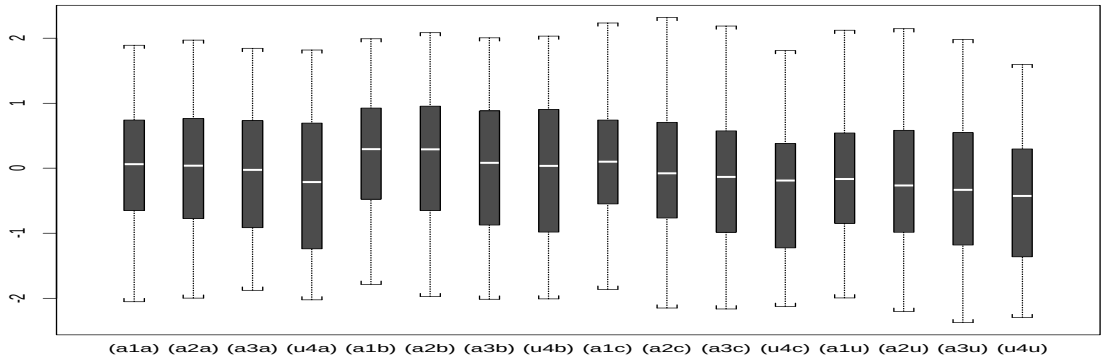

(a)

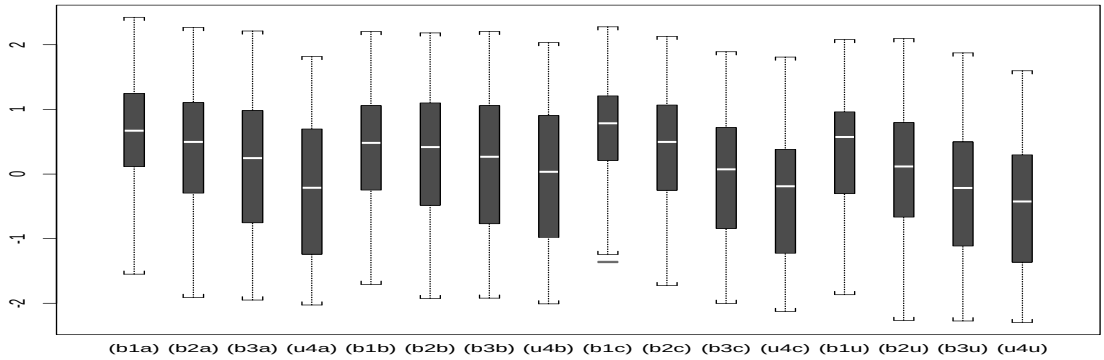

(b)

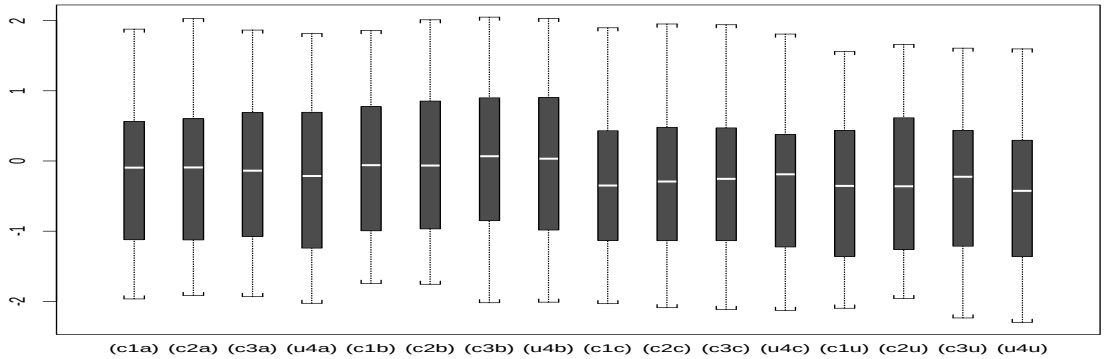

(c)

Figure 18: Second component of variability by fault structure, fault density and PDO. Fault structure a, b and c are displayed in the corresponding figures. In each figure the first four boxplots are for PDO a, the next four for PDO b, next four PDO c, and last four for PDO u. In the four boxplots having the same fault structure and PDO, the fault density ranges from fully faulted to none faulting, i.e. 1 through 4. The unfaulted model is identical for all three fault structures. The data in each boxplot correspond to assigning the three different fault permeability predictors to each of the 81 geological models.

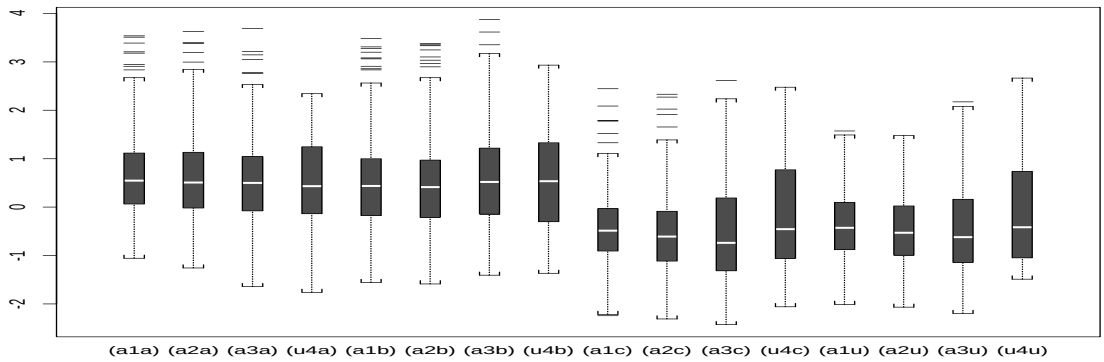

(a)

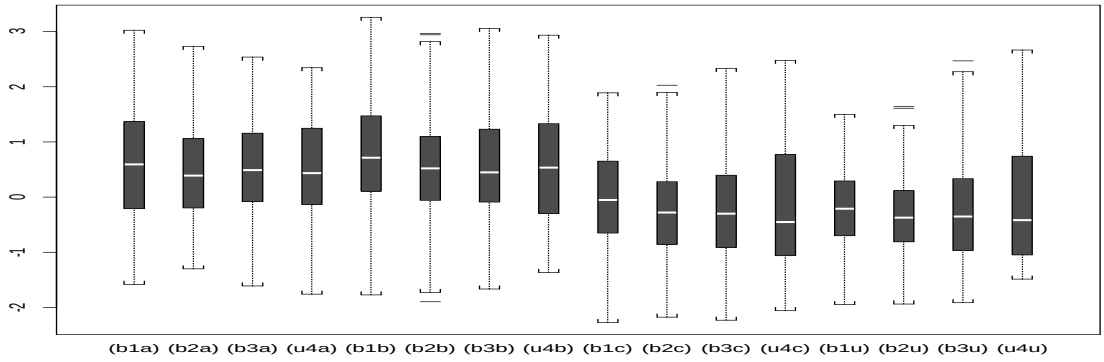

(b)

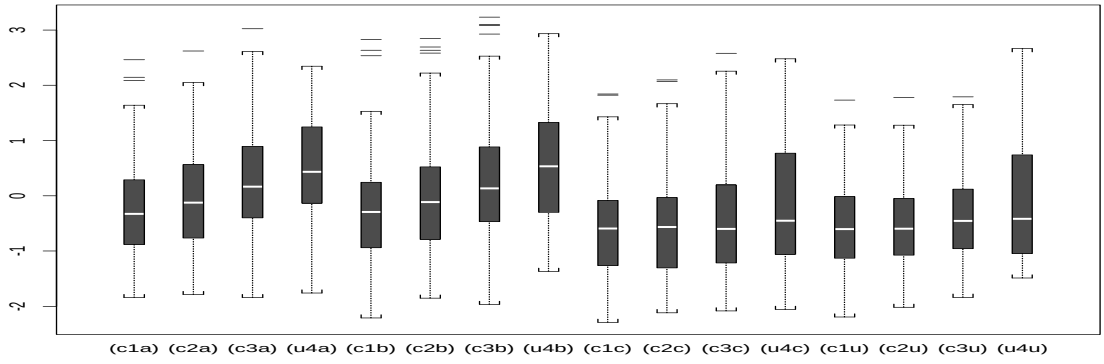

(c)

Figure 19: Third component of variability by fault structure, fault density and PDO. Fault structure a, b and c are displayed in the corresponding figures. In each figure the first four boxplots are for PDO a, the next four for PDO b, next four PDO c, and last four for PDO u. In the four boxplots having the same fault structure and PDO, the fault density ranges from fully faulted to none faulting, i.e. 1 through 4. The unfaulted model is identical for all three fault structures. The data in each boxplot correspond to assigning the three different fault permeability predictors to each of the 81 geological models.

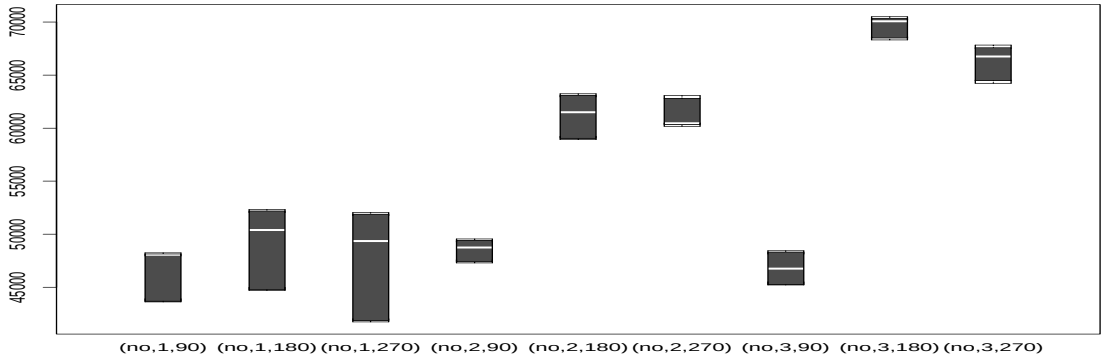

(a)

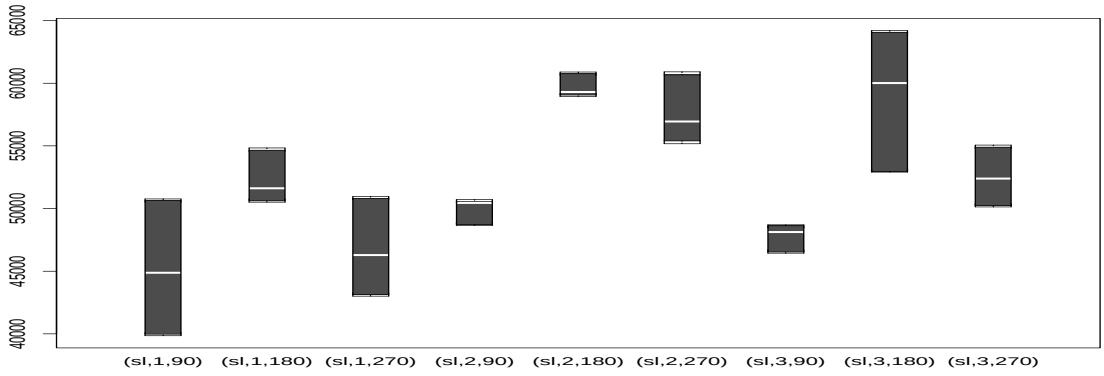

(b)

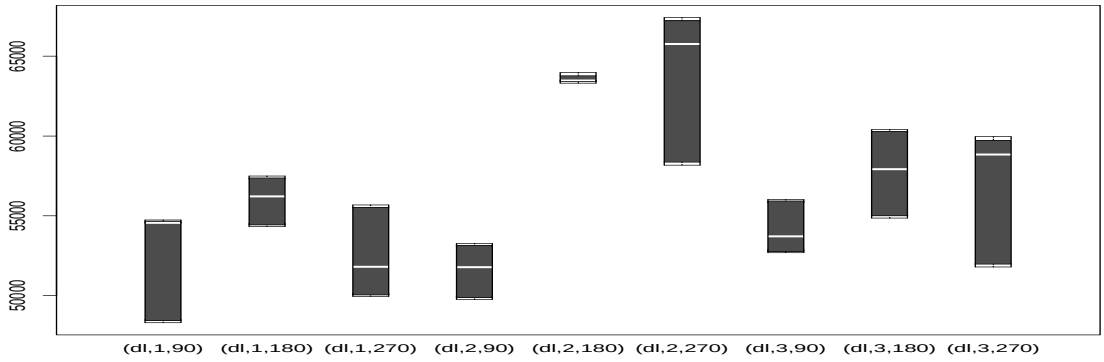

(c)

Figure 20: Oil in place by curvature, aggradation angle and progradation direction. The curvature is no curvature (a); single lobe (b); and double lobe (c). The aggradation angle is on three levels, see Section 2 , and the progradation angle is 90, 180 and 270. The data in each boxplot correspond to assign the barriers at three different levels PDO's at four levels for all 28 fault models. For oil in place PDO and fault structure have no effect hence there is essentially only 3 observations in each boxplot.

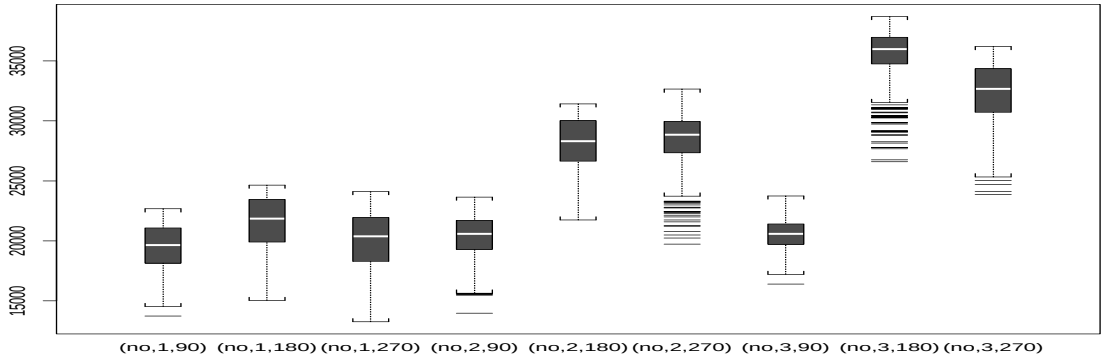

(a)

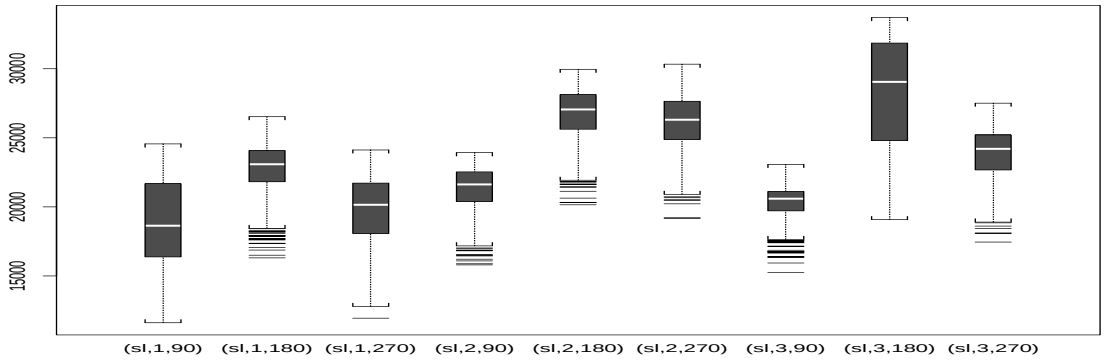

(b)

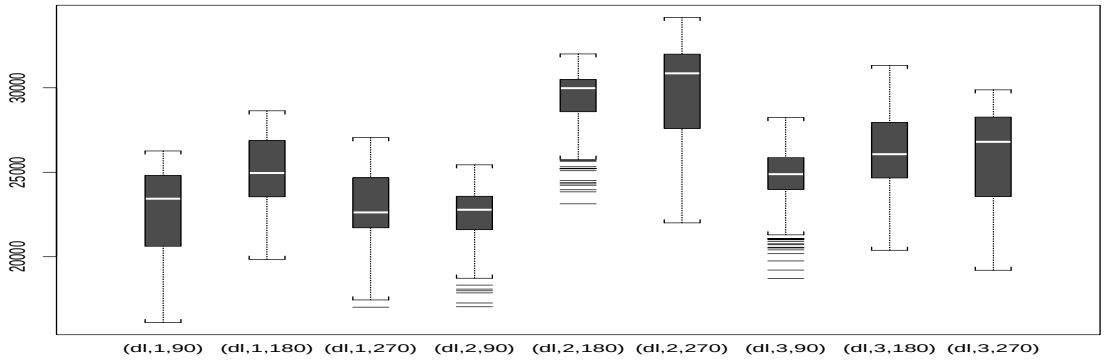

(c)

Figure 21: Total oil production by curvature, aggradation angle and progradation direction. The curvature is no curvature (a); single lobe (b); and double lobe (c). The aggradation angle is on three levels, see Section 2 , and the progradation angle is 90, 180 and 270. There are 336 observations in each boxplot.

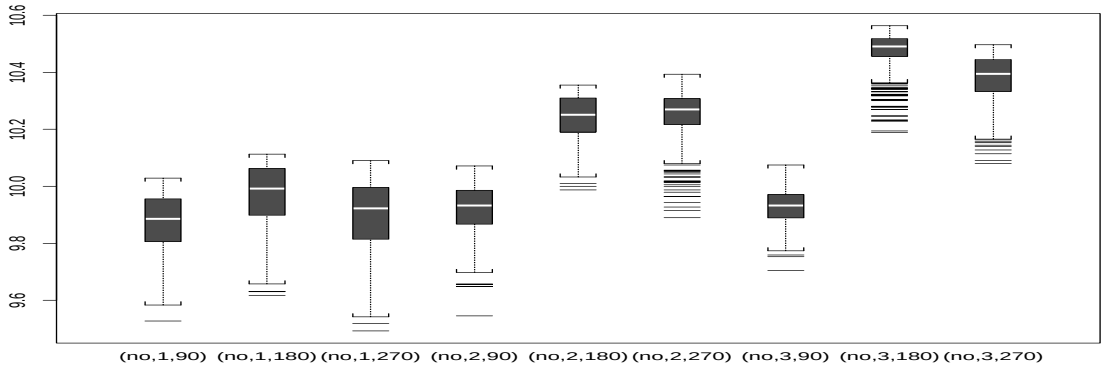

(a)

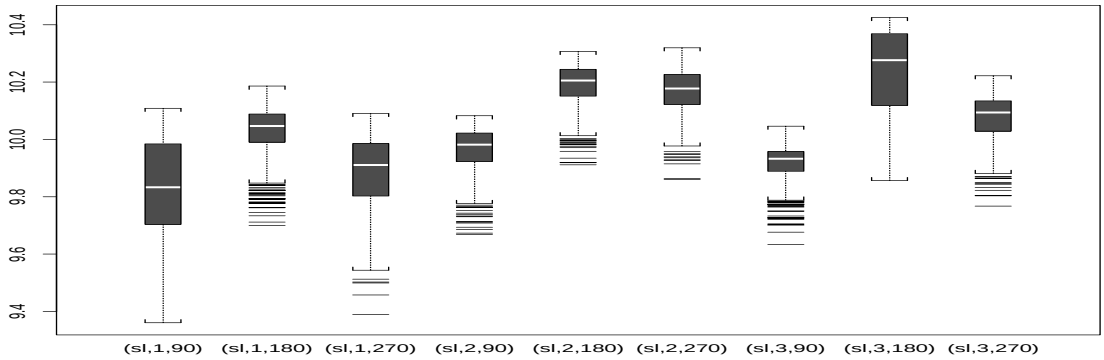

(b)

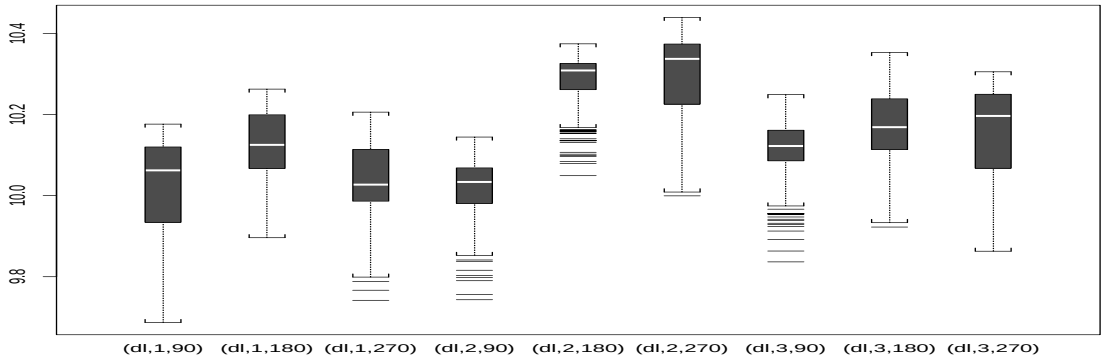

(c)

Figure 22: Logarithm of total oil production by curvature, aggradation angle and progradation direction. The curvature is no curvature (a); single lobe (b); and double lobe (c). The aggradation angle is on three levels, see Section 2 , and the progradation angle is 90, 180 and 270. There are 336 observations in each boxplot.

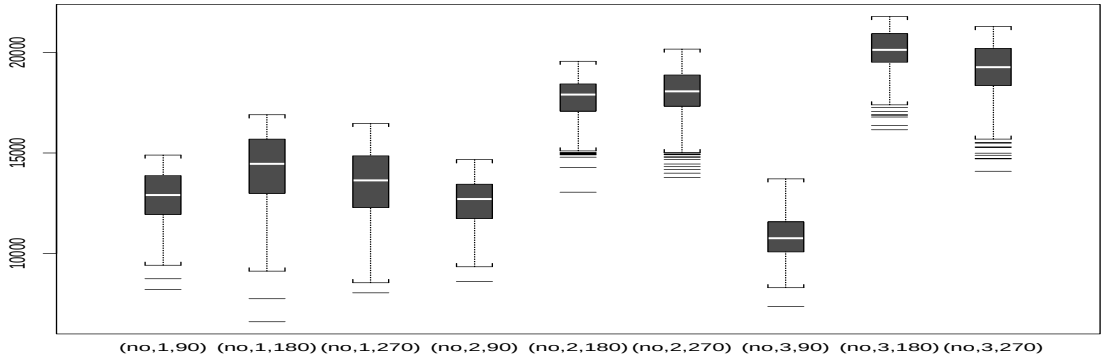

(a)

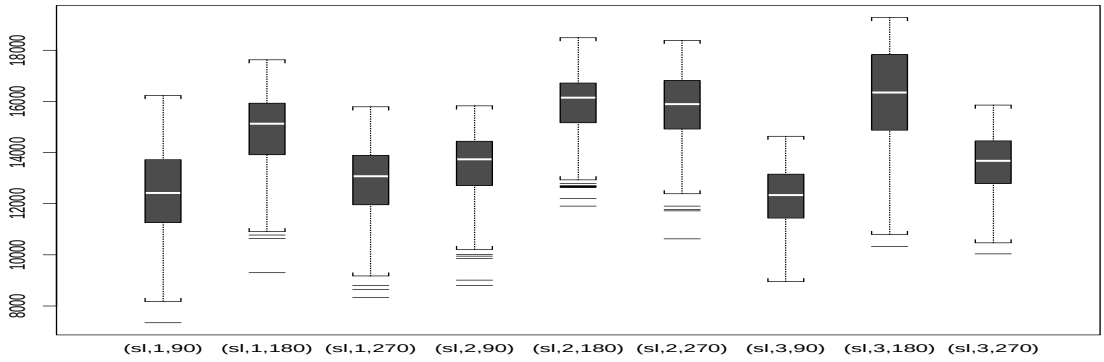

(b)

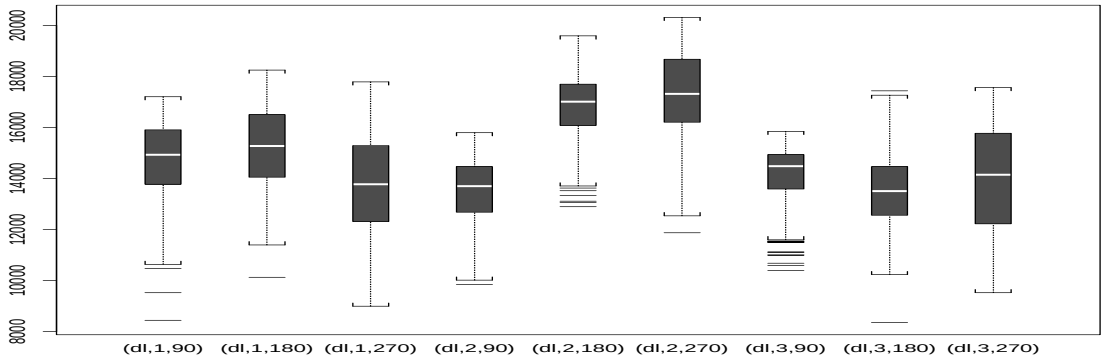

(c)

Figure 23: Discounted oil production by curvature, aggradation angle and progradation direction. The curvature is no curvature (a); single lobe (b); and double lobe (c). The aggradation angle is on three levels, see Section 2 , and the progradation angle is 90, 180 and 270. There are 336 observations in each boxplot.

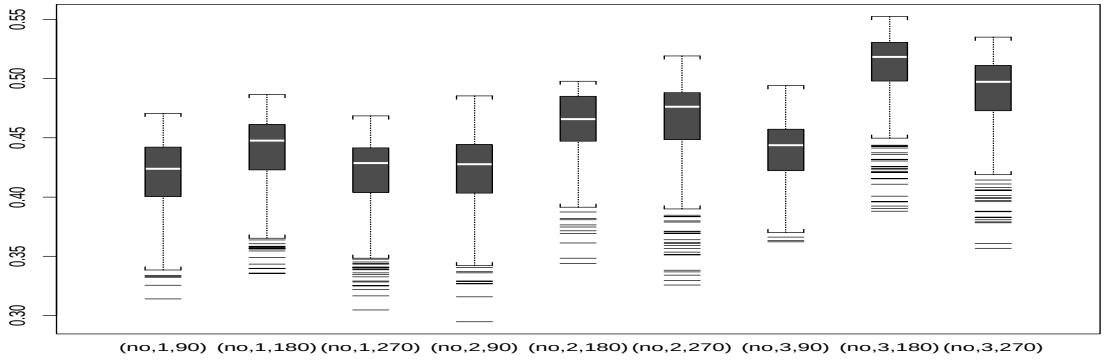

(a)

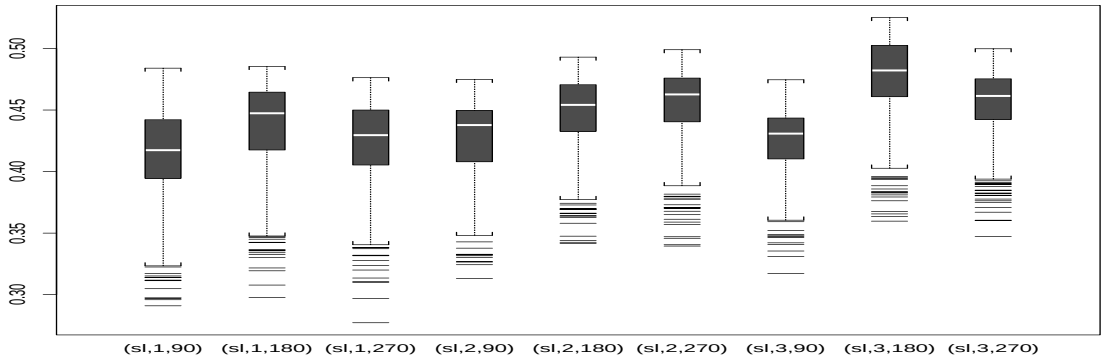

(b)

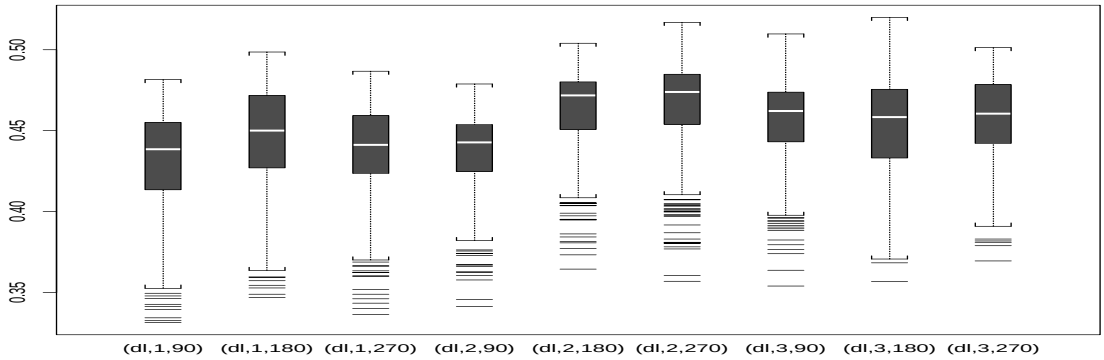

(c)

Figure 24: Recovery factor by curvature, aggradation angle and progradation direction. The curvature is no curvature (a); single lobe (b); and double lobe (c). The aggradation angle is on three levels, see Section 2 , and the progradation angle is 90, 180 and 270. There are 336 observations in each boxplot.

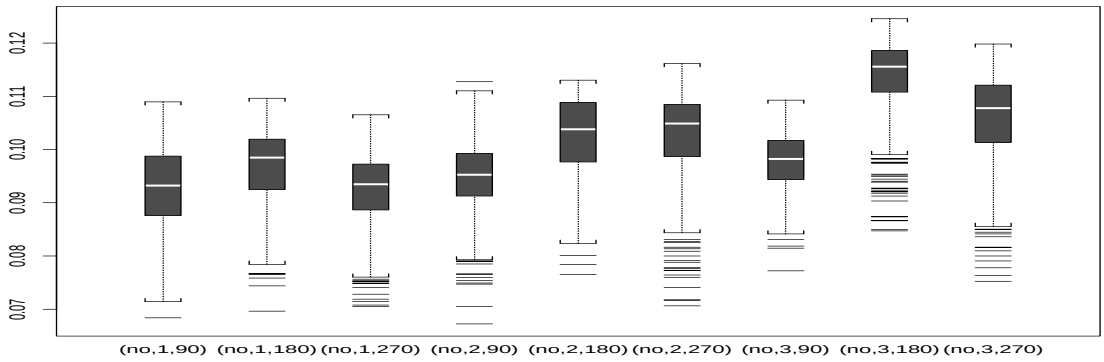

(a)

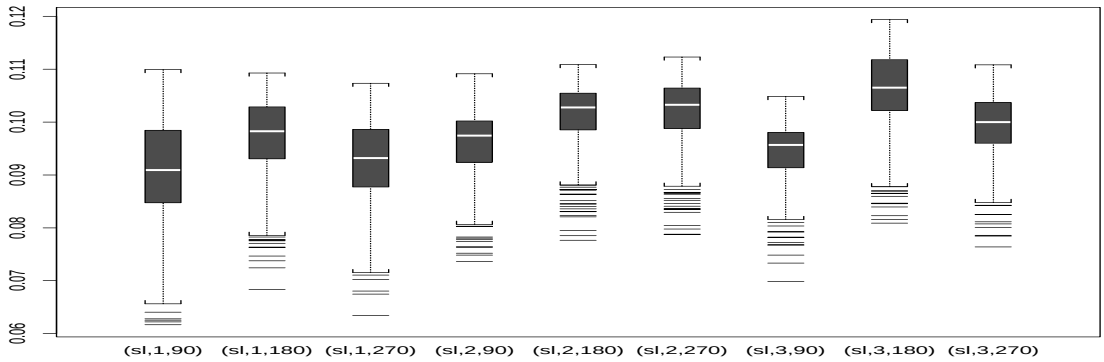

(b)

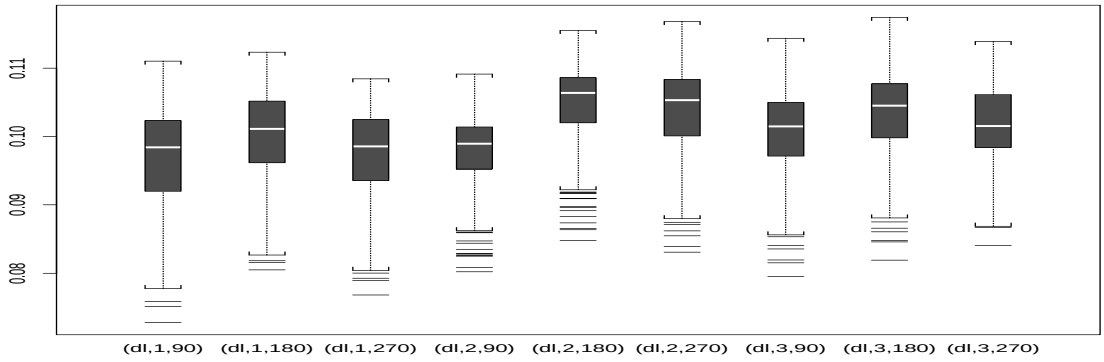

(c)

Figure 25: Recovery factor at 20% water injection by curvature, aggradation angle and progradation direction. The curvature is no curvature (a); single lobe (b); and double lobe (c). The aggradation angle is on three levels, see Section 2 , and the progradation angle is 90, 180 and 270. There are 336 observations in each boxplot.

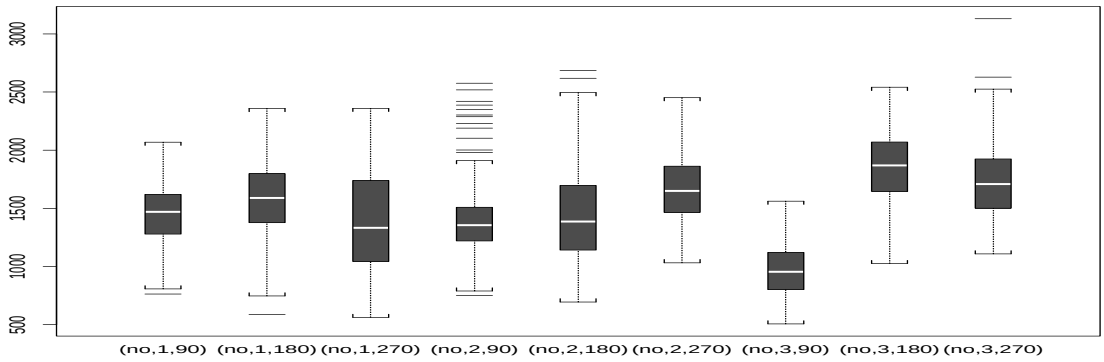

(a)

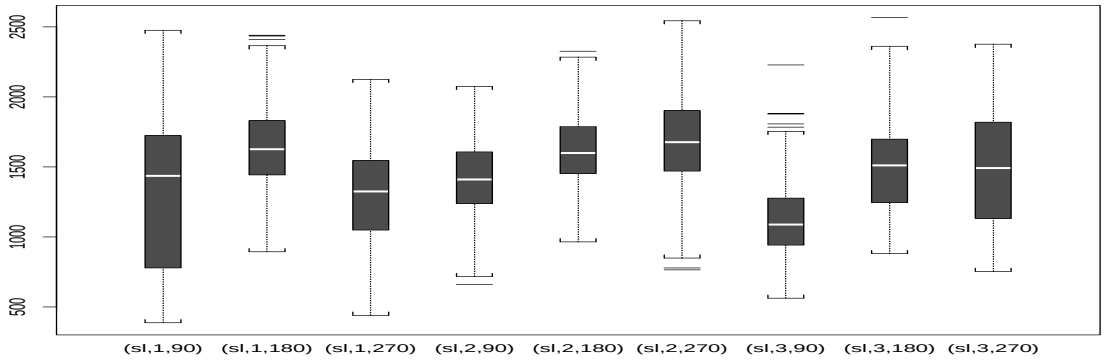

(b)

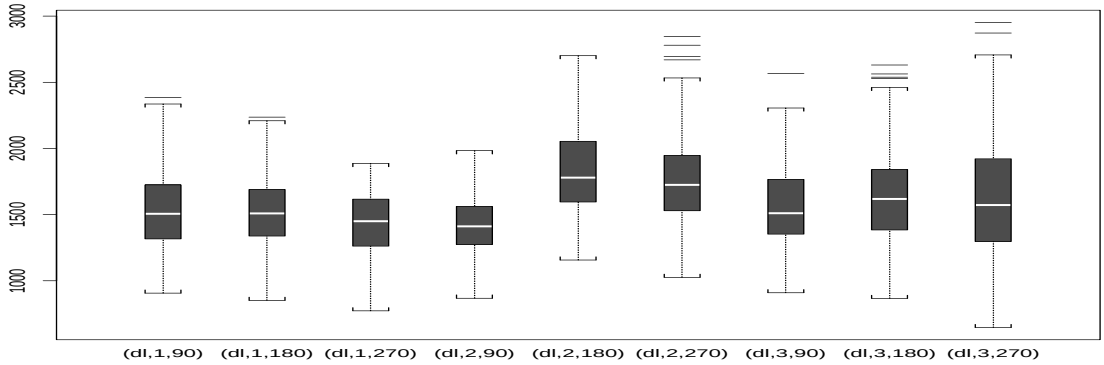

(c)

Figure 26: Total water production by curvature, aggradation angle and progradation direction. The curvature is no curvature (a); single lobe (b); and double lobe (c). The aggradation angle is on three levels, see Section 2 , and the progradation angle is 90, 180 and 270. There are 336 observations in each boxplot.

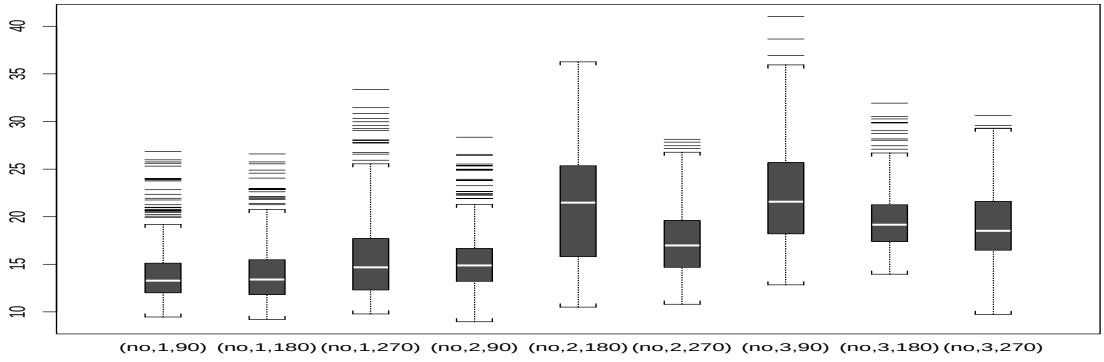

(a)

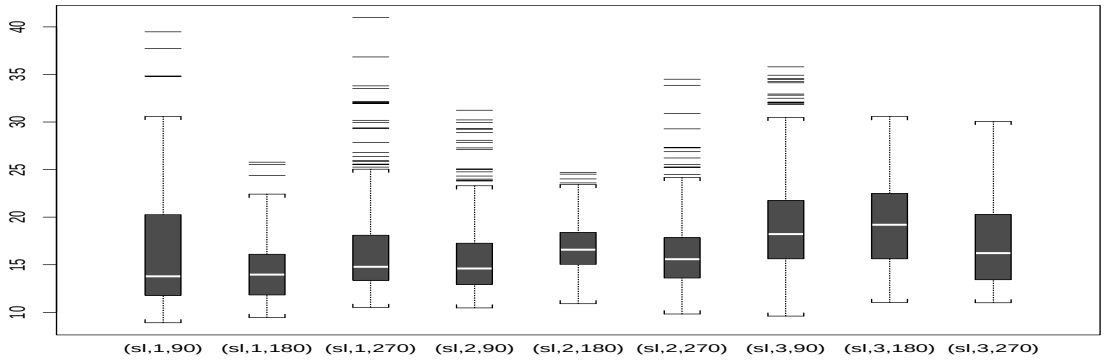

(b)

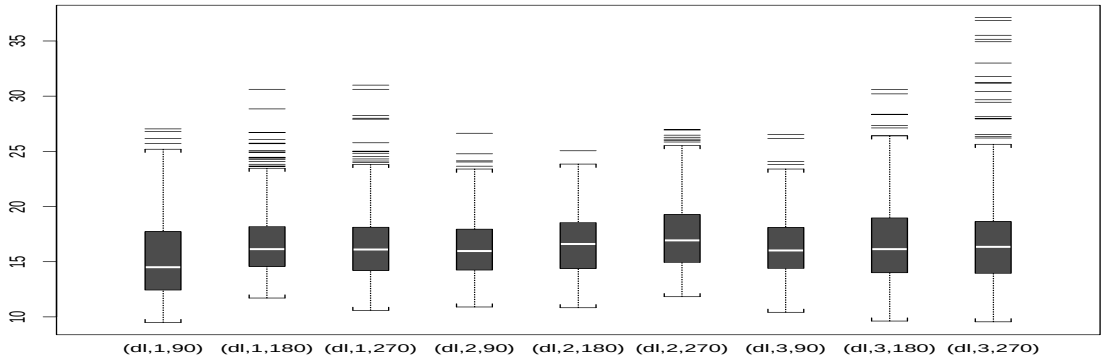

(c)

Figure 27: Ratio of oil/water production by curvature, aggradation angle and progradation direction. The curvature is no curvature (a); single lobe (b); and double lobe (c). The aggradation angle is on three levels, see Section 2 , and the progradation angle is 90, 180 and 270. There are 336 observations in each boxplot.

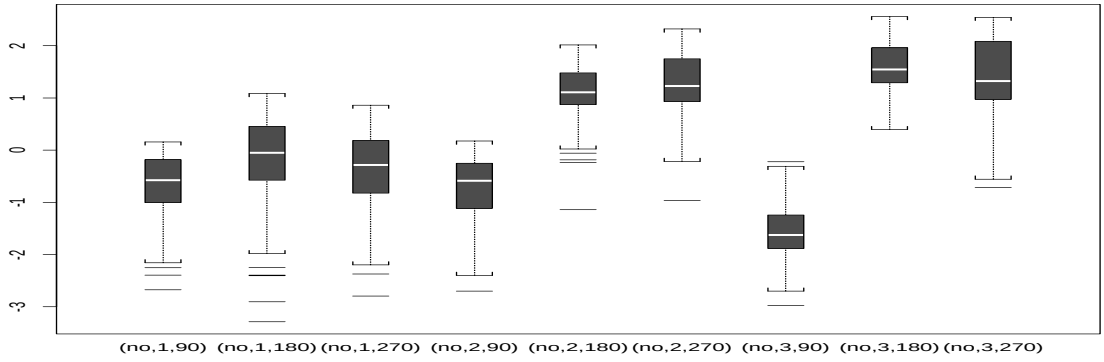

(a)

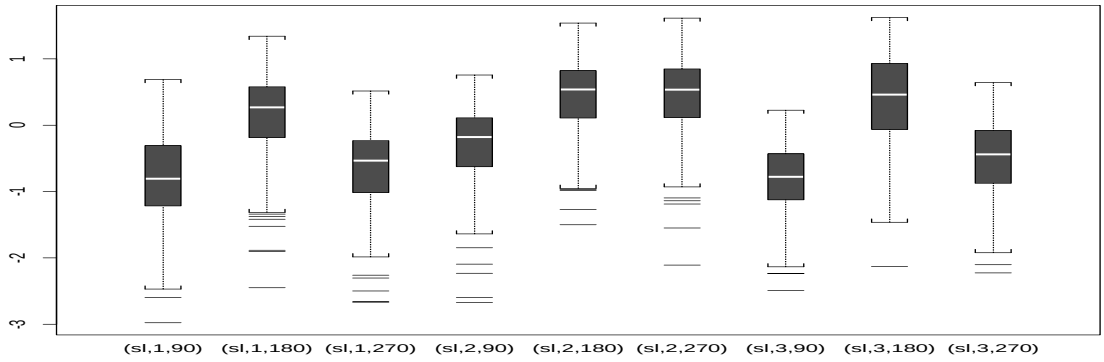

(b)

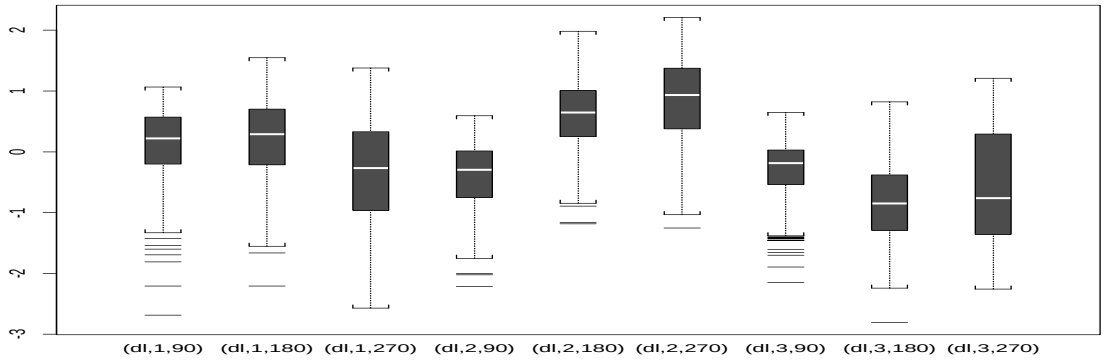

(c)

Figure 28: First component of variability by curvature, aggradation angle and progradation direction. The curvature is no curvature (a); single lobe (b); and double lobe (c). The aggradation angle is on three levels, see Section 2 , and the progradation angle is 90, 180 and 270. There are 336 observations in each boxplot.

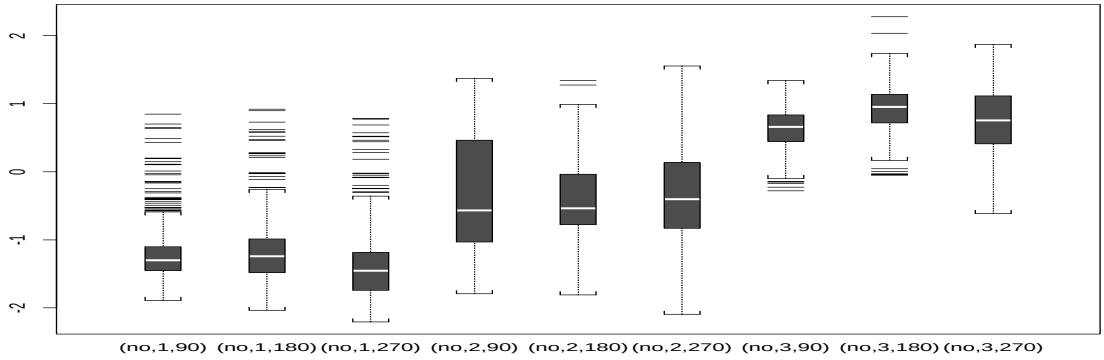

(a)

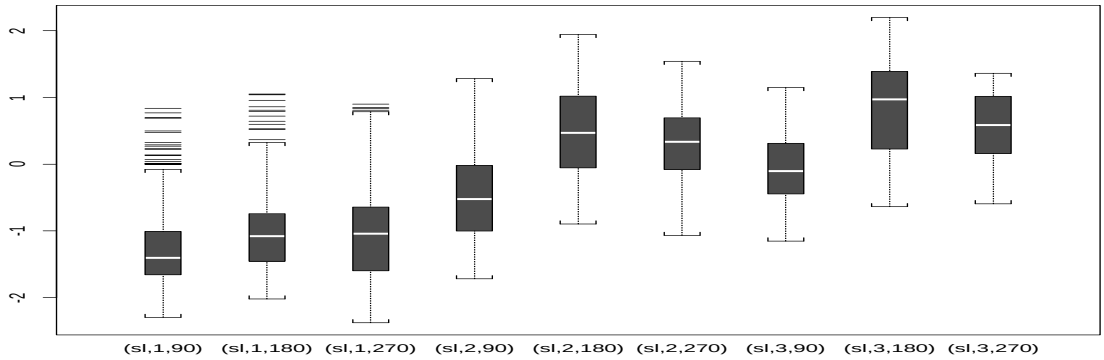

(b)

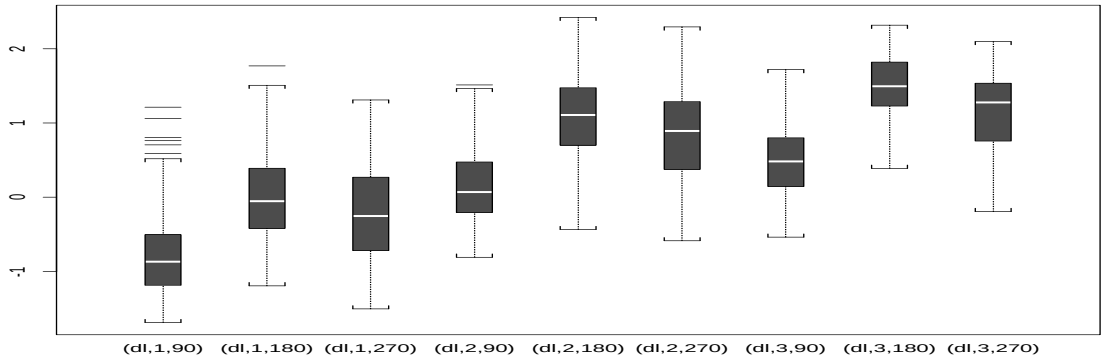

(c)

Figure 29: Second component of variability by curvature, aggradation angle and progradation direction. The curvature is no curvature (a); single lobe (b); and double lobe (c). The aggradation angle is on three levels, see Section 2 , and the progradation angle is 90, 180 and 270. There are 336 observations in each boxplot.

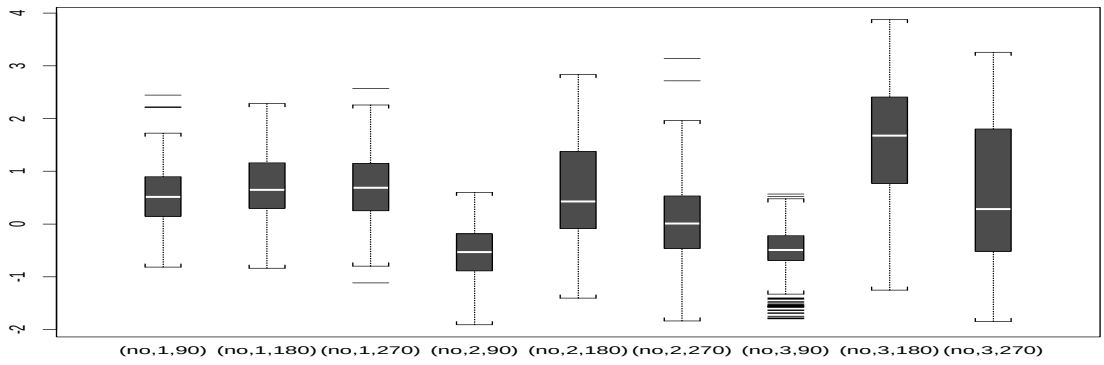

(a)

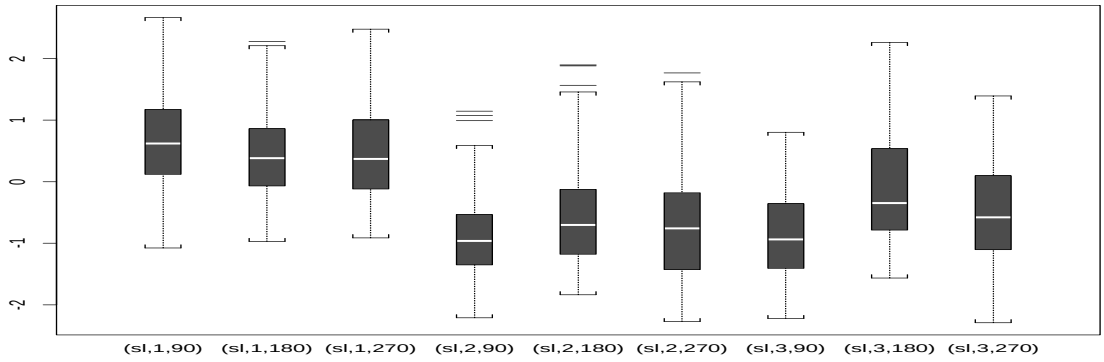

(b)

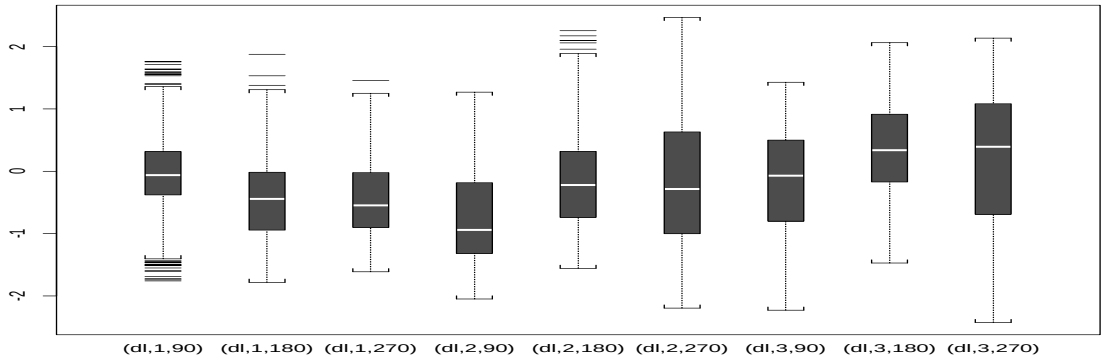

(c)

Figure 30: Third component of variability by curvature, aggradation angle and progradation direction. The curvature is no curvature (a); single lobe (b); and double lobe (c). The aggradation angle is on three levels, see Section 2, and the progradation angle is 90, 180 and 270. There are 336 observations in each boxplot.

4 Statistical methodology

The statistical analysis account for variance components, due to the dependency structure in the data, i.e. $81+28+4 = 113$ independent factors in the input, are combined to $81 \cdot 28 \cdot 4 = 9072$ outputs. The statistical analysis uses two approaches. In the first part the objective is to determine the relative magnitude of the functions $K_{\mathbf{G}}(\mathbf{G})$, $K_{\mathbf{F}}(\mathbf{F})$, $K_{\mathbf{P}}(\mathbf{P})$, $K_{\mathbf{GF}}(\mathbf{G},\mathbf{F})$, $K_{\mathbf{GP}}(\mathbf{G},\mathbf{P})$, $K_{\mathbf{FP}}(\mathbf{F},\mathbf{P})$, and $K_{\mathbf{GFP}}(\mathbf{G},\mathbf{F},\mathbf{P})$, see Expression (2), and to further break down the main effects of geology and faulting to determine the relative effect of the design parameters for the geological models and the fault models, i.e. $K_{\mathbf{G}}(\mathbf{G})$ and $K_{\mathbf{F}}(\mathbf{F})$. Next the objective is to identify the most influential variables related to geology in order to approximate the main effects, i.e. $K_{\mathbf{G}}(\mathbf{G})$.The statistical analysis is preformed using the statistical program Splus.

4.1 Determining the relative magnitude of effects

The production variable is interpreted as a sum of independent variance components,

$$y_{ijk} = K_0 + \varepsilon_i + \varepsilon_j + \varepsilon_k + \varepsilon_{ij} + \varepsilon_{ik} + \varepsilon_{jk} + \varepsilon_{ijk} \; ; \;\; i = 1, ...81; \;\; j = 1, ..., 28; \;\; k = 1, ..., 4; \qquad (4)$$

with K_0 being the average level, see Expression (1); ε_i, ε_j and ε_k being variables explaining the main effects of geology, faulting and production strategy respectively; ε_{ij}, ε_{ik} ε_{jk} being variables explaining second order interactions and ε_{ijk} explaining third order interactions. These random effects correspond to the orthogonal components in Expression (2).

The variance of the components in Expression (4) are estimated by a moment method, based on sum of squares from aggregate levels of the data. The sum of squares computed are, $\sum_{ijk} (y_{ijk} - \bar{y})^2$, $\sum_{jk} (y_{\cdot jk} - \bar{y})^2$, $\sum_{ik} (y_{i \cdot k} - \bar{y})^2$, $\sum_{ij} (y_{ij \cdot} - \bar{y})^2$, $\sum_{i} (y_{i \cdot \cdot} - \bar{y})^2$, $\sum_{j} (y_{\cdot j \cdot} - \bar{y})^2$, and $\sum_{k} (y_{\cdot \cdot k} - \bar{y})^2$, where by standard statistical notation a dot replaces the indices that are averaged out. A simple set of linear equations relates the variance of the random effects in Expression (4) to the expected value of sum of squares above these are reported in Appendix A. The variances computed are the least squares solution of this system of equations subject to a non-negativity constraint. The ratio of the standard deviation in the components to the total standard deviation is reported in tables. The uncertainty assessment is based on a parametric bootstrap using Gaussian variance components.

4.2 Approximating the main effects

In order to compute the main effects of geology, the observations are averaged over fault patterns and production strategy, yielding 81 aggregate observations. The statistical model that is used to compute the main effects of geology is then

$$y_{i \cdot \cdot} = \beta_0^* + \beta_G^T \, \mathbf{x}_i^G + \varepsilon_i^* \; ; \;\; i = 1, ...81 \qquad (5)$$

with $y_{i \cdot \cdot}$ being the aggregate observations; β_0^* being a scalar coefficient; β_G being a coefficient vector related to geology; $\mathbf{x}_i^G$ being explanatory variables related to geology; and ε_i^* being independent errors. The function $\beta_G^T \, \mathbf{x}_i^G$ approximate the main effect of geology, i.e. $K_{\mathbf{G}}(\mathbf{G}) \approx \beta_G^T \, \mathbf{x}^G$.

The reason for using the aggregate data is that this approach is robust to dependency structures such as in Expression (4), and little efficiency is lost when the main effects are estimated.

The variables listed in Table 1 are proposed as candidate variables in the regression. The standardised variables are used through out the analysis, see Table 2 for mean and standard deviation. In order to identify the most influential variables, all combinations of the variables are investigated. The models are fitted by classical least squares. For models having the same number of explanatory variables, the one with the lowest residual sum of squares is preferred. For models having different number of explanatory variables cross validation (CV) is used to discriminate. The CV criterion measures the predictive strength, see Stone (1974) for reference. For comparison the model corresponding to the standard stepwise regression using Efroymson's method (Efroymson 1960) is computed these results are reported in Appendix B. The resulting models are very similar. The exhaustive search, and Efroymson's method are standard functions in Splus.

5 Data analysis of production data

The dependent variable, y, is one of the variables listed in Table 4. The standardised variables are used through out the analysis, see Table 5 for mean and standard deviation of the production data. For each dependent variable the results are presented as follows. First the breakdown of the total variability and the break down for main effects of geology and faulting in terms of design variables are reported in tables listing the relative effect of the components and a 80 % confidence interval, leaving 10 % probability at each side of the interval. Next the regression equations explaining the main effects of geology is given in terms of the standardised variables. The prediction is plotted versus the aggregate variable, i.e. $y_{i\cdots}$, in order to visualise the fit. In this plot the variables are transformed back to the original scales.

5.1 Oil in place

Table 7 shows how the variability is broken down into components due to main effects related to geology, faulting, production strategy and interaction effects. The volume of oil in place is fully explained by geology.

Table 7: Relative effects for oil in place

Effect	Estimate	80 % CI
Geology	1.00	1.00 - 1.00
Fault	0.01	0.01 - 0.01
PDO	0.00	0.00 - 0.00
Geology and Fault	0.00	0.00 - 0.00
Geology and PDO	0.00	0.00 - 0.00
Fault and PDO	0.00	0.00 - 0.00
Geology, Fault and PDO	0.00	0.00 - 0.00

The main effect of geology can be further broken down into components due to the design factors

Table 8: Relative effect of geological design factors for oil in place

Effect	Estimate	80 % CI
Agg.ang	0.44	0.00 - 0.67
Prog.dir	0.56	0.00 - 0.76
Barrier	0.00	0.00 - 0.14
Curvature	0.12	0.00 - 0.35
Agg.ang, Prog.dir	0.34	0.09 - 0.49
Agg.ang, Barrier	0.00	0.00 - 0.13
Agg.ang, Curvature	0.33	0.11 - 0.49
Prog.dir, Barrier	0.14	0.00 - 0.23
Prog.dir, Curvature	0.22	0.00 - 0.33
Barrier, Curvature	0.00	0.00 - 0.13
Residuals	0.44	0.33 - 0.61

The main effect of faulting is of no interest for oil in place since all fault models are adjusted such that the geological model determines the net gross.

The main effect of geology can also be broken down into a regression equation of the form in Expression (5). In the regression the variables above the line in Table 1 excluding v-shale are used as candidate variables. Below the model computed by an exhaustive search is presented.

Exhaustive search:

```
Coefficients:
                      Value Std. Error  t value Pr(>|t|)
            AGGR.aZ   0.2101   0.0639     3.2889   0.0016
         KXmY.ARITH   0.0716   0.0360     1.9922   0.0502
          OFFSET.aZ  -0.1370   0.0683    -2.0075   0.0485
       THICK.LSF.aZ  -0.0414   0.0271    -1.5268   0.1312
           CH.FM.aZ   0.1021   0.0335     3.0468   0.0032
           CP.FM.aZ  -1.2300   0.0684   -17.9782   0.0000
          LSF.FM.aZ  -0.4849   0.0646    -7.5002   0.0000
          OFF.FM.aZ  -0.6605   0.0483   -13.6815   0.0000
          OTZ.FM.aZ  -0.9952   0.0543   -18.3163   0.0000
           COS.PDIR  -0.1149   0.0288    -3.9972   0.0002

Residual standard error: 0.224 on 71 degrees of freedom
Multiple R-Squared: 0.9555, CV=0.059
```

The model above is used to predict the main effect of geology on oil in place. In Figure 31 the prediction is plotted versus the aggregated value computed from the data, i.e. $y_{i\cdots}$.

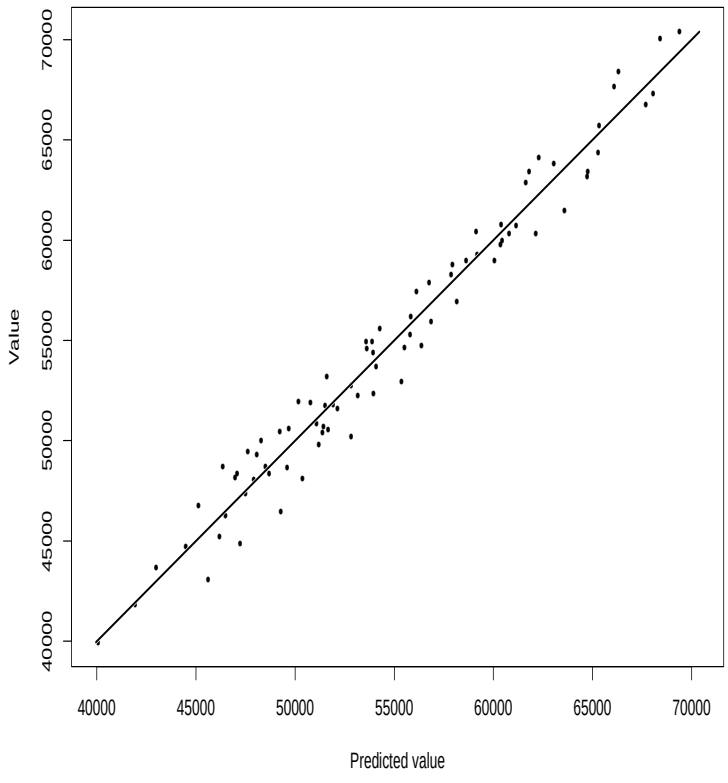

Figure 31: Prediction of oil in place versus the aggregated value computed from the data.

5.2 Total oil production

Table 9 shows how the variability is broken down into components due to main effects related to geology, faulting, production strategy and interaction effects.

Table 9: Relative effects for total oil production

Effect	Estimate	80 % CI
Geology	0.94	0.91 - 0.95
Fault	0.29	0.23 - 0.34
PDO	0.10	0.04 - 0.14
Geology and Fault	0.11	0.10 - 0.12
Geology and PDO	0.07	0.06 - 0.07
Fault and PDO	0.13	0.11 - 0.15
Geology, Fault and PDO	0.08	0.08 - 0.09

The main effect of geology can be further broken down into components due to the design factors

Table 10: Relative effect of geological design factors for total oil production

Effect	Estimate	80 % CI
Agg.ang	0.45	0.00 - 0.72
Prog.dir	0.55	0.00 - 0.74
Barrier	0.00	0.00 - 0.10
Curvature	0.01	0.00 - 0.30
Agg.ang, Prog.dir	0.33	0.12 - 0.50
Agg.ang, Barrier	0.00	0.00 - 0.12
Agg.ang, Curvature	0.36	0.12 - 0.48
Prog.dir, Barrier	0.09	0.00 - 0.18
Prog.dir, Curvature	0.23	0.00 - 0.34
Barrier, Curvature	0.00	0.00 - 0.12
Residuals	0.44	0.32 - 0.60

Similarly the main effect of faulting can be further broken down into components due to the design factors.

Table 11: Relative effect of fault design factors for total production

Effect	Estimate	80 % CI
Structure	0.84	0.42 - 0.93
Density	0.37	0.00 - 0.66
Perm	0.02	0.00 - 0.19
Structure, Density	0.28	0.16 - 0.50
Structure, Perm	0.26	0.15 - 0.48
Density, Perm	0.09	0.07 - 0.18
Residuals	0.00	0.00 - 0.16

The main effect of geology can also be broken down into a regression equation of the form in Expression (5). In the regression all variables in Table 1 are used as candidate variables. Below the model computed by an exhaustive search is presented.

Exhaustive search :

```
Coefficients:
                      Value Std. Error t value Pr(>|t|)
               HETRZ  0.1097  0.0348     3.1490  0.0024
        KY.PRES.SOLVE -0.1320  0.0606    -2.1783  0.0327
              AGGR.aZ  0.3147  0.0404     7.7824  0.0000
            KZ.ARITH   0.2249  0.0724     3.1084  0.0027
       PORO.ARITH.aZ   0.6419  0.0759     8.4561  0.0000
         THICK.USF.aZ -0.0813  0.0290    -2.8009  0.0066
      VSHALE.ARITH.aZ -0.3700  0.0782    -4.7303  0.0000
            LSF.FM.aZ -0.1602  0.0564    -2.8415  0.0059
            OFF.FM.aZ  0.2368  0.0346     6.8435  0.0000
             COS.PDIR -0.0968  0.0305    -3.1757  0.0022

Residual standard error: 0.232 on 71 degrees of freedom
Multiple R-Squared: 0.9522, CV=  0.063
```

The model above is used to predict the main effect of geology on total oil production. In Figure 32 the prediction is plotted versus the aggregated value computed from the data, i.e. $y_{i\cdots}$.

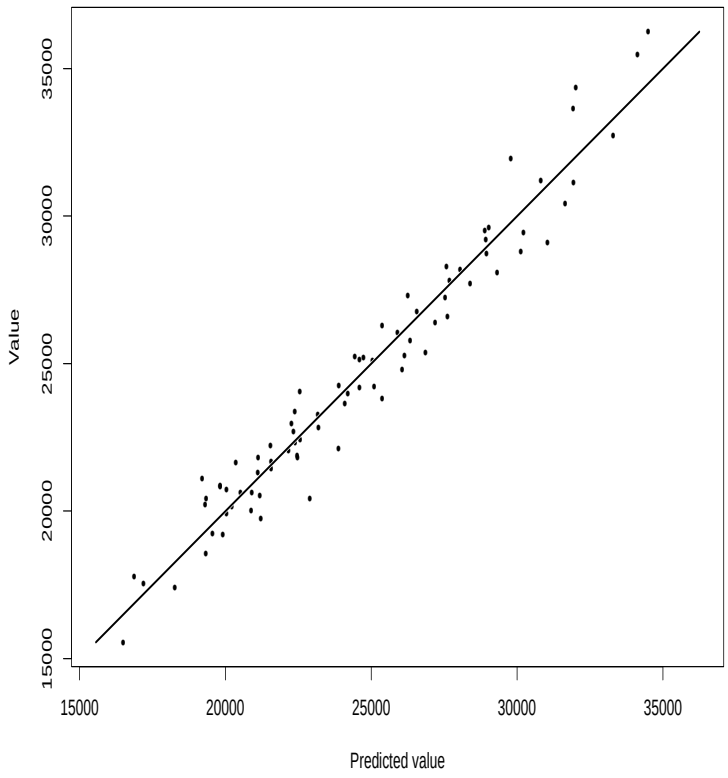

Figure 32: Prediction of total production versus the aggregated value computed from the data.

5.3 Total oil production log transformed

Table 12 shows how the variability is broken down into components due to main effects related to geology, faulting, production strategy and interaction effects.

Table 12: Relative effects for log transform of total production

Effect	Estimate	80% CI
Geology	0.93	0.90 - 0.94
Fault	0.31	0.25 - 0.36
PDO	0.10	0.04 - 0.16
Geology and Fault	0.11	0.10 - 0.12
Geology and PDO	0.07	0.06 - 0.07
Fault and PDO	0.14	0.12 - 0.16
Geology, Fault and PDO	0.09	0.08 - 0.10

The main effect of geology can be further broken down into components due to the design factors

Table 13: Relative effect of geological design factors for logarithm of total oil production

Effect	Estimate	80 % CI
Agg.ang	0.48	0.00 - 0.72
Prog.dir	0.56	0.00 - 0.75
Barrier	0.00	0.00 - 0.11
Curvature	0.12	0.00 - 0.34
Agg.ang, Prog.dir	0.30	0.10 - 0.46
Agg.ang, Barrier	0.00	0.00 - 0.13
Agg.ang, Curvature	0.32	0.11 - 0.49
Prog.dir, Barrier	0.11	0.00 - 0.19
Prog.dir, Curvature	0.22	0.00 - 0.35
Barrier, Curvature	0.00	0.00 - 0.13
Residuals	0.43	0.31 - 0.59

Similarly the main effect of faulting can be further broken down into components due to the design factors.

Table 14: Relative effect of fault design factors for logarithm of total oil production

Effect	Estimate	80 % CI
Structure	0.82	0.36 - 0.92
Density	0.39	0.00 - 0.68
Perm	0.06	0.00 - 0.27
Structure, Density	0.30	0.17 - 0.56
Structure, Perm	0.26	0.14 - 0.47
Density, Perm	0.07	0.02 - 0.13
Residuals	0.06	0.04 - 0.10

The main effect of geology can also be broken down into a regression equation of the form in Expression (5). In the regression all variables in Table 1 are used as candidate variables. Below the model computed by an exhaustive search is presented.

Exhaustive search :

```
Coefficients:
                      Value Std. Error t value Pr(>|t|)
               HETRY -0.1055  0.0374    -2.8208  0.0062
        KZ.PRES.SOLVE  0.2422  0.0595     4.0730  0.0001
              AGGR.aZ  0.3012  0.0423     7.1256  0.0000
        PORO.ARITH.aZ  0.5243  0.0685     7.6489  0.0000
         THICK.LSF.aZ -0.0582  0.0278    -2.0974  0.0395
         THICK.USF.aZ -0.0554  0.0267    -2.0717  0.0419
      VSHALE.ARITH.aZ -0.3608  0.0652    -5.5329  0.0000
            OFF.FM.aZ  0.2165  0.0326     6.6455  0.0000
                 BARR  0.1029  0.0502     2.0514  0.0439
             COS.PDIR -0.0830  0.0286    -2.9065  0.0049

Residual standard error: 0.2255 on 71 degrees of freedom
Multiple R-Squared: 0.9549, CV=0.060
```

The model above is used to predict the main effect of geology on the logarithm of total production In Figure 33 the prediction is plotted versus the aggregated value computed from the data, i.e. y_i...

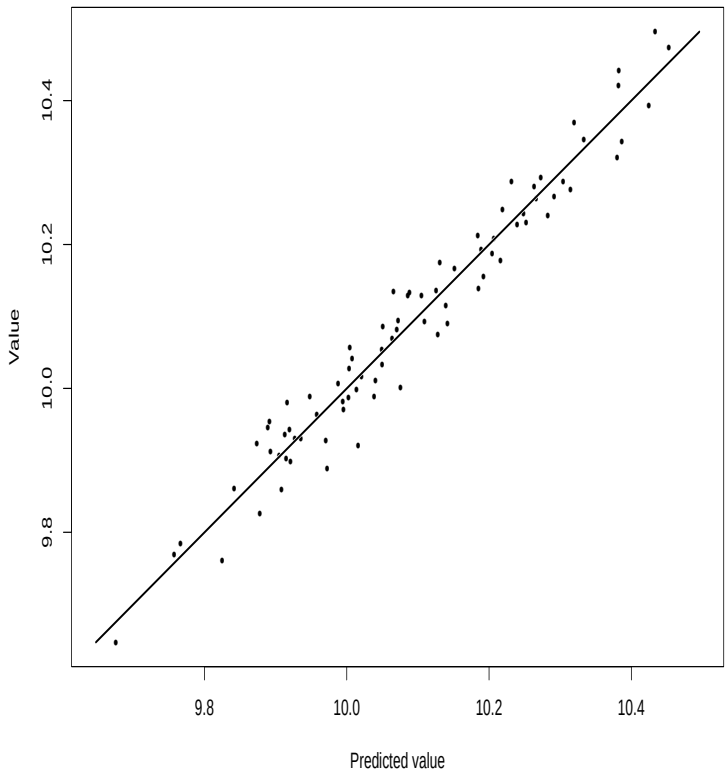

Figure 33: Prediction of logarithm of total production versus the aggregated value computed from the data.

5.4 Discounted production

The value of getting oil early in the production is larger than getting it later due too investments made for production. Oil companies would usually discount production by 15 % in order to get the investments back quickly. The government discount the production by 5% in order to assure a high recovery factor. In the current variable an intermediate rate of 10 % is used. This means that the first year all of the production is added to the total, the second year 90 % of the production is added, from the second year is added, the third year 81 % of the production the third year is added, and so on, i.e. $100 \cdot 0.9^{n-1}$ % of the production is added the n^{th} year. Table 15 shows how the variability is broken down into components due to main effects related to geology, faulting, production strategy and interaction effects.

Table 15: Relative effects for discounted production

Effect	Estimate	80 % CI
Geology	0.89	0.85 - 0.91
Fault	0.32	0.25 - 0.37
PDO	0.20	0.08 - 0.29
Geology and Fault	0.11	0.10 - 0.12
Geology and PDO	0.16	0.14 - 0.18
Fault and PDO	0.20	0.17 - 0.22
Geology, Fault and PDO	0.10	0.09 - 0.11

The main effect of geology can be further broken down into components due to the design factors.

Table 16: Relative effect of geological design factors for discounted production

Effect	Estimate	80 % CI
Agg.ang	0.19	0.00 - 0.46
Prog.dir	0.52	0.00 - 0.74
Barrier	0.00	0.00 - 0.10
Curvature	0.00	0.00 - 0.40
Agg.ang, Prog.dir	0.36	0.08 - 0.49
Agg.ang, Barrier	0.00	0.00 - 0.15
Agg.ang, Curvature	0.32	0.06 - 0.45
Prog.dir, Barrier	0.03	0.00 - 0.14
Prog.dir, Curvature	0.41	0.12 - 0.54
Barrier, Curvature	0.00	0.00 - 0.15
Residuals	0.54	0.42 - 0.68

Similarly the main effect of faulting can be further broken down into components due to the design factors.

Table 17: Relative effect of fault design factors for discounted production

Effect	Estimate	80 % CI
Structure	0.58	0.13 - 0.81
Density	0.61	0.16 - 0.83
Perm	0.45	0.00 - 0.69
Structure, Density	0.00	0.00 - 0.17
Structure, Perm	0.07	0.00 - 0.20
Density, Perm	0.18	0.00 - 0.35
Residuals	0.24	0.00 - 0.41

The main effect of geology can also be broken down into a regression equation of the form in Expression (5). In the regression all variables in Table 1 are used as candidate variables. Below the model computed by an exhaustive search is presented.

Exhaustive search :

```
Coefficients:
                      Value Std. Error  t value Pr(>|t|)
           AGGR.aZ   0.0825   0.0258     3.1995   0.0021
      PORO.ARITH.aZ   0.6994   0.0601    11.6337   0.0000
       THICK.USF.aZ  -0.0474   0.0230    -2.0591   0.0432
    VSHALE.ARITH.aZ  -0.1873   0.0645    -2.9057   0.0049
          CH.FM.aZ  -0.1145   0.0263    -4.3503   0.0000
          CP.FM.aZ  -0.2633   0.0426    -6.1890   0.0000
         LSF.FM.aZ  -0.3436   0.0446    -7.6996   0.0000
         OTZ.FM.aZ  -0.4814   0.0437   -11.0181   0.0000
              BARR  -0.0718   0.0195    -3.6769   0.0005
          SIN.PDIR   0.0504   0.0361     1.3975   0.1667
          COS.PDIR  -0.0517   0.0263    -1.9676   0.0531

Residual standard error: 0.1715 on 70 degrees of freedom
Multiple R-Squared: 0.9743, CV=0.034
```

The model above is used to predict the main effect of geology on discounted production. In Figure 34 the prediction is plotted versus the aggregated value computed from the data, i.e. y_i..

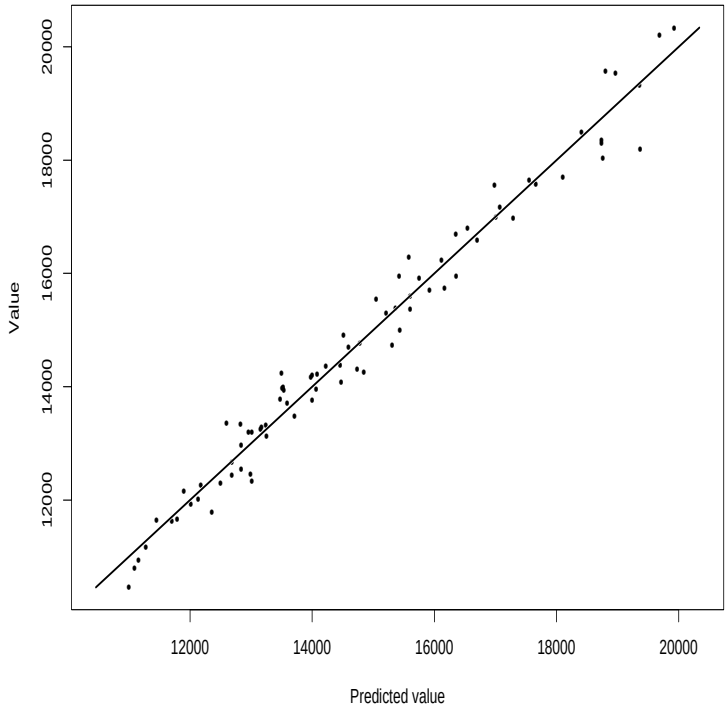

Figure 34: Prediction of discounted production versus the aggregated value computed from the data.

5.5 Recovery factor

The recovery factor is the total amount of oil produced at end divided by the amount of oil in place. Table 18 shows how the variability is broken down into components due to main effects related to geology, faulting, production strategy and interaction effects.

Table 18: Relative effects for recovery factor

Effect	Estimate	80 % CI
Geology	0.62	0.56 - 0.67
Fault	0.64	0.55 - 0.69
PDO	0.21	0.08 - 0.31
Geology and Fault	0.23	0.21 - 0.24
Geology and PDO	0.15	0.13 - 0.16
Fault and PDO	0.29	0.25 - 0.32
Geology, Fault and PDO	0.19	0.17 - 0.20

The main effect of geology can be further broken down into components due to the design factors

Table 19: Relative effect of geological design factors for recovery factor

Effect	Estimate	80 % CI
Agg.ang	0.54	0.00 - 0.74
Prog.dir	0.50	0.00 - 0.72
Barrier	0.00	0.00 - 0.09
Curvature	0.00	0.00 - 0.30
Agg.ang, Prog.dir	0.26	0.00 - 0.40
Agg.ang, Barrier	0.07	0.00 - 0.19
Agg.ang, Curvature	0.32	0.08 - 0.44
Prog.dir, Barrier	0.00	0.00 - 0.14
Prog.dir, Curvature	0.23	0.00 - 0.35
Barrier, Curvature	0.00	0.00 - 0.14
Residuals	0.48	0.35 - 0.64

Similarly the main effect of faulting can be further broken down into components due to the design factors.

Table 20: Relative effect of fault design factors for recovery factor

Effect	Estimate	80 % CI
Structure	0.83	0.40 - 0.92
Density	0.40	0.00 - 0.71
Perm	0.07	0.00 - 0.30
Structure, Density	0.27	0.15 - 0.50
Structure, Perm	0.25	0.13 - 0.42
Density, Perm	0.06	0.02 - 0.12
Residuals	0.05	0.03 - 0.08

The main effect of geology can also be broken down into a regression equation of the form in Expression (5). In the regression all variables in Table 1 are used as candidate variables. Below the model computed by an exhaustive search is presented.

Exhaustive search :

```
Coefficients:
                      Value Std. Error  t value Pr(>|t|)
               HETRY   0.3761   0.1075     3.4991   0.0008
        KY.PRES.SOLVE  -0.4859   0.1940    -2.5048   0.0145
              AGGR.aZ   0.5826   0.0547    10.6573   0.0000
              CLIN.aZ  -0.0905   0.0443    -2.0428   0.0447
            KZ.ARITH   0.3433   0.1417     2.4227   0.0179
        PORO.ARITH.aZ   0.8166   0.0691    11.8173   0.0000
         THICK.USF.aZ  -0.0893   0.0469    -1.9034   0.0609
            OFF.FM.aZ   0.1539   0.0531     2.8975   0.0050

Residual standard error: 0.387 on 73 degrees of freedom
Multiple R-Squared: 0.8633, CV=0.168
```

The model above is used to predict the main effect of geology on the recovery factor. In Figure 35 the prediction is plotted versus the aggregated value computed from the data, i.e. $y_{i\cdots}$.

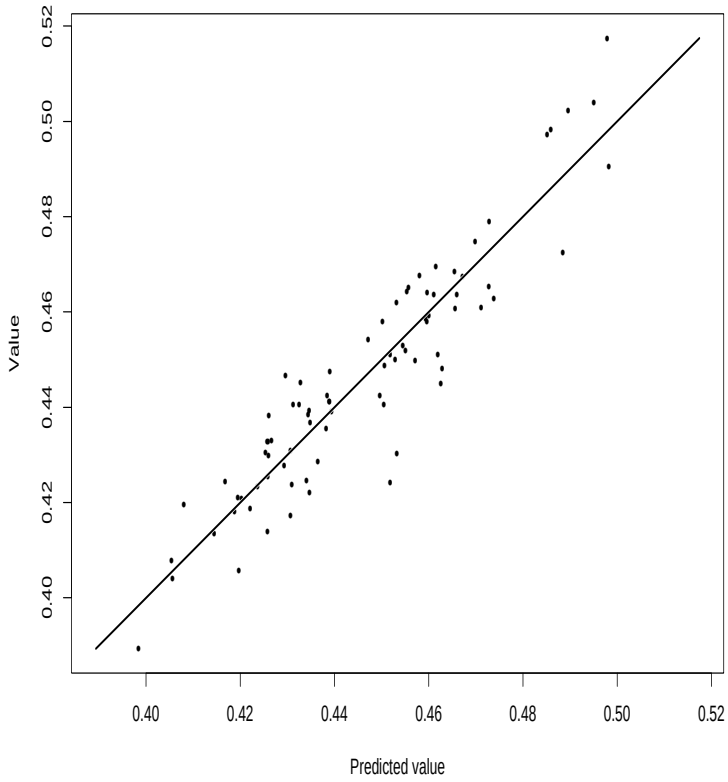

Figure 35: Prediction of recovery factor versus the aggregated value computed from the data.

5.6 Recovery at 20 % of injected water volume

The recovery at 20 % of injected water volume, is the amount of oil produced at the time when 20 % of the total water amount is injected, divided by oil in place. Table 21 shows how the variability is broken down into components due to main effects related to geology, faulting, production strategy and interaction effects.

Table 21: Relative effects for recovery at 20 % of injected water volume

Effect	Estimate	80 % CI
Geology	0.65	0.59 - 0.70
Fault	0.59	0.49 - 0.65
PDO	0.12	0.00 - 0.18
Geology and Fault	0.23	0.21 - 0.24
Geology and PDO	0.17	0.15 - 0.19
Fault and PDO	0.35	0.30 - 0.39
Geology, Fault and PDO	0.20	0.18 - 0.21

The main effect of geology can be further broken down into components due to the design factors

Table 22: Relative effect of geological design factors on recovery at 20 % of injected water volume

Effect	Estimate	80 % CI
Agg.ang	0.54	0.00 - 0.74
Prog.dir	0.51	0.00 - 0.73
Barrier	0.05	0.00 - 0.16
Curvature	0.16	0.00 - 0.32
Agg.ang, Prog.dir	0.26	0.00 - 0.40
Agg.ang, Barrier	0.00	0.00 - 0.15
Agg.ang, Curvature	0.30	0.07 - 0.44
Prog.dir, Barrier	0.11	0.00 - 0.21
Prog.dir, Curvature	0.10	0.00 - 0.21
Barrier, Curvature	0.00	0.00 - 0.15
Residuals	0.49	0.36 - 0.66

Similarly the main effect of faulting can be further broken down into components due to the design factors.

Table 23: Relative effect of fault design factors on recovery at 20 % of injected water volume

Effect	Estimate	80 % CI
Structure	0.77	0.36 - 0.91
Density	0.53	0.13 - 0.80
Perm	0.23	0.00 - 0.44
Structure, Density	0.19	0.09 - 0.34
Structure, Perm	0.18	0.09 - 0.32
Density, Perm	0.07	0.03 - 0.13
Residuals	0.04	0.02 - 0.07

The main effect of geology can also be broken down into a regression equation of the form in Expression (5). In the regression all variables in Table 1 are used as candidate variables. Below the model computed by an exhaustive search is presented.

Exhaustive search :

```
Coefficients:
                Value Std. Error t value Pr(>|t|)
        HETRX  0.3383  0.1009     3.3545  0.0013
        HETRY -0.2040  0.0784    -2.6028  0.0112
      AGGR.aZ  0.5965  0.0609     9.7971  0.0000
      CLIN.aZ -0.1054  0.0460    -2.2940  0.0248
   KXmY.ARITH -0.1641  0.0826    -1.9870  0.0508
     KZ.ARITH  0.1381  0.0742     1.8612  0.0669
PORO.ARITH.aZ  0.6488  0.0726     8.9309  0.0000
 THICK.USF.aZ -0.1165  0.0483    -2.4136  0.0184
     COS.PDIR -0.1687  0.0513    -3.2920  0.0016

Residual standard error: 0.399 on 72 degrees of freedom
Multiple R-Squared: 0.8587, CV=0.180
```

The model above is used to predict the main effect of geology on recovery at 20 % of injected water volume. In Figure 36 the prediction is plotted versus the aggregated value computed from the data, i.e. y_i...

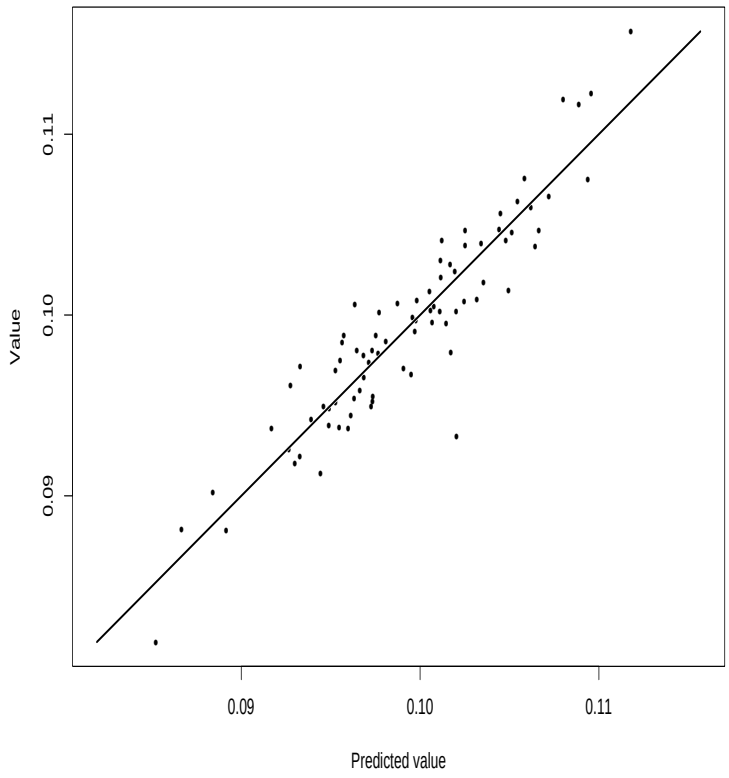

Figure 36: Prediction of recovery at 20 % of injected water volume versus the aggregated value computed from the data.

5.7 Total water production

Table 24 shows how the variability is broken down into components due to main effects related to geology, faulting, production strategy and interaction effects.

Table 24: Relative effects for Total water production

Effect	Estimate	80% CI
Geology	0.75	0.70 - 0.78
Fault	0.33	0.26 - 0.38
PDO	0.20	0.08 - 0.28
Geology and Fault	0.37	0.35 - 0.40
Geology and PDO	0.22	0.20 - 0.24
Fault and PDO	0.13	0.11 - 0.15
Geology, Fault and PDO	0.32	0.30 - 0.34

The main effect of geology can be further broken down into components due to the design factors

Table 25: Relative effects for total water production

Effect	Estimate	80 % CI
Agg.ang	0.00	0.00 - 0.29
Prog.dir	0.40	0.00 - 0.59
Barrier	0.47	0.00 - 0.65
Curvature	0.18	0.00 - 0.28
Agg.ang, Prog.dir	0.34	0.00 - 0.46
Agg.ang, Barrier	0.00	0.00 - 0.21
Agg.ang, Curvature	0.00	0.00 - 0.21
Prog.dir, Barrier	0.10	0.00 - 0.26
Prog.dir,Curvature	0.00	0.00 - 0.22
Barrier, Curvature	0.00	0.00 - 0.21
Residuals	0.68	0.52 - 0.81

Similarly the main effect of faulting can be further broken down into components due to the design factors.

Table 26: Relative effect of fault design factors for total water production

Effect	Estimate	80 % CI
Structure	0.62	0.16 - 0.86
Density	0.68	0.20 - 0.89
Perm	0.00	0.00 - 0.21
Structure, Density	0.17	0.00 - 0.33
Structure, Perm	0.27	0.01 - 0.43
Density, Perm	0.00	0.00 - 0.14
Residuals	0.22	0.12 - 0.35

The main effect of geology can also be broken down into a regression equation of the form in Expression (5). In the regression all variables in Table 1 are used as candidate variables. Below the model computed by an exhaustive search is presented.

Exhaustive search :

```
Coefficients:
                      Value Std. Error t value Pr(>|t|)
               HETRX  1.0178  0.5397     1.8859  0.0636
               HETRY -0.1734  0.0836    -2.0742  0.0418
        KX.PRES.SOLVE -1.8872  0.9405    -2.0065  0.0488
        KZ.PRES.SOLVE -0.5059  0.1072    -4.7206  0.0000
              AGGR.aZ  0.1942  0.1074     1.8072  0.0752
              CLIN.aZ -0.1330  0.0561    -2.3732  0.0205
            KXY.ARITH  2.1726  0.9227     2.3545  0.0214
        PORO.ARITH.aZ  0.6730  0.1704     3.9494  0.0002
         THICK.LSF.aZ -0.2561  0.0613    -4.1743  0.0001
         THICK.USF.aZ -0.1547  0.0637    -2.4288  0.0178
            LSF.FM.aZ  0.2323  0.1122     2.0696  0.0423
            OFF.FM.aZ  0.2868  0.0846     3.3888  0.0012
             SIN.PDIR  0.1582  0.0773     2.0479  0.0444

Residual standard error: 0.4829 on 68 degrees of freedom
Multiple R-Squared: 0.8018, CV=0.28
```

The model above is used to predict the main effect of geology on total water production. In Figure 37 the prediction is plotted versus the aggregated value computed from the data, i.e. $y_{i\cdots}$.

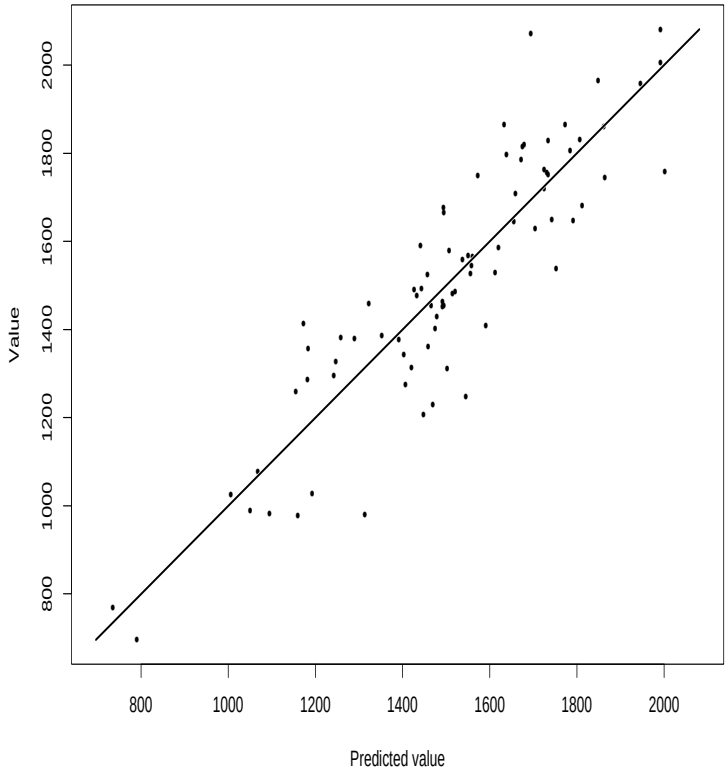

Figure 37: Prediction of total water production versus the aggregated value computed from the data.

5.8 Ratio total oil to total water production

Table 27 shows how the variability is broken down into components due to main effects related to geology, faulting, production strategy and interaction effects.

Table 27: Relative effects for ratio total oil to total water production

Effect	Estimate	80 % CI
Geology	0.67	0.61 - 0.70
Fault	0.40	0.33 - 0.46
PDO	0.27	0.12 - 0.37
Geology and Fault	0.41	0.38 - 0.43
Geology and PDO	0.23	0.20 - 0.24
Fault and PDO	0.11	0.09 - 0.12
Geology, Fault and PDO	0.35	0.32 - 0.37

The main effect of geology can be further broken down into components due to the design factors

Table 28: Relative effect of geological design factors for ratio total oil to total water production

Effect	Estimate	80 % CI
Agg.ang	0.39	0.00 - 0.63
Prog.dir	0.00	0.00 - 0.15
Barrier	0.54	0.00 - 0.72
Curvature	0.00	0.00 - 0.28
Agg.ang, Prog.dir	0.17	0.00 - 0.29
Agg.ang, Barrier	0.15	0.00 - 0.30
Agg.ang, Curvature	0.32	0.00 - 0.45
Prog.dir, Barrier	0.00	0.00 - 0.17
Prog.dir, Curvature	0.00	0.00 - 0.18
Barrier, Curvature	0.00	0.00 - 0.21
Residuals	0.63	0.48 - 0.79

Similarly the main effect of faulting can be further broken down into components due to the design factors.

Table 29: Relative effect of fault design factors for ratio total oil to total water production

Effect	Estimate	80 % CI
Structure	0.83	0.34 - 0.91
Density	0.27	0.00 - 0.59
Perm	0.00	0.00 - 0.28
Structure, Density	0.33	0.16 - 0.58
Structure, Perm	0.29	0.11 - 0.47
Density, Perm	0.07	0.00 - 0.19
Residuals	0.21	0.13 - 0.35

The main effect of geology can also be broken down into a regression equation of the form in Expression (5). In the regression all variables in Table 1 are used as candidate variables. Below the model computed by an exhaustive search is presented.

Exhaustive search :

```
Coefficients:
                      Value Std. Error  t value Pr(>|t|)
               HETRX  -1.1220   0.5670    -1.9788   0.0517
        KX.PRES.SOLVE   2.0031   1.0412     1.9238   0.0584
        KZ.PRES.SOLVE   0.8621   0.0861    10.0100   0.0000
              CLIN.aZ   0.1310   0.0645     2.0298   0.0461
            KXY.ARITH  -2.5796   1.0084    -2.5580   0.0127
             KZ.ARITH   0.3166   0.2308     1.3713   0.1746
          THICK.LSF.aZ   0.3078   0.0703     4.3789   0.0000
       VSHALE.ARITH.aZ  -0.3477   0.1558    -2.2312   0.0288
              CH.FM.aZ  -0.2064   0.0796    -2.5933   0.0115
             LSF.FM.aZ  -0.4637   0.1274    -3.6390   0.0005

Residual standard error: 0.5681 on 71 degrees of freedom
Multiple R-Squared: 0.7135, CV=0.37
```

The model above is used to predict the main effect of geology on the ratio of total oil to total water production. In Figure 38 the prediction is plotted versus the aggregated value computed from the data, i.e. $y_{i\cdots}$

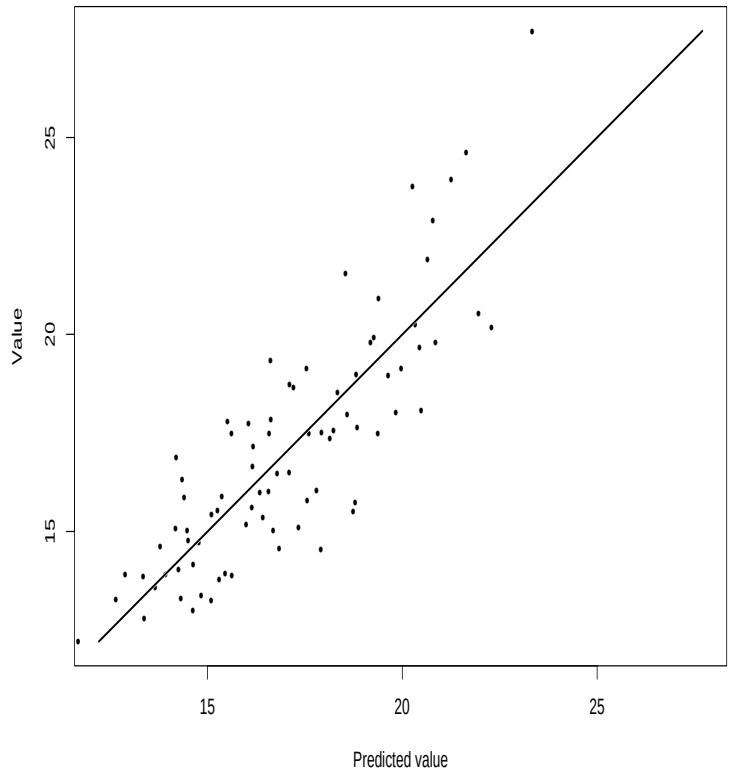

Figure 38: Prediction of ratio of total oil to total water production versus the aggregated value computed from the data.

5.9 First principal production component

Table 30 shows how the variability is broken down into components due to main effects related to geology, faulting, production strategy and interaction effects.

Table 30: Relative effects for first principal production component

Effect	Estimate	80 % CI
Geology	0.84	0.78 - 0.86
Fault	0.34	0.28 - 0.40
PDO	0.28	0.12 - 0.39
Geology and Fault	0.13	0.12 - 0.14
Geology and PDO	0.24	0.21 - 0.26
Fault and PDO	0.21	0.18 - 0.23
Geology, Fault and PDO	0.13	0.12 - 0.14

The main effect of geology can be further broken down into components due to the design factors

Table 31: Relative effect of geological design factors for first principal production component

Effect	Estimate	80 % CI
Agg.ang	0.22	0.00 - 0.45
Prog.dir	0.44	0.00 - 0.65
Barrier	0.04	0.00 - 0.11
Curvature	0.00	0.00 - 0.44
Agg.ang, Prog.dir	0.33	0.02 - 0.46
Agg.ang, Barrier	0.00	0.00 - 0.16
Agg.ang, Curvature	0.32	0.00 - 0.42
Prog.dir, Barrier	0.00	0.00 - 0.17
Prog.dir, Curvature	0.46	0.18 - 0.59
Barrier, Curvature	0.00	0.00 - 0.15
Residuals	0.58	0.45 - 0.71

Similarly the main effect of faulting can be further broken down into components due to the design factors.

Table 32: Relative effect of fault design factors for first principal production component

Effect	Estimate	80 % CI
Structure	0.39	0.00 - 0.62
Density	0.62	0.17 - 0.82
Perm	0.53	0.00 - 0.77
Structure, Density	0.00	0.00 - 0.22
Structure, Perm	0.17	0.00 - 0.35
Density, Perm	0.22	0.00 - 0.40
Residuals	0.33	0.00 - 0.53

The main effect of geology can also be broken down into a regression equation of the form in Expression (5). In the regression all variables in Table 1 are used as candidate variables. Below the model computed by an exhaustive search is presented.

Exhaustive search :

```
Coefficients:
                      Value Std. Error t value Pr(>|t|)
               HETRZ  0.0614  0.0384     1.5988  0.1143
        PORO.ARITH.aZ -0.5526  0.1501    -3.6818  0.0004
             CH.FM.aZ  0.1086  0.0264     4.1101  0.0001
             CP.FM.aZ  0.4473  0.1894     2.3616  0.0209
            LSF.FM.aZ  0.3334  0.0732     4.5559  0.0000
            OFF.FM.aZ  0.2593  0.1474     1.7587  0.0829
            OTZ.FM.aZ  0.7078  0.1227     5.7679  0.0000
                 BARR  0.1357  0.0361     3.7566  0.0003
             COS.PDIR  0.0436  0.0272     1.6012  0.1137

Residual standard error: 0.2095 on 72 degrees of freedom
Multiple R-Squared: 0.960, CV=0.05
```

The model above is used to predict the main effect of geology on the first principal production component. In Figure 39 the prediction is plotted versus the aggregated value computed from the data, i.e. y_i...

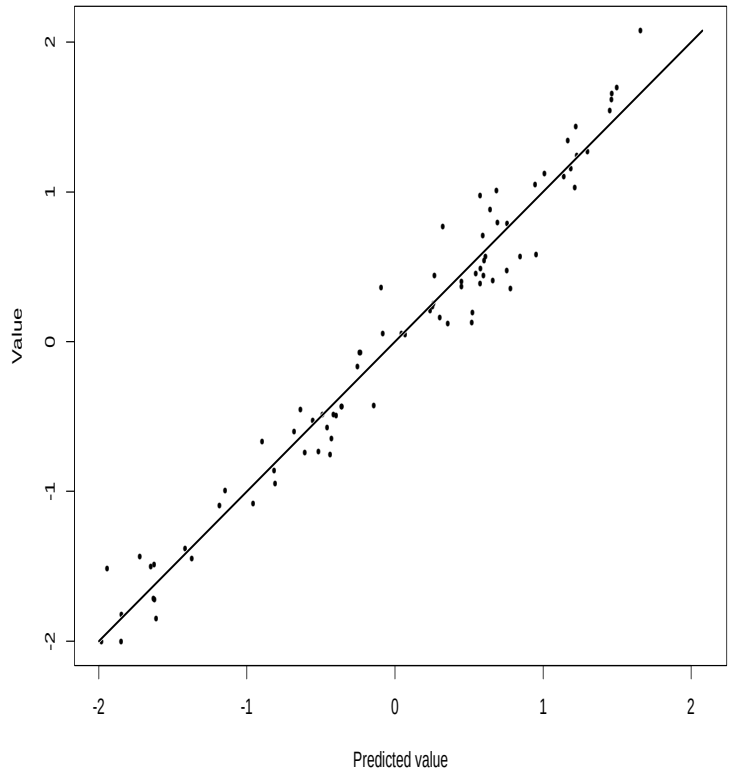

Figure 39: Prediction of first principal production component versus the aggregated value computed from the data.

5.10 Second principal production component

Table 33 shows how the variability is broken down into components due to main effects related to geology, faulting, production strategy and interaction effects.

Table 33: Relative effects for second principal production component

Effect	Estimate	80 % CI
Geology	0.87	0.84 - 0.89
Fault	0.28	0.22 - 0.32
PDO	0.13	0.05 - 0.20
Geology and Fault	0.22	0.20 - 0.23
Geology and PDO	0.25	0.22 - 0.27
Fault and PDO	0.13	0.11 - 0.14
Geology, Fault and PDO	0.18	0.17 - 0.20

The main effect of geology can be further broken down into components due to the design factors

Table 34: Relative effect of geological design factors for second principal production component

Effect	Estimate	80 % CI
Agg.ang	0.79	0.37 - 0.90
Prog.dir	0.25	0.00 - 0.46
Barrier	0.00	0.00 - 0.10
Curvature	0.35	0.00 - 0.60
Agg.ang, Prog.dir	0.00	0.00 - 0.12
Agg.ang, Barrier	0.10	0.00 - 0.19
Agg.ang, Curvature	0.20	0.05 - 0.34
Prog.dir, Barrier	0.04	0.00 - 0.11
Prog.dir, Curvature	0.20	0.03 - 0.36
Barrier, Curvature	0.00	0.00 - 0.11
Residuals	0.33	0.23 - 0.54

Similarly the main effect of faulting can be further broken down into components due to the design factors.

Table 35: Relative effect of fault design factors for second principal production component

Effect	Estimate	80 % CI
Structure	0.66	0.00 - 0.83
Density	0.24	0.00 - 0.56
Perm	0.26	0.00 - 0.50
Structure, Density	0.41	0.22 - 0.63
Structure, Perm	0.47	0.24 - 0.70
Density, Perm	0.07	0.00 - 0.19
Residuals	0.20	0.00 - 0.30

The main effect of geology can also be broken down into a regression equation of the form in Expression (5). In the regression all variables in Table 1 are used as candidate variables. Below the model computed by an exhaustive search is presented.

Exhaustive search :

```
Coefficients:
                      Value Std. Error t value Pr(>|t|)
       KX.PRES.SOLVE  0.1936  0.1198     1.6162  0.1104
       KY.PRES.SOLVE -0.6267  0.1299    -4.8255  0.0000
       KZ.PRES.SOLVE  0.5370  0.1318     4.0748  0.0001
             AGGR.aZ  0.5511  0.0780     7.0615  0.0000
        THICK.LSF.aZ -0.0904  0.0485    -1.8634  0.0665
     VSHALE.ARITH.aZ -0.2941  0.0766    -3.8391  0.0003
           CH.FM.aZ  0.1920  0.0557     3.4463  0.0010
           CP.FM.aZ -0.3422  0.0582    -5.8778  0.0000
               BARR  0.3317  0.0887     3.7394  0.0004

Residual standard error: 0.3973 on 72 degrees of freedom
Multiple R-Squared: 0.8579, CV=0.18
```

The model above is used to predict the main effect of geology on the second principal production component. In Figure 40the prediction is plotted versus the aggregated value computed from the data, i.e. y_i...

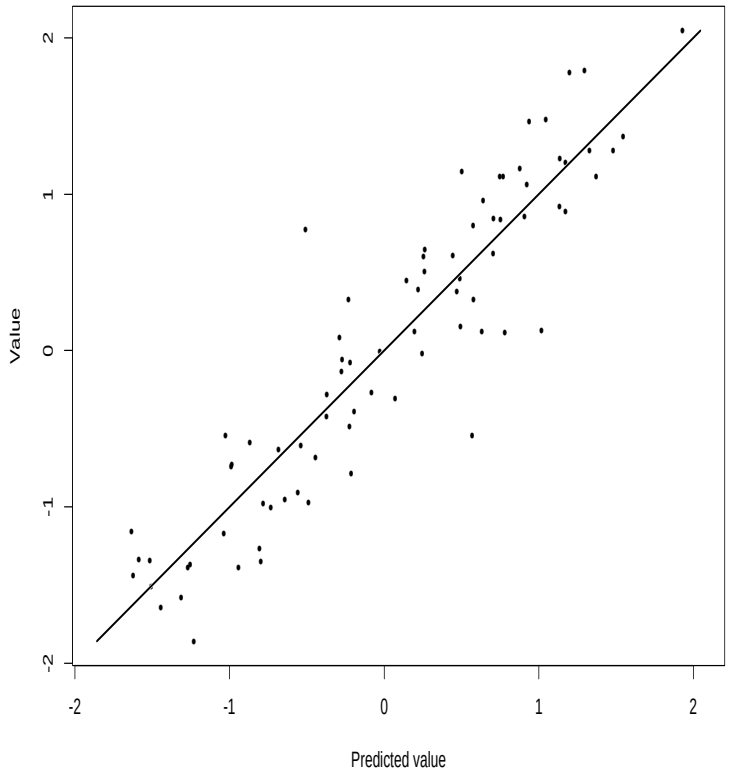

Figure 40: Prediction of second principal production component versus the aggregated value computed from the data.

5.11 Third principal production component

Table 36 shows how the variability is broken down into components due to main effects related to geology, faulting, production strategy and interaction effects.

Table 36: Relative effects for third principal production component

Effect	Estimate	80 % CI
Geology	0.62	0.54 - 0.67
Fault	0.27	0.22 - 0.31
PDO	0.43	0.20 - 0.57
Geology and Fault	0.34	0.30 - 0.36
Geology and PDO	0.39	0.34 - 0.42
Fault and PDO	0.16	0.13 - 0.18
Geology, Fault and PDO	0.34	0.30 - 0.36

The main effect of geology can be further broken down into components due to the design factors

Table 37: Relative effect of geological design factors for third principal production component

Effect	Estimate	80 % CI
Agg.ang	0.15	0.00 - 0.52
Prog.dir	0.21	0.00 - 0.50
Barrier	0.00	0.00 - 0.20
Curvature	0.34	0.00 - 0.60
Agg.ang, Prog.dir	0.46	0.21 - 0.58
Agg.ang, Barrier	0.18	0.00 - 0.26
Agg.ang, Curvature	0.53	0.24 - 0.63
Prog.dir, Barrier	0.14	0.00 - 0.21
Prog.dir, Curvature	0.33	0.13 - 0.45
Barrier, Curvature	0.17	0.00 - 0.25
Residuals	0.38	0.28 - 0.47

Similarly the main effect of faulting can be further broken down into components due to the design factors.

Table 38: Relative effect of fault design factors for third principal production component

Effect	Estimate	80 % CI
Structure	0.64	0.00 - 0.78
Density	0.00	0.00 - 0.38
Perm	0.23	0.00 - 0.50
Structure, Density	0.24	0.00 - 0.46
Structure, Perm	0.40	0.00 - 0.58
Density, Perm	0.20	0.00 - 0.43
Residuals	0.53	0.31 - 0.76

The main effect of geology can also be broken down into a regression equation of the form in Expression (5). In the regression all variables in Table 1 are used as candidate variables. Below the model computed by an exhaustive search is presented.

Exhaustive search :

```
Coefficients:
                      Value Std. Error t value Pr(>|t|)
               HETRX  0.5013  0.1777     2.8206  0.0063
               HETRZ  0.3468  0.1968     1.7623  0.0826
      KZ.PRES.SOLVE -0.7481  0.2772    -2.6990  0.0088
            AGGR.aZ  0.9889  0.1890     5.2326  0.0000
          KXY.ARITH  0.7155  0.1472     4.8616  0.0000
         KXmY.ARITH -0.3000  0.1276    -2.3515  0.0216
          OFFSET.aZ  1.0889  0.1762     6.1798  0.0000
       THICK.LSF.aZ  0.1503  0.0742     2.0261  0.0467
       THICK.USF.aZ -0.1395  0.0771    -1.8080  0.0751
    VSHALE.ARITH.aZ -0.6584  0.1721    -3.8257  0.0003
           CH.FM.aZ -0.1839  0.0922    -1.9938  0.0502
          LSF.FM.aZ -0.5079  0.1321    -3.8452  0.0003
          OFF.FM.aZ  0.2879  0.0863     3.3352  0.0014
           COS.PDIR -0.2437  0.0764    -3.1898  0.0022

Residual standard error: 0.5891 on 67 degrees of freedom
Multiple R-Squared: 0.7094, CV=0.41
```

The model above is used to predict the main effect of geology on the third principal production component. In Figure 41 the prediction is plotted versus the aggregated value computed from the data, i.e. $y_{i\cdots}$

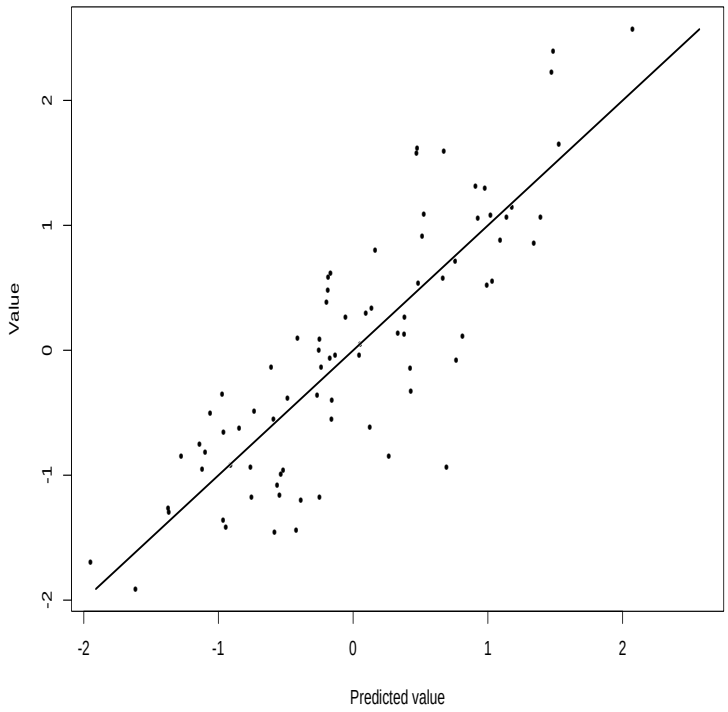

Figure 41: Prediction of third principal production component versus the aggregated value computed from the data.

6 Data analysis of deduced geological variables

The variables KX.PRES.SOLVE, KY.PRES.SOLVE and KZ.PRES.SOLVE, are upscaled permeabilities in X,Y and Z direction respectively. The variables HETRX, HETRY and HETRZ are heterogeneity measures, these are defined as the upscaled permeability divided by the arithmetic average of the permeability, i.e. HETRX= KX.PRES.SOLVE/KX.ARITH etc., these variables are dimensionless. In the previous analysis KX.PRES.SOLVE, KY.PRES.SOLVE, KZ.PRES.SOLVE, HETRX, HETRY and HETRZ variables are regarded as summary variables of the geological models, these variables are also complex function of the geological input variables. The variability is broken down into variance components due to geological design parameters. A regression analysis is performed to see if these variables can be described by the raw geological variables above the line in Table 1.

6.1 Upscaled permeability X direction (log transformed)

Table 39: Relative effect of geological design factors for upscaled permeability in X direction (log transformed)

Effect	Estimate	80 % CI
Agg.ang	0.26	0.00 - 0.49
Prog.dir	0.00	0.00 - 0.43
Barrier	0.35	0.00 - 0.58
Curvature	0.39	0.00 - 0.60
Agg.ang, Prog.dir	0.36	0.13 - 0.47
Agg.ang, Barrier	0.00	0.00 - 0.14
Agg.ang, Curvature	0.27	0.00 - 0.37
Prog.dir, Barrier	0.37	0.13 - 0.50
Prog.dir, Curvature	0.31	0.07 - 0.42
Barrier, Curvature	0.08	0.00 - 0.17
Residuals	0.46	0.34 - 0.56

Exhaustive search :

```
Coefficients:
               Value Std. Error  t value Pr(>|t|)
     AGGR.aZ  -0.1396   0.0292    -4.7880   0.0000
   KXY.ARITH   1.0012   0.0289    34.5941   0.0000
  KXmY.ARITH   0.3289   0.0312    10.5261   0.0000
THICK.LSF.aZ  -0.0539   0.0276    -1.9547   0.0543
        BARR  -0.2924   0.0268   -10.8945   0.0000

Residual standard error: 0.2364 on 76 degrees of freedom
Multiple R-Squared: 0.9469, CV=0.065
```

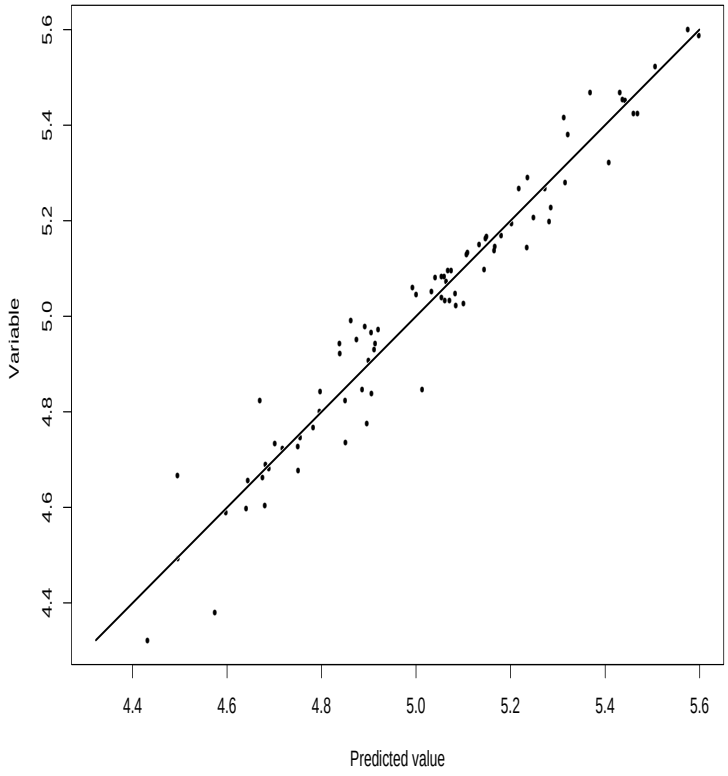

Figure 42: Predicted upscaled permeability X direction (log transformed) versus computed, for the model selected by an exhaustive search.

6.2 Upscaled permeability Y direction (log transformed)

Table 40: Relative effect of geological design factors for for upscaled permeability in Y direction (log transformed)

Effect	Estimate	80 % CI
Agg.ang	0.15	0.00 - 0.38
Prog.dir	0.00	0.00 - 0.47
Barrier	0.24	0.00 - 0.42
Curvature	0.31	0.00 - 0.62
Agg.ang, Prog.dir	0.29	0.07 - 0.41
Agg.ang, Barrier	0.00	0.00 - 0.14
Agg.ang, Curvature	0.29	0.07 - 0.40
Prog.dir, Barrier	0.29	0.09 - 0.37
Prog.dir, Curvature	0.58	0.27 - 0.69
Barrier, Curvature	0.16	0.00 - 0.25
Residuals	0.45	0.35 - 0.55

Exhaustive search ::

```
Coefficients:

                     Value Std. Error  t value Pr(>|t|)
         KXY.ARITH   0.8205   0.0498    16.4915   0.0000
        KXmY.ARITH  -0.1347   0.0338    -3.9897   0.0002
         OFFSET.aZ   0.1255   0.0311     4.0399   0.0001
      PORO.ARITH.aZ   0.0990   0.0497     1.9939   0.0498
           CH.FM.aZ  -0.2327   0.0329    -7.0686   0.0000
           CP.FM.aZ   0.1594   0.0368     4.3380   0.0000
               BARR  -0.2528   0.0260    -9.7140   0.0000

Residual standard error: 0.2312 on 74 degrees of freedom
Multiple R-Squared: 0.9506, CV=0.060
```

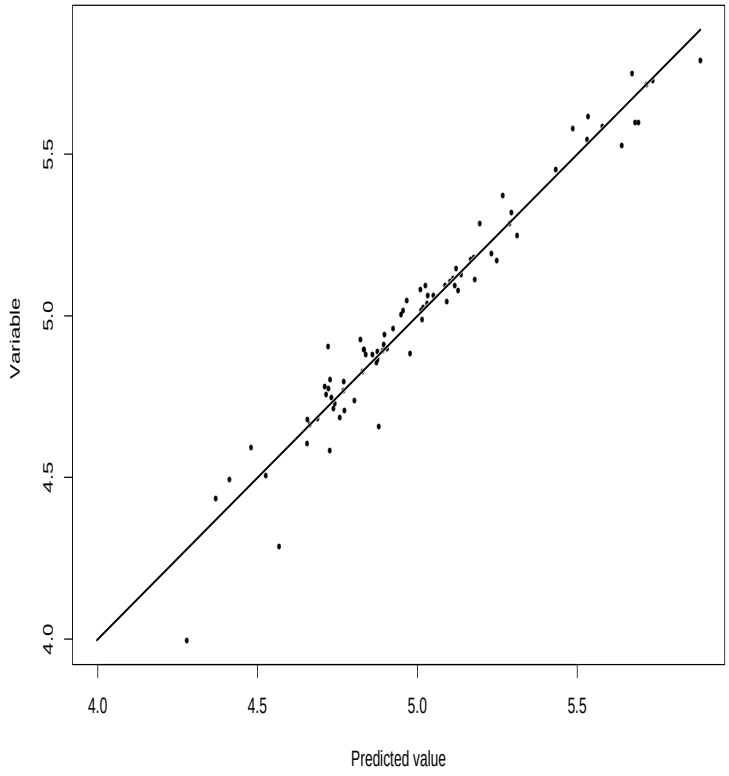

Figure 43: Predicted upscaled permeability Y direction (log transformed) versus computed, for the model selected by an exhaustive search.

6.3 Upscaled permeability Z direction (log transformed)

Table 41: Relative effect of geological design factors for upscaled permeability in Z direction (log transformed)

Effect	Estimate	80 % CI
Agg.ang	0.48	0.00 - 0.74
Prog.dir	0.00	0.00 - 0.20
Barrier	0.68	0.21 - 0.85
Curvature	0.00	0.00 - 0.27
Agg.ang, Prog.dir	0.13	0.00 - 0.21
Agg.ang, Barrier	0.23	0.09 - 0.38
Agg.ang, Curvature	0.34	0.14 - 0.50
Prog.dir, Barrier	0.15	0.01 - 0.25
Prog.dir, Curvature	0.15	0.00 - 0.23
Barrier, Curvature	0.08	0.00 - 0.16
Residuals	0.28	0.20 - 0.41

Exhaustive search :

```
Coefficients:
                        Value Std. Error  t value Pr(>|t|)
             AGGR.aZ   0.1816   0.0892     2.0366   0.0453
          KXmY.ARITH   0.0891   0.0485     1.8366   0.0703
            OFFSET.aZ -0.2360   0.0937    -2.5178   0.0140
       PORO.ARITH.aZ   0.7239   0.1098     6.5937   0.0000
     VSHALE.ARITH.aZ   0.2761   0.1267     2.1783   0.0326
           LSF.FM.aZ  -0.3372   0.0672    -5.0184   0.0000
           OTZ.FM.aZ  -0.3620   0.0724    -5.0005   0.0000
                BARR  -0.6973   0.0381   -18.2977   0.0000

Residual standard error: 0.3368 on 73 degrees of freedom
Multiple R-Squared: 0.8965, CV=0.131
```

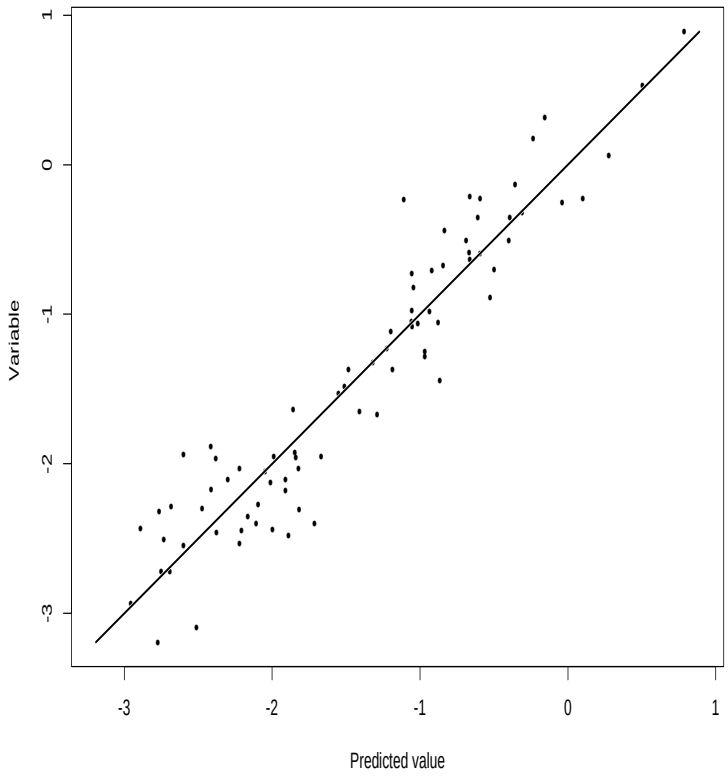

Figure 44: Predicted upscaled permeability Y direction (log transformed) versus computed, for the model selected by an exhaustive search.

6.4 Heterogeneity X direction

Table 42: Relative effect of geological design factors for heterogeneity in X direction

Effect	Estimate	80 % CI
Agg.ang	0.54	0.17 - 0.74
Prog.dir	0.00	0.00 - 0.31
Barrier	0.60	0.09 - 0.79
Curvature	0.00	0.00 - 0.37
Agg.ang, Prog.dir	0.00	0.00 - 0.10
Agg.ang, Barrier	0.14	0.00 - 0.24
Agg.ang, Curvature	0.00	0.00 - 0.10
Prog.dir, Barrier	0.13	0.00 - 0.22
Prog.dir, Curvature	0.41	0.19 - 0.53
Barrier, Curvature	0.26	0.11 - 0.39
Residuals	0.29	0.21 - 0.41

Exhaustive search :

```
Coefficients:
                      Value Std. Error  t value Pr(>|t|)
            AGGR.aZ  -0.2884   0.0515    -5.5989   0.0000
         KXmY.ARITH   0.5322   0.0572     9.3077   0.0000
       THICK.LSF.aZ  -0.0777   0.0486    -1.5990   0.1140
          CH.FM.aZ   -0.0942   0.0554    -1.7014   0.0930
          CP.FM.aZ    0.0941   0.0522     1.8041   0.0752
              BARR   -0.5540   0.0465   -11.9241   0.0000

Residual standard error: 0.4111 on 75 degrees of freedom
Multiple R-Squared: 0.8416,CV=0.193
```

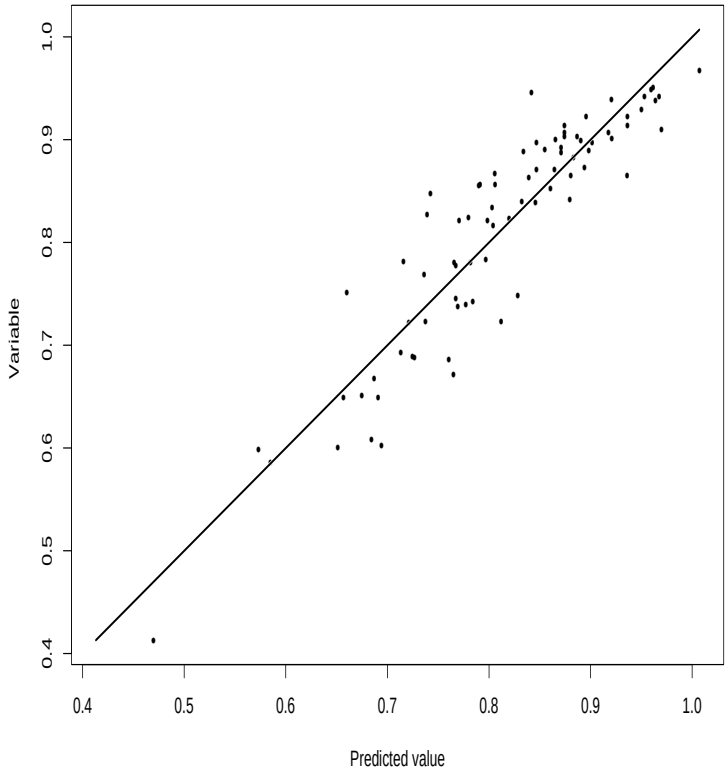

Figure 45: Predicted versus heterogeneity measure in Y direction versus computed heterogeneity measure, for the model selected by an exhaustive search.

6.5 Heterogeneity Y direction

Table 43: Relative effect of geological design factors for heterogeneity in Y direction

Effect	Estimate	80 % CI
Agg.ang	0.19	0.00 - 0.34
Prog.dir	0.00	0.00 - 0.30
Barrier	0.56	0.00 - 0.77
Curvature	0.41	0.00 - 0.69
Agg.ang, Prog.dir	0.14	0.00 - 0.22
Agg.ang, Barrier	0.00	0.00 - 0.12
Agg.ang, Curvature	0.14	0.00 - 0.23
Prog.dir, Barrier	0.08	0.00 - 0.16
Prog.dir, Curvature	0.39	0.19 - 0.54
Barrier, Curvature	0.41	0.19 - 0.60
Residuals	0.33	0.24 - 0.45

Exhaustive search :

```
Coefficients:
                      Value Std. Error  t value Pr(>|t|)
          KXmY.ARITH  -0.3258   0.0670    -4.8634   0.0000
           OFFSET.aZ   0.2594   0.0596     4.3553   0.0000
        PORO.ARITH.aZ   0.3161   0.0592     5.3438   0.0000
         THICK.LSF.aZ  -0.0882   0.0546    -1.6155   0.1105
             CH.FM.aZ  -0.5712   0.0642    -8.9040   0.0000
             CP.FM.aZ   0.3579   0.0637     5.6171   0.0000
                 BARR  -0.5635   0.0524   -10.7576   0.0000

Residual standard error: 0.4601 on 74 degrees of freedom
Multiple R-Squared: 0.8042, CV=0.239
```

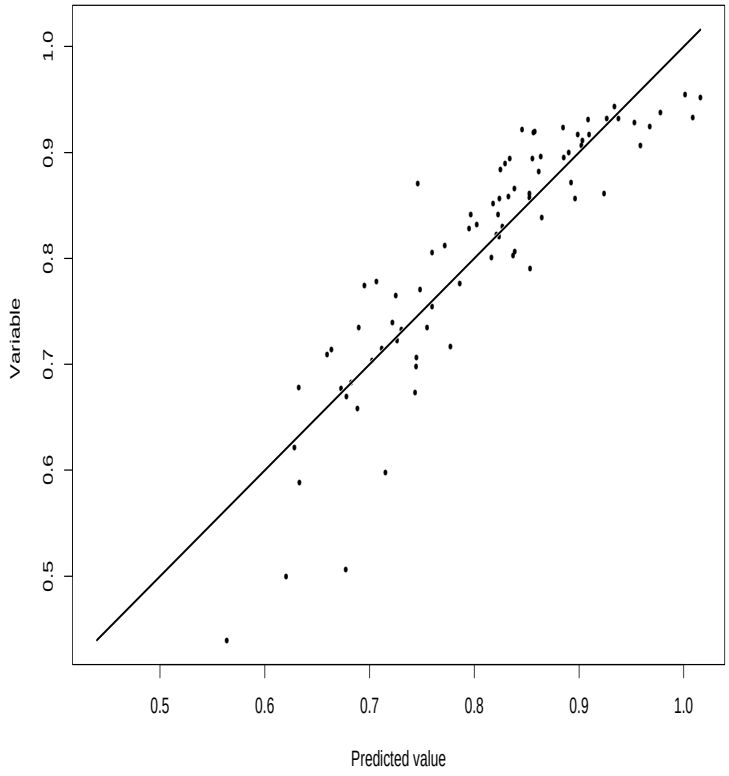

Figure 46: Predicted versus heterogeneity measure in Y direction versus computed heterogeneity measure, for the model selected by an exhaustive search.

6.6 Heterogeneity Z direction

Table 44: Relative effect of geological design factors for heterogeneity in Z direction

Effect	Estimate	80 % CI
Agg.ang	0.37	0.00 - 0.67
Prog.dir	0.00	0.00 - 0.13
Barrier	0.69	0.00 - 0.87
Curvature	0.00	0.00 - 0.19
Agg.ang, Prog.dir	0.13	0.03 - 0.22
Agg.ang, Barrier	0.52	0.26 - 0.77
Agg.ang, Curvature	0.18	0.06 - 0.29
Prog.dir, Barrier	0.10	0.00 - 0.18
Prog.dir, Curvature	0.04	0.00 - 0.09
Barrier, Curvature	0.15	0.04 - 0.23
Residuals	0.20	0.14 - 0.32

Exhaustive search :

```
Coefficients:
                       Value Std. Error  t value Pr(>|t|)
             AGGR.aZ   0.2413   0.1306     1.8476   0.0688
             CLIN.aZ  -0.1010   0.0574    -1.7600   0.0827
           KXY.ARITH  -0.4651   0.1781    -2.6111   0.0110
           OFFSET.aZ  -0.2215   0.1449    -1.5288   0.1308
       PORO.ARITH.aZ   0.9375   0.2620     3.5777   0.0006
     VSHALE.ARITH.aZ   0.6098   0.2129     2.8636   0.0055
            CH.FM.aZ  -0.1061   0.0698    -1.5199   0.1330
           LSF.FM.aZ  -0.2698   0.1233    -2.1882   0.0319
           OTZ.FM.aZ  -0.4991   0.1876    -2.6608   0.0096
                BARR  -0.7321   0.0564   -12.9702   0.0000

Residual standard error: 0.4958 on 71 degrees of freedom
Multiple R-Squared: 0.7819, CV=0.286
```

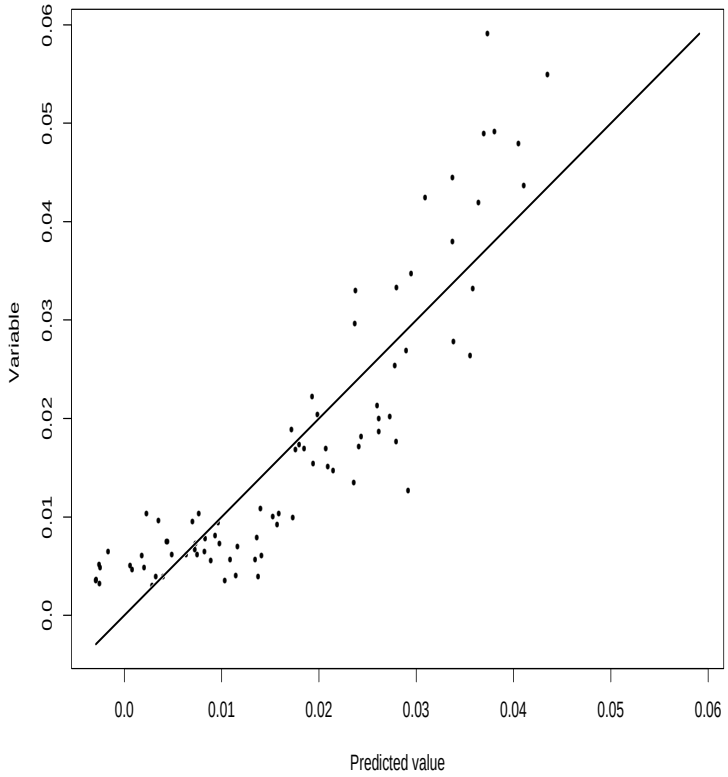

Figure 47: Predicted versus heterogeneity measure in Z direction versus computed heterogeneity measure, for the model selected by an exhaustive search.

7 Discussion of the results

In the current section the results from the statistical analysis are discussed. The discussion at the SAIGUP meeting 2002 and communication following this meeting, e.g. Matthews (2002), have given contributions to the current section. First the effects of geology, fault and PDO are discussed, then the geological factors are discussed, at last fault factors and PDO are discussed. The analysis of the variance components in the two last subsections is troubled by large uncertainties in the analysis, hence conclusions are weak.

7.1 Main effects of geology, fault and PDO

Geology is the dominant factor for variables related to production volumes, i.e. oil in place, total oil volume produced, log transform of total oil volume produced, discounted production, and the production components, see Tables 7, 9, 12, 15, 30, 33, and 36. This is partly because the fault models are adjusted such that the net gross is determined by the geological model, hence oil in place is determined by geological factors alone, see Table 7. The range of oil in place is 39860 kSM3 to 70500 kSM3, which is quite large. The assertion that it is the influence of oil in place that make geology dominant for the production variables is supported by the correlations in Table 6, and the boxplots in Section 3. Oil in place is correlated with all of the variables related to oil production and recovery, more with those related to oil volumes than to those related to recovery. The box plots indicate the same effect as the correlations The pattern in the boxplots for oil in place is also seen for the variables related oil volume production, in particular total oil volume produced, log transform of total oil volume produced, discounted production, and the first production component (PROD.PC1), compare Figure 20 with Figures 21, 22, 23, and 28. The second and third production components are not as strongly correlated to oil in place, see Table 6. The geological effect is dominating also for these variables. Hence, the dominant effect of geology on production variables can not only be contributed to oil in place. Geology is also the dominant effect for the total water production and the ratio of total oil to water production, see Tables 24, and 27.

Fault and geology have an equally dominant effect on variables related to recovery, i.e. recovery factor after 30 years of production and recovery factor for production at an injected pore volume of 20%, see Tables 18 and 21. Fault is the largest effect on the recovery factor after 30 years of production.

PDO generally has a minor effect, the largest effect is on the third production component, see Table 36. This variable can be given the interpretation as a variable that shift production, see Figure 4 (d). Hence, the largest contribution of PDO is regarding the time when oil is produced, not as much the amount of oil. This is also seen when comparing the effect of PDO in total production, Table 9, and discounted production, Table 15. The influence is larger on the discounted production, which gives unequal weight to oil volume produced at different times.

Each PDO is designed to a particular fault structure. In order to account for this it is natural to evaluate the effect of PDO by combining its main effect and its interaction with fault effects. When this is done for recovery factor and recovery at 20 % injected water volume, see Table 18 and 21, the joint effect is $\sqrt{0.21^2 + 0.29^2} = 0.37$ and $\sqrt{0.12^2 + 0.35^2} = 0.36$ respectively. The influence of PDO on recovery is hence larger than it seems when only the main effect is accounted for.

It can also be argued that the variability due to interaction of fault and PDO should be contributed to fault, since this variability is given by nature while the effect of PDO is man made. By adding the interaction effect of fault and PDO to fault, the effect of faults will be slightly increased, but the general picture will not be altered.

7.2 The influence of geological factors

Aggradation angle, progradation direction, interaction of these two effects and the residual term dominate the effect of geological design variables on variables related to oil production and recovery, see Tables 8, 10, 13, 16, 19, 22, 31, 34, and 37. The residual term is caused by heterogeneity in the geological models that is introduced when modelling facies and petrophysical properties, but is also caused by third and fourth order interaction of geological design variables. The two first effects are believed to be dominant, but the effects can not be separated in the current design. So even though the residual term give a significant contribution in the analysis, it cannot be given a physical interpretation.

As commented in the previous subsection oil in place correlate strongly with other variables related to production, i.e. total oil volume produced, log transform of total oil volume produced, discounted production, and the first production component. Since aggradation angle and progradation direction have the dominating effect on oil in place, it is also natural that these two dominate the other production variables, compare Figure 20 with Figures 21, 22, 23 and 28. The importance of aggradation angle and progradation direction is however not only related to oil in place, since these factors are dominant also for the recovery and second production component, see Table 19, 22, and 34.

Barriers have relatively large influence on water production, ratio of produced oil to water, upscaled permeabilities and heterogeneity measures (in particular in Z direction), see Tables 25, 28, 39, 40, 41, 42, 43 and 44. For variables related to oil production and recovery the effect of barriers is almost absent, see Tables 8, 10, 13, 16, 19, 21, 31, 34, and 37. The barrier variable is present in many regression equations, either directly or by its influence through heterogeneity measures. The effect is however typically small, although it is highly significant in statistical terms, the physical impact is not large.

The missing influence of the barriers on variables related to oil production and recovery, can be caused by the range of barrier coverage present in the SAIGUP project, i.e. the range 10% - 90% is not enough to see an effect. It is likely that barriers are of larger importance when the coverage is close to 100 %. In addition, the faulting of the reservoir brake up the barriers, this allow flow through areas that is sealed in unfaulted models.

Curvature has the largest influence on heterogeneity measure in Y direction, see Table 43 and on upscaled permeabilities in the lateral direction, see Tables 39 and 40. When variables related to production and recovery are considered, curvature generally have a small effect. The largest contribution is to the second and third production component, see Table 34 and 37.

7.3 The influence of fault factors and PDO

Fault structure is the dominating effect in most of the variables, i.e. total oil production, the logarithm of total oil production, recovery factor, recovery at 20 % injected water volume, total oil to water production, second and third production component, see Tables 11, 14, 20, 20, 23, 29, 35 and 38. It is also large for those it does not dominate, i.e discounted production, total water production and first principal production component, see Tables 17, 26, and 32. The main reason why the fault structure dominate is that fault structure c gives worse production results than the two other, see Figures 10 through 19.

Fault density is the second most important fault factor, it dominates discounted production, total water production and first principal production component, see Tables 17, 26, and 32, and is large for most other variables. The effect of fault density is monotone in the sense that lower fault density gives better production results, see Figures 10 through 19. This is in particular seen for fault structure c where high fault density give particularly bad results with respect to production and recovery. For fault structure a and b the effect of fault density is generally larger for variables that give credit to early production, i.e the effect of fault density in fault structure a and b is less for total production than for discounted production, and less for recovery factor than for recovery at 20 % water injection, compare Figure 10 with 12 and Figure 13 with 14. Lower fault density also gives larger water production. The effect is large for both fault structure b and c, but less for fault structure a. Fault structure a tend to have an overall water production that is larger than the two other fault structures, see Figure 15. For the ratio of total produced oil to water the fault density effect is largest for fault structure b, see Figure 16. In fault structure a; total oil produced and total water produced is little influenced by the density, hence there is no effect for the ratio of the two. In fault structure b; total oil produced is little influenced by fault density while the effect on total water produced is large, resulting in a large effect on the ratio. In fault structure c; both total oil produced and total water produced are influenced equally much such that ratio of the two is not much affected.

The fault permeability predictor generally have a small effect, but it has larger influence on variables that give credit to early production, hence the permeability predictor seem to have some influence on the time of the production, i.e compare the contribution of fault permeability predictor on total production versus discounted production and recovery at thirty years versus recovery at an injected pore volume of 20%, i.e. Table 11 versus 17 and Table 20 versus 23.

An interesting interaction effect between fault factors and production strategy is that the fault density has less effect when the correct production strategy is used for a fault structure. This can be seen in Figures

10 through 19, by comparing the shifts in the distributions when the fault density decreases. The shifts are smaller when the correct PDO is used. In particular the very low recovery rates are avoided in fault structure c when the correct production strategy is used, see Figures 13 and 14.

8 Summary

The data analysis is performed based on 9072 reservoir simulations from all combinations of 81 geological models, 28 fault models and 4 production strategies. The 81 geological models are constructed by varying structural factors, i.e. curvature of the facies borders, progradation angle, aggradation angle and barrier coverage, and adding heterogeneity to these main structures, i.e facies borders and petrophysical properties. The 28 fault models are constructed by varying the fault structure, fault density and permeability in the fault zone. In addition there is one unfaulted reservoir. The data analysis of these reservoir simulations has given the following main conclusions:

- The geological parameters dominate the estimates for oil in place, total oil produced, discounted production and have the largest effect on almost all other production parameters. The geological parameters are varied such that the largest reservoir has 1,75 times as much oil in place as the smallest reservoir.
- Fault parameters have a significant influence on total oil production, recovery, water production and the production profiles. The fault parameters are introduced such that they have no influence on the oil in place.
- The aggradation and progradation parameters are the most important geological parameters.
- The fault structure and density are the most important fault parameters.
- The barriers and the fault permeabilities influence how fast the reservoir is drained, but has less effect on total recovery.
- When the PDO that corresponds to the fault structure is chosen, this reduces the effect of the fault density and removes the very low recovery reservoirs.
- The aggradation angle, barriers, curvature and the residual are dominating the heterogeneity measures.
- The geology dominates the two first principal components of the production. The PDO, heterogeneities and permeabilities have an important influence on the third production component that influence when the oil is produced.

Note that how the test have been performed have had a major influence on the results. Some of the factors are:

- How much a parameter is varied has a major influence on how dominant it will be in a data analysis like this. In a real uncertainty study is the knowledge about a parameter as important as the influence of the parameter.
- Only a very limited number of geological and fault models are tested.
- The production scenarios are fixed and not optimised based on the knowledge about each reservoir and knowledge that is gained from the reservoir so far.

Acknowledgements

This is a project funded by the European Community under the Energy, Environment and sustainable development Programme, project number NNE5-2000-20095. The partners are; Fault Analysis Group, Department of Geology, University College Dublin; (co-ordinator); Department of Petroleum Engineering, Heriot-Watt University; Department of Earth Science and Engineering, Imperial College of science, technology and medicine; The Netherlands Institute of Applied Geoscience-National Geological Survey, Department of Geo-Energy; Badley Technology Ltd; BG International Limited; ROXAR Software Solution ASA; Shell International Exploration and production; Stratigraphy Group, Department of Earth Sciences, University of Liverpool; and SAND department at the Norwegian Computing Center.

References

Box,G.E.P.;Hunter,W.G. and Hunter,J.S (1978) "Statistics for experiments". Wiley

Efroymson,M.A. (1960) Multiple regression analysis, in A.Ralston & H. Wilf,eds, Mathematical methods for digital computers,Wiley,New York, pp 191-203

Egeland, Thore; Omre, Henning; Lia, Oddvar; Tjelmeland, Håkon; Holden, Lars and Andersen, Tove: "GRUS data analysis" Nr. SAND/17/94, 1994. Notat

Lia, Oddvar; Omre, Henning; Tjelmeland, Håkon; Holden, Lars; Egeland, Thore and Andersen, Tove; MacDonald, Alister; Hustad, Odd Steve (IKU Petroleum Research); Qi, Yuanchang (IBM/EPAC): "The great reservoir uncertainty study - GRUS". PROFIT 1990-1994. Project summary reports. Norwegian Petroleum Directorate, Stavanger 1995. Artikkel.

Matthews John D.; (2002) "Sweep efficiency in the SAIGUP reservoir simulation model.", SAIGUP internal report.

Stone, M. (1974) "Cross-validation Choice and Assessment of Statistical Predictions" Journal of the Royal Statistical Society, series B, Vol. 36, No.2, pp 111-133.

Weisberg Sanford (1985) "Applied linear regression" 2nd edition, Wiley, New York.

A Expectations of sum of squares

In the variance component model,

$$y_{ijk} = K_0 + \varepsilon_i + \varepsilon_j + \varepsilon_k + \varepsilon_{ij} + \varepsilon_{ik} + \varepsilon_{jk} + \varepsilon_{ijk}\ ;\ \ i = 1, ...n_I;\ \ j = 1, ..., n_J;\ \ k = 1, ..., n_K;$$

with all random components, i.e. the ε's, being independent. Let σ_I denote the standard deviation of ε_i; $\forall\ i$, σ_J that of $\varepsilon_j\ \forall\ j$ and so on. The expected sum of squares from aggregate levels of data is used in order to estimate the variances of the random components. This appendix, see Expression (6), list the expected value of the relevant sum of squares. A standard statistical notation where a dot replaces the indices that is averaged out is used.

$$
\begin{array}{rcllllll}
\mathrm{E}\left\{\sum_{ijk}(y_{ijk}-\bar{y})^2\right\} &=& (n_I-1)n_Jn_K & \sigma_I^2 & +(n_J-1)n_In_K & \sigma_J^2 & +(n_K-1)n_In_J & \sigma_K^2 \\
&+& n_K(n_In_J-1) & \sigma_{IJ}^2 & +n_J(n_In_K-1) & \sigma_{IK}^2 & +n_I(n_Kn_J-1) & \sigma_{JK}^2 \\
&+& (n_In_Jn_K-1) & \sigma_{IJK}^2 & & & & \\
\mathrm{E}\left\{\sum_{jk}(y_{\cdot jk}-\bar{y})^2\right\} &=& & & +(n_J-1)n_K & \sigma_J^2 & +(n_K-1)n_J & \sigma_K^2 \\
&+& (n_J-1)n_K/n_I & \sigma_{IJ}^2 & +(n_K-1)n_J/n_I & \sigma_{IK}^2 & +(n_Kn_J-1) & \sigma_{JK}^2 \\
&+& (n_Jn_K-1)/n_I & \sigma_{IJK}^2 & & & & \\
\mathrm{E}\left\{\sum_{ik}(y_{i\cdot k}-\bar{y})^2\right\} &=& (n_I-1)n_K & \sigma_I^2 & & & +(n_K-1)n_I & \sigma_K^2 \\
&+& (n_I-1)n_K/n_J & \sigma_{IJ}^2 & +(n_In_K-1) & \sigma_{IK}^2 & +(n_K-1)n_I/n_J & \sigma_{JK}^2 \\
&+& (n_In_K-1)/n_J & \sigma_{IJK}^2 & & & & \\
\mathrm{E}\left\{\sum_{ij}(y_{ij\cdot}-\bar{y})^2\right\} &=& (n_I-1)n_J & \sigma_I^2 & +(n_J-1)n_I & \sigma_J^2 & & \\
&+& (n_In_J-1) & \sigma_{IJ}^2 & +(n_I-1)n_J/n_K & \sigma_{IK}^2 & +(n_J-1)n_I/n_K & \sigma_{JK}^2 \\
&+& (n_In_J-1)/n_K & \sigma_{IJK}^2 & & & & \\
\mathrm{E}\left\{\sum_{k}(y_{\cdot\cdot k}-\bar{y})^2\right\} &=& & & & & +(n_K-1) & \sigma_K^2 \\
&+& & & (n_K-1)/n_I & \sigma_{IK}^2 & +(n_K-1)/n_J & \sigma_{JK}^2 \\
&+& (n_K-1)/n_In_J & \sigma_{IJK}^2 & & & & \\
\mathrm{E}\left\{\sum_{j}(y_{\cdot j\cdot}-\bar{y})^2\right\} &=& & & (n_J-1) & \sigma_J^2 & & \\
&+& (n_J-1)/n_I & \sigma_{IJ}^2 & & & +(n_J-1)/n_K & \sigma_{JK}^2 \\
&+& (n_J-1)/n_In_K & \sigma_{IJK}^2 & & & & \\
\mathrm{E}\left\{\sum_{i}(y_{i\cdot\cdot}-\bar{y})^2\right\} &=& (n_I-1) & \sigma_I^2 & & & & \\
&+& (n_I-1)/n_J & \sigma_{IJ}^2 & +(n_I-1)/n_K & \sigma_{IK}^2 & & \\
&+& (n_I-1)/n_Jn_K & \sigma_{IJK}^2 & & & &
\end{array}
\tag{6}
$$

B Result from stepwise regression using Efroymson's method

The current section contains the regression models that are computed using stepwise regression with Efroymson's selection rule. The results for each variable are listed in the same order as in Table 5 in the subsection to follow. The same analysis is performed on the upscaled permeability and the heterogeneity measure and is listed in the last subsection.

B.1 Production variables

Oil in place , stepwise model:

```
Coefficients:
                    Value Std. Error  t value Pr(>|t|)
            AGGR.aZ  0.2418   0.0373   6.4850   0.0000
          KXY.ARITH -0.3475   0.1012  -3.4322   0.0010
           KZ.ARITH  0.3585   0.0908   3.9497   0.0002
      PORO.ARITH.aZ  0.8814   0.0512  17.2168   0.0000
           CH.FM.aZ  0.0837   0.0307   2.7266   0.0080
          OFF.FM.aZ  0.2733   0.0347   7.8821   0.0000
          OTZ.FM.aZ -0.2121   0.0556  -3.8170   0.0003
           COS.PDIR -0.0859   0.0325  -2.6448   0.0100

Residual standard error: 0.2449 on 73 degrees of freedom
Multiple R-Squared: 0.9453, CV=0.069
```

Total oil production, stepwise model:

```
Coefficients:
                      Value Std. Error t value Pr(>|t|)
        KZ.PRES.SOLVE  0.1878  0.0651     2.8844  0.0052
              AGGR.aZ  0.3324  0.0429     7.7543  0.0000
        PORO.ARITH.aZ  0.6048  0.0812     7.4451  0.0000
         THICK.USF.aZ -0.0698  0.0292    -2.3901  0.0195
      VSHALE.ARITH.aZ -0.4317  0.0704    -6.1358  0.0000
            LSF.FM.aZ -0.1824  0.0549    -3.3235  0.0014
            OFF.FM.aZ  0.2607  0.0350     7.4536  0.0000
                 BARR  0.1070  0.0527     2.0302  0.0460
             COS.PDIR -0.0952  0.0304    -3.1305  0.0025

Residual standard error: 0.2376 on 72 degrees of freedom
Multiple R-Squared: 0.9492, CV=0.066
```

Total oil production log transformed, stepwise model:

```
Coefficients:
                      Value Std. Error t value Pr(>|t|)
               HETRY -0.0994  0.0374    -2.6578  0.0097
        KZ.PRES.SOLVE  0.2311  0.0596     3.8798  0.0002
              AGGR.aZ  0.3073  0.0422     7.2855  0.0000
              CLIN.aZ -0.0372  0.0261    -1.4257  0.1584
        PORO.ARITH.aZ  0.5226  0.0681     7.6776  0.0000
         THICK.LSF.aZ -0.0583  0.0276    -2.1144  0.0380
         THICK.USF.aZ -0.0588  0.0267    -2.2060  0.0307
      VSHALE.ARITH.aZ -0.3668  0.0649    -5.6542  0.0000
            OFF.FM.aZ  0.2212  0.0325     6.8035  0.0000
                 BARR  0.0968  0.0500     1.9381  0.0566
             COS.PDIR -0.0771  0.0287    -2.6883  0.0090

Residual standard error: 0.2239 on 70 degrees of freedom
Multiple R-Squared: 0.9561, CV=0.060
```

Discounted production, stepwise model:

```
Coefficients:
                       Value Std. Error  t value Pr(>|t|)
        KZ.PRES.SOLVE   0.0870   0.0257     3.3892   0.0012
              AGGR.aZ   0.1127   0.0470     2.3999   0.0191
            OFFSET.aZ   0.0919   0.0515     1.7857   0.0785
        PORO.ARITH.aZ   0.6077   0.0589    10.3215   0.0000
         THICK.USF.aZ  -0.0395   0.0219    -1.8066   0.0751
      VSHALE.ARITH.aZ  -0.2175   0.0653    -3.3320   0.0014
             CH.FM.aZ  -0.0818   0.0237    -3.4520   0.0009
             CP.FM.aZ  -0.2198   0.0330    -6.6583   0.0000
            LSF.FM.aZ  -0.2864   0.0435    -6.5760   0.0000
            OTZ.FM.aZ  -0.4481   0.0450    -9.9614   0.0000
             COS.PDIR  -0.0725   0.0224    -3.2339   0.0019

Residual standard error: 0.1735 on 70 degrees of freedom
Multiple R-Squared: 0.9737, CV=0.035
```

Recovery factor, stepwise model:

```
Coefficients:
                        Value Std. Error  t value Pr(>|t|)
               HETRY   0.1386   0.0482     2.8769   0.0052
             AGGR.aZ   0.6209   0.0463    13.4095   0.0000
             CLIN.aZ  -0.0842   0.0455    -1.8501   0.0682
        PORO.ARITH.aZ   0.7687   0.0528    14.5639   0.0000
         THICK.USF.aZ  -0.0792   0.0459    -1.7256   0.0885
            OFF.FM.aZ   0.1455   0.0541     2.6905   0.0088

Residual standard error: 0.3985 on 75 degrees of freedom
Multiple R-Squared: 0.8512, CV=0.175
```

Recovery at 20 % injected water,stepwise model:

```
Coefficients:
                Value Std. Error t value Pr(>|t|)
        HETRX  0.3383  0.1009     3.3545  0.0013
        HETRY -0.2040  0.0784    -2.6028  0.0112
      AGGR.aZ  0.5965  0.0609     9.7971  0.0000
      CLIN.aZ -0.1054  0.0460    -2.2940  0.0248
   KXmY.ARITH -0.1641  0.0826    -1.9870  0.0508
     KZ.ARITH  0.1381  0.0742     1.8612  0.0669
PORO.ARITH.aZ  0.6488  0.0726     8.9309  0.0000
 THICK.USF.aZ -0.1165  0.0483    -2.4136  0.0184
     COS.PDIR -0.1687  0.0513    -3.2920  0.0016

Residual standard error: 0.399 on 72 degrees of freedom
Multiple R-Squared: 0.8587, CV=0.186
```

Total water production , stepwise model:

```
Coefficients:
                       Value Std. Error t value Pr(>|t|)
               HETRX -0.1551  0.0876    -1.7698  0.0810
               HETRZ -0.2243  0.0911    -2.4625  0.0162
             CLIN.aZ -0.1487  0.0613    -2.4258  0.0178
        PORO.ARITH.aZ  0.4929  0.1212     4.0684  0.0001
         THICK.LSF.aZ -0.2203  0.0634    -3.4739  0.0009
             CH.FM.aZ  0.1349  0.0732     1.8433  0.0694
            LSF.FM.aZ  0.3694  0.1110     3.3263  0.0014
            OFF.FM.aZ  0.2844  0.0749     3.7949  0.0003
                 BARR  0.1796  0.1083     1.6591  0.1014

Residual standard error: 0.524 on 72 degrees of freedom
Multiple R-Squared: 0.7529, CV=0.32
```

Ratio total oil to total water production, stepwise model:

```
 Coefficients:
                        Value Std. Error  t value Pr(>|t|)
       KX.PRES.SOLVE  -0.3934   0.1102    -3.5700   0.0006
       KZ.PRES.SOLVE   0.9669   0.0877    11.0278   0.0000
             CLIN.aZ   0.1460   0.0658     2.2203   0.0295
          KXmY.ARITH   0.1860   0.0926     2.0079   0.0483
        THICK.LSF.aZ   0.2735   0.0723     3.7843   0.0003
     VSHALE.ARITH.aZ  -0.4202   0.1419    -2.9610   0.0041
           CH.FM.aZ  -0.2049   0.0812    -2.5222   0.0138
          LSF.FM.aZ  -0.5345   0.1167    -4.5819   0.0000

Residual standard error: 0.5821 on 73 degrees of freedom
Multiple R-Squared: 0.6908, CV=0.39
```

First principal production component, stepwise model:

```
Coefficients:
                        Value Std. Error  t value Pr(>|t|)
       PORO.ARITH.aZ  -0.7158   0.0702   -10.2027   0.0000
        THICK.OTZ.aZ  -0.0351   0.0245    -1.4313   0.1566
     VSHALE.ARITH.aZ   0.1457   0.0793     1.8374   0.0702
           CH.FM.aZ   0.1175   0.0264     4.4471   0.0000
           CP.FM.aZ   0.1224   0.0381     3.2092   0.0020
          LSF.FM.aZ   0.2366   0.0483     4.9014   0.0000
          OTZ.FM.aZ   0.4348   0.0453     9.6045   0.0000
               BARR   0.0905   0.0240     3.7701   0.0003

Residual standard error: 0.2114 on 73 degrees of freedom
Multiple R-Squared: 0.9592, CV=0.051
```

Second principal production component, stepwise model:

```
oefficients:
                        Value Std. Error t value Pr(>|t|)
            AGGR.aZ  0.5194  0.1153     4.5064  0.0000
            CLIN.aZ -0.1246  0.0479    -2.6024  0.0112
         KXmY.ARITH  0.1178  0.0609     1.9354  0.0569
          OFFSET.aZ -0.4005  0.1103    -3.6319  0.0005
       THICK.LSF.aZ -0.0928  0.0501    -1.8525  0.0680
       THICK.USF.aZ -0.0714  0.0501    -1.4247  0.1586
           CH.FM.aZ  0.2942  0.0591     4.9739  0.0000
           CP.FM.aZ -0.5653  0.0621    -9.1032  0.0000
          OFF.FM.aZ -0.1773  0.0630    -2.8154  0.0063

Residual standard error: 0.4211 on 72 degrees of freedom
Multiple R-Squared: 0.8404, CV=0.22
```

Third principal production component, stepwise model:

```
Coefficients:
                        Value Std. Error t value Pr(>|t|)
       KY.PRES.SOLVE  0.4135  0.1442     2.8671  0.0054
             AGGR.aZ  0.8324  0.1686     4.9380  0.0000
          KZ.ARITH  0.3458  0.1589     2.1760  0.0328
          OFFSET.aZ  1.2544  0.1788     7.0171  0.0000
       THICK.LSF.aZ  0.1586  0.0769     2.0616  0.0428
          OFF.FM.aZ  0.2618  0.0862     3.0381  0.0033
           COS.PDIR -0.2515  0.0737    -3.4139  0.0010

Residual standard error: 0.6435 on 74 degrees of freedom
Multiple R-Squared: 0.617, CV=0.46
```

B.2 Deduced Geological variables

Upscaled permeability X direction (log transformed), stepwise search :

```
Coefficients:
               Value Std. Error  t value Pr(>|t|)
     AGGR.aZ  -0.1396   0.0292    -4.7880   0.0000
   KXY.ARITH   1.0012   0.0289    34.5941   0.0000
  KXmY.ARITH   0.3289   0.0312    10.5261   0.0000
THICK.LSF.aZ  -0.0539   0.0276    -1.9547   0.0543
        BARR  -0.2924   0.0268   -10.8945   0.0000

Residual standard error: 0.2364 on 76 degrees of freedom
Multiple R-Squared: 0.9469, CV=0.065
```

Upscaled permeability Y direction (log transformed) , stepwise search :

```
Coefficients:
                         Value Std. Error  t value Pr(>|t|)
           KXY.ARITH   0.8747   0.0333    26.2619   0.0000
          KXmY.ARITH  -0.1410   0.0338    -4.1761   0.0001
           OFFSET.aZ   0.1154   0.0330     3.5007   0.0008
            CH.FM.aZ  -0.2309   0.0331    -6.9746   0.0000
            CP.FM.aZ   0.0857   0.0334     2.5683   0.0122
           OFF.FM.aZ  -0.0590   0.0343    -1.7220   0.0893
                BARR  -0.2541   0.0263    -9.6676   0.0000

Residual standard error: 0.2327 on 74 degrees of freedom
Multiple R-Squared: 0.9499, CV=0.062
```

Upscaled permeability Z direction (log transformed), stepwise search: :

```
Coefficients:
                         Value Std. Error  t value Pr(>|t|)
            AGGR.aZ   0.1541   0.0896     1.7198   0.0896
           KZ.ARITH   0.2755   0.0668     4.1228   0.0001
          OFFSET.aZ  -0.2723   0.0948    -2.8737   0.0053
       PORO.ARITH.aZ   0.3217   0.0919     3.5003   0.0008
           LSF.FM.aZ  -0.1760   0.0720    -2.4436   0.0169
                BARR  -0.7135   0.0394   -18.1021   0.0000

Residual standard error: 0.3502 on 75 degrees of freedom
Multiple R-Squared: 0.885, CV=0.139
```

Heterogeneity X direction , stepwise search:

```
Coefficients:
               Value Std. Error  t value Pr(>|t|)
     AGGR.aZ  -0.2886   0.0517    -5.5846   0.0000
  KXmY.ARITH   0.5509   0.0525    10.4889   0.0000
THICK.LSF.aZ  -0.0960   0.0482    -1.9916   0.0500
        BARR  -0.5524   0.0473   -11.6785   0.0000

Residual standard error: 0.4189 on 77 degrees of freedom
Multiple R-Squared: 0.8311, CV=0.193
```

Heterogeneity Y direction , stepwise search :

```
Coefficients:
                        Value Std. Error  t value Pr(>|t|)
           KXmY.ARITH  -0.3017   0.0681    -4.4314   0.0000
            OFFSET.aZ   0.3168   0.0693     4.5689   0.0000
         PORO.ARITH.aZ   0.4657   0.1116     4.1721   0.0001
          THICK.LSF.aZ  -0.0833   0.0542    -1.5386   0.1282
              CH.FM.aZ  -0.5590   0.0640    -8.7351   0.0000
              CP.FM.aZ   0.5111   0.1160     4.4072   0.0000
             OFF.FM.aZ   0.1808   0.1148     1.5745   0.1197
                  BARR  -0.5577   0.0520   -10.7258   0.0000

Residual standard error: 0.4556 on 73 degrees of freedom
Multiple R-Squared: 0.8106, CV=0.239
```

Heterogeneity Z direction, stepwise search :

```
Coefficients:
                 Value Std. Error  t value Pr(>|t|)
      AGGR.aZ   0.4782   0.0583     8.1978   0.0000
      CLIN.aZ  -0.1296   0.0584    -2.2197   0.0294
PORO.ARITH.aZ   0.1158   0.0588     1.9695   0.0525
         BARR  -0.7338   0.0583   -12.5895   0.0000

Residual standard error: 0.5179 on 77 degrees of freedom
Multiple R-Squared: 0.7418, CV=0.295
```